Synthesis and biological assessment of organometallic tamoxifen derivatives for the diagnosis and the treatment of breast cancer

Anh Nguyen

UNIVERSITE PIERRE & MARIE CURIE
LA SCIENCE A PARIS

Ecole doctorale de Chimie Moléculaire Paris-Centre (ED406)

Spécialité: Chimie BioOrganométallique

Thèse de doctorat

de l'université de Pierre et Marie Curie (Paris VI)

Présentée par **Anh NGUYEN**

Pour obtenir le grade de Docteur de l'universite Paris VI

Synthèse et évaluation biologique
de nouveaux dérivés organométalliques du tamoxifène
pour le diagnostic et le traitement du Cancer du Sein

Soutenue le 30 Octobre 2007

devant le jury composé de:

Pr.	Giovanni POLI, Professeur à l'université Paris VI	Président
Pr.	Roger ALBERTO, Professeur à l'université de Zürich, Suisse	Rapporteur
Pr.	Nils METZLER-NOLTE, Professeur à l'université de Bochum, Allemagne	Rapporteur
Dr.	Jack-Michel RENOIR, Directeur de recherche à la Faculté de Châtenay-Malabry	Examinateur
Dr.	Siden TOP, Directeur de recherche à l'ENSCP	Examinateur
Pr.	Gérard JAOUEN, Professeur à l'ENSCP	Directeur de thèse

Préparée à l'Ecole Nationale Supérieure de Chimie de Paris

"Une chime unitaire [sur laquelle] les natures organique et inorganique reposeraient"

La Recherche de l'Absolu, Honoré de BALZAC

Balzac pressentait-il déjà en 1834 l'avènement de la Chimie Organométallique?

A la mémoire de mon père

Ce travail de thèse a été effectué au

This thesis work has been performed at the

Laboratoire de Chimie et Biochimie des Complexes Moléculaires, UMR7576

Ecole Nationale Supérieure de Chime de Paris (ENSCP)

11 rue Pierre et Marie Curie, 75005 PARIS, FRANCE

sous la direction du Pr. Gérard JAOUEN et du Dr. Siden TOP

under the supervision of Prof. Gérard JAOUEN and Dr. Siden TOP

Title: Synthesis and biological assessment of organometallic tamoxifen derivatives for the diagnosis and the treatment of breast cancer

Résumé

Puisque le cancer du sein reste l'une des premières causes de mortalité chez la femme, le diagnostic et le traitement de cette maladie ont plus que jamais besoin d'être améliorés. L'intérêt des composés organométalliques robustes, ciblant le récepteur des œstrogènes, est qu'on peut moduler leurs applications en fonction du métal introduit.

Pour la première fois, une entité organométallique stable et lipophilique, le groupement ferrocénique, a été substituée à la chaîne-clé aminée du squelette triphényléthylénique de l'antiœstrogène hydroxytamoxifène, tenue pour être responsable de l'activité du médicament. La chaîne amine des ferrocifènes a également été remplacée par une fonction acide carboxylique. Différentes variations structurelles ont été explorées, afin d'optimiser les propriétés biologiques de ces composés ferrocéniques, qui peuvent être cytotoxiques.

Cependant certains de ces composés ont non seulement une activité antiproliférative, mais peuvent aussi servir de précurseurs stables pour la synthèse de radiopharmaceutiques. Il est en effet possible de remplacer le Fer par le Rhénium ou le Technétium suivant une réaction d'échange de ligands, qui est chimiosélective. Les composés organométalliques résultants peuvent être de bons agents ciblés pour la radiothérapie (^{188}Re) ou pour l'imagerie médicale (^{99m}Tc).

Finalement, afin d'améliorer leur biodisponibilité, deux composés ferrocéniques ont été incorporés dans deux types de nanovecteurs: les nanosphères et les nanocapsules. Leur petite taille et la libération tardive des principes actifs, associés à une activité apoptotique exacerbée sont en accord avec une persistance accrue dans la circulation sanguine, et une activité anticancéreuse prometteuse.

Mots-clés : ferrocène, SERM, tamoxifène, cancer du sein, chimie bioorganométallique, radiopharmaceutiques, technétium, rhénium, nanoparticules, encapsulation

Abstract

Since breast cancer is still a leading cause of cancer death among women, improvements in diagnosis and therapy for this disease have to be explored more than ever. Using robust organometallic compounds and targeting them to the estrogen receptor, enables us to broaden their applications by choosing the appropriate metal.

For the first time were described compounds where the key amino side-chain of hydroxytamoxifen has been replaced by a lipophilic and stable organometallic entity, a ferrocenyl moiety. This amino side-chain was deemed essential for the anti-estrogenic activity. Additionally, the amino side-chain of the ferrocifens was also substituted by a carboxylate group. Various parameters were tested to optimise the biological activity of the ferrocenyl compounds.

The versatility of some of the ferrocenyl derivatives synthetized lies in their ability to be both a potential drug and a stable precursor for the synthesis of radiopharmaceuticals. The compounds were successfully labeled by a double ligand exchange reaction with Re and Tc, which proved to be chemioselective. These high affinity organometallic compounds could be potential site-specific radiotherapeutic (^{188}Re derivatives) or radioimaging (^{99m}Tc derivatives) agents.

Finally, in order to improve their bioavailability, the two most interesting organometallic tamoxifen-like compounds were incorporated in two types of stealth nanoparticles: nanospheres and nanocapsules. An efficient anticancer organometallic triphenylethylene-loaded nanosystem has been developed for the first time. Their small size and delayed drug release, combined with their enhanced apoptotic potential, are compatible with an increased persistence in the blood and a promising antitumour activity.

Keywords: ferrocene, SERM, tamoxifen, breast cancer, bioorganometallic chemistry, radiopharmaceuticals, technetium, rhenium, nanoparticles, encapsulation

Remerciements

Cette thèse a été réalisée au sein du laboratoire de Chimie et Biochimie des Complexes Moléculaires (UMR7576), dirigé par le Professeur Gérard JAOUEN. Je tiens à lui exprimer mes plus sincères remerciements pour m'avoir acceptée dans son laboratoire et toute ma reconnaissance pour la formation qui m'a été dispensée. En plus de sa grande disponibilité et de son implication personnelle dans mon projet de thèse, il a aussi ouvert mon horizon en me donnant la possibilité d'établir deux collaborations réussies. Sa confiance en mes capacités et ses encouragements pendant des moments difficiles m'ont été d'un grand secours. Mes remerciements vont également à Monsieur Siden TOP qui m'a guidée et soutenue au jour le jour. Sa ténacité (surtout concernant le dérivé rhénié) et son expertise en chimie organométallique m'ont aidé à surmonter bien des obstacles. Je remercie sincèrement Madame Anne Vessières d'avoir non seulement veillé aux tests biologiques de tous mes composés, mais aussi à la rigueur des interprétations les concernant.

I would like to thank Prof. Roger ALBERTO and Prof. Nils METZLER-NOLTE for being part of my thesis committee, and for their time evaluating my research work.

Je voudrais également remercier le Professeur Giovanni POLI et Monsieur Jack-Michel RENOIR de m'avoir fait l'honneur de faire partie de mon jury de thèse.

I would like to say many thanks to Prof. ALBERTO and Dr. RENOIR for welcoming me in their groups, and for sharing their experience in radiopharmaceutics and nanoparticles. My stays in their laboratories were great experiences, both scientifically and personnally.

Un grand merci à deux personnes en particulier qui m'ont énormément aidé tout le long de mon travail de thèse: Pascal PIGEON (en synthèse) et Elizabeth HILLARD (en électrochimie et résolution de structure R-X).

Merci Pascal pour m'avoir accueillie à mon arrivée, pour ton aide en synthèse durant toute ma thèse (pardon d'avoir parfois tardé à rendre tes produits), et pour avoir relu mes parties expérimentales (le plus pénible).

Thank you Elizabeth for your kind involvement in my thesis training. You were always ready to give me a hand and your valuable remarks were terribly useful for my manuscripts. Your help and friendship meant a lot to me.

Je remercie Monsieur Michel HUCHE pour son travail en modélisation moléculaire. Ses résultats ont apporté quelques éléments de réponse aux comportements biologiques de mes composés.

Mes remerciements vont à l'ensemble des membres du laboratoire du Professeur JAOUEN et en particulier à Emilie BRULE, Julia HEILMANN et Barisa TALBI. Merci à Emilie d'avoir lu ma thèse, même en avion. Merci Barisa pour m'avoir remplacée maintes fois au passeur. Et merci Julia pour m'avoir supportée et aidée durant ma dernière année de thèse, en tant que voisine de paillasse et de bureau. Cela a été un vrai plaisir de travailler avec toi. Je pense aussi aux bons moments (musicaux *et al.*) avec Benoît FERBER, mon autre voisin de paillasse durant ma première année de thèse. Je garderai en mémoire l'efficacité et la gentillesse de Nathalie, notre secrétaire de choc, qui a dû parfois supporter des odeurs pas toujours agréables venant de ma paillasse.

Je n'oublie certainement pas les techniciennes de la partie bio, Annie CORDAVILLE et Marie-Aude PLAMONT, qui ont testé mes composés. Désolée Marie-Aude de t'avoir parfois un peu harcelée pour avoir au plus vite les résultats biologiques de mes composés.

J'ai une pensée chaleureuse pour Marie-Noëlle RAGER et Lauriane JUGE (du service de RMN), ainsi que pour Claudine FLEURANT et Delphine FOSSE (du service de masse), qui m'ont toutes aidée à analyser mes produits.

Je remercie les membres des laboratoires du Professeur ALBERTO et de Monsieur RENOIR de m'avoir apporté leur aide durant mes collaborations. Je voudrais témoigner ma reconnaissance à Monsieur Philippe LEGRAND de m'avoir guidé dans les méandres des paramètres physico-chimiques des nanoparticules. Je pense également à Lukas KROMER (thanks for showing me how to handle radioactive technetium!), Véronique MARSAUD et Céline BOUCLIER (pour la culture de cellules).

Finalement, je voudrais remercier ma famille et Pierre-Jean de m'avoir soutenue durant ces longues années de thèse, malgré leur impatience à me voir terminer.

I would like to conclude my aknowledgements by thanking the COST (European Co-Operation in the field of Scientific and Technical research) for financing my stays in Zürich, to work with Prof. ALBERTO.

Je remercie également la Société Française de Chimie et l'Association Lapervenchelif (Institut de Chimie des Substances Naturelles, Gif-sur-Yvette) pour avoir financé ma participation à deux congrès internationaux: le "European Chemistry Congress" (Budapest, Hongrie) et le "International Conference on Organometallic Chemistry" (Saragosse, Espagne).

Contents

Chapter 1

Overview of diagnosis techniques and treatments of breast cancer

Breast cancer is a malignant growth that begins in the tissue of the breast, usually the ducts and lobules. It occurs in both men and women although male breast cancer is rare (<1% all breast cancer cases) [1]. Dated from the XVIIth century BC, an Egyptian papyrus (the Edwin Smith Papyrus) contains the first accounts of tumours in the breast [2]. Its dooming verdict was: "There is no treatment". Later surgeons recommended excising the tumour, or even the entire breast. The VIth century Byzantine empress Theodora chose to die in pain rather than lose her breast.

Despite progress made in preventing, detecting, diagnosing and treating this disease beyond surgical disfiguration, it still elicits many fears, including those relating to surgery, death, loss of body image and loss of sexuality. This chapter provides some information about diagnosis methods and available treatments for breast cancer, and on how they could be improved by the use of organometallic compounds.

1.1 What is breast cancer?

1.1.1 Facts and figures

Breast cancer is the leading cause of cancer death among women in France (Fig. 1-1) [3], while in the US it has been only surpassed by lung cancer since the 1980s (Fig. 1-2) [4]. Breast cancer accounts for 23% of all female cancer cases worldwide [3]. Nearly one in three cancers diagnosed in US women is for breast cancer, according to the American Cancer Society [1]. Each year, about 42 000 new cases are expected to occur in France, 270 000 cases in the US, and more than 1 million in the world. Approximately 11 000 women are expected to die from breast cancer in France annually, 40 000 in the US, and ten times more in the world. In terms of incidence rate, breast cancer touches one woman in eight in the Western World.

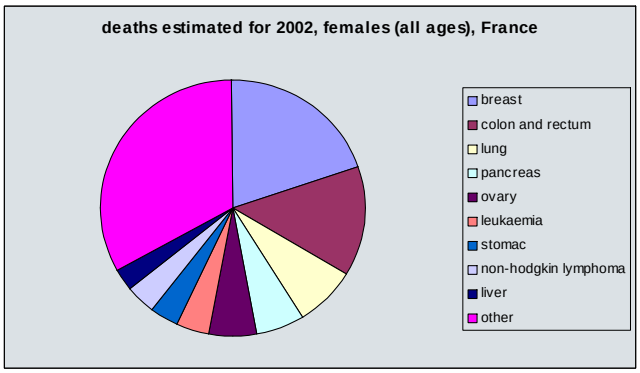

Figure 1-1: Cancer death rates among females in France, estimated for 2002, from GLOBOCAN 2002

1.1.2 Diagnosis

If a physical examination by a medical doctor suggests the presence of a breast tumour, additional tests may be made to confirm and describe more accurately the diagnosis: [1, 5, 6]

- X-ray mammography to identify the breast mass
- Sonogram (ultrasound) to determine whether the lump is solid or fluid-filled
- Needle aspiration or needle biopsy of breast lumps for confirmation of malignancy and a better analysis in case of a fluid-filled tumour
- Surgical biopsy for laboratory study

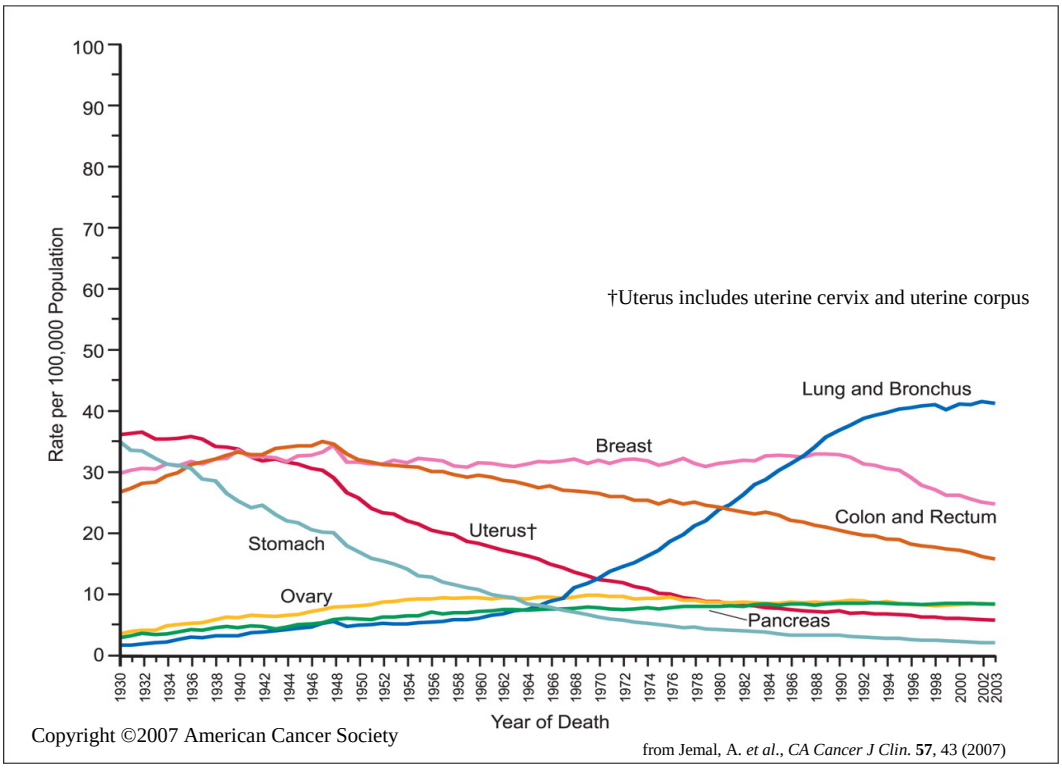

Figure 1-2: Cancer death rates among females for selected cancers, US, 1930 to 2003 (rates are age-adjusted to the 2000 US standard population)

On the average, mammography helps to detect about 80-90% of breast cancers in women without symptoms. This low dose X-ray procedure allows accurate visualization of the internal structure of the breast. But it is neither sensitive nor specific enough to be free of false-positive (suggests disease when there is none) and false-negative (fails to detect a malignant lesion) results. According to a study led by Smith-Bindman *et al.,* the mean sensitivity is 77% and the mean false-positive rate is 10% [7]. In the best scenario, about 30% of cancers will be missed. These limitations, mainly because of high breast density and fast tumour growth rate [8], have led to a highly litigious climate of malpractice lawsuits [9, 10].

Since mammography relies on anatomical differences between normal and cancerous tissues, it does not provide specific information about the molecular changes at the cellular level. Detection using probes that differentiate normal from cancerous cells at the molecular level could provide more specific and accurate information. Methods such as PET (Positron Emission Tomogaphy), SPECT (Single Photon Emission Computed Tomogaphy), and MRI (Magnetic Resonance Imaging) offer functional imaging, and therefore have gained increased importance in breast cancer detection [11–15].

1.1.3 Types of breast cancer

Although most breast abnormalities are benign, two main types of breast cancers are distinguished.

- *In situ* breast cancers are still confined within the ducts (ductal carcinoma) or lobules (lobular carcinoma) of the breast, and have not yet spread beyond the area where they originated. Nearly all cancers at this stage can be cured.

- Other breast tumours are called invasive or infiltrating. Starting in the ducts or the lobules of the breast, they have invaded the surrounding fatty tissue of the breast. When they have spread to other organs, they are called distant metastases.

In the late 1890s, evidence was found that the ovaries were involved in breast carcinoma and that their removal was beneficial to the patient [16]. Oophorectomy caused tumour regression in approximately one-third of premenopausal women with metastatic breast cancer. It was only then that the role of hormones in stimulating the growth of certain malignancies in breast cancer began to be recognized. However, their mechanism of action on the target cells was not understood until Jensen *et al.* characterized the estrogen receptor in the early sixties [17, 18].

It has been found that the female hormone estradiol plays a critical role in controlling the female reproductive system. One of its many functions is to regulate the proliferation and differentiation of the healthy breast epithelium. Thus it is not surprising that this molecule is involved in two-thirds of breast tumours. These hormone-dependent cancer cells exhibit a higher accumulation of specific intracellular receptor proteins, the α isoform of the estrogen receptor (ER) [19,20], and are traditionally classified as ER+. The hormone-independent breast tumours, which lack ERα, are called ER negative (ER-).

ER can also be found in another isoform: ERβ [21–23], discovered later. Both ERα and ERβ are transcription factors of the thyroid/steroid superfamily, which include receptors for androgens, progestins, glucocorticoids, and Vitamin D. [24]. ERα is predominantly found in breast, uterus and vagina, while ERβ is expressed in the central nervous system, cardiovascular system, immune system, gastrointestinal system, kidneys, lungs, bones and in limited amount in the breast. In addition to their expression pattern differences, they also differ slightly in their amino acid sequence. ERα and ERβ are highly homologous in their DNA-binding sequence ($\sim$97%), but they have only a moderate similarity in the ligand binding domain, or LBD, ($\sim$56%) [25–27].

1.1.4 Treatments: surgery, radiotherapy and chemotherapy

As stated above, most women with breast cancer will undergo some type of surgical excision, often combined with other treatments such as radiation therapy, chemotherapy, hormone therapy, and very recently biology therapy [1]. Surgery is meant to remove the tumour from the breast and lymph nodes. It is almost always followed by radiotherapy. In this procedure, high powered X-rays or gamma-rays should destroy remaining breast cancer cells. Radiotherapy helps to reduce the chance of cancer recurrence, but is less effective in prolonging patient survival. Since the radiation destroys normal cells as well as cancer cells within the treated area, the patient may experience red and itchy skin and sore throat. However, the normal healthy cells should be able to repair themselves afterwards, unlike the cancer cells and the side-effects should be temporary. Biology therapy refers to the treatment with Herceptin®, a monoclonal antibody, for patients overexpressing a specific "protein" (HER2) [28, 29].

In the case of ER- breast tumours, chemotherapy is then often prescribed to kill cancer cells that could not be removed by other means, or that may have already invaded other parts of the body. It has been established that a combination of drugs is more effective than just

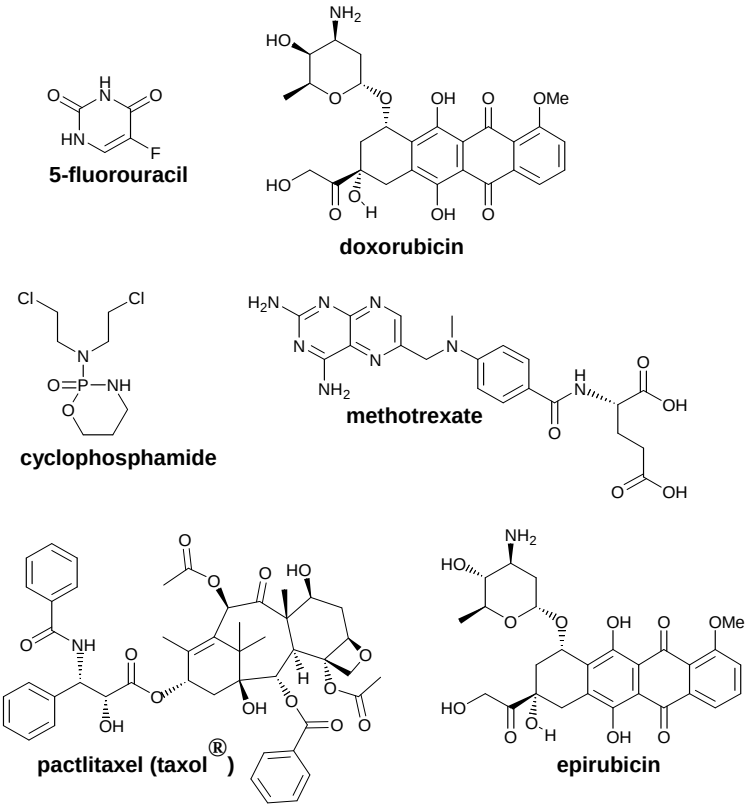

Figure 1-3: Molecules used in chemotherapy (ER- breast cancer cases)

one drug alone for breast cancer treatment. The first-line therapies are usually a combination of 5-fluorouracil, doxorubicin (adriamycin®), cyclophosphamide, methotrexate, paclitaxel (taxol®), and epirubicin (Fig. 1-3) [30].

The molecules used in chemotherapy are highly cytotoxic, and can reduce mortality by up to 20% [31]. They affect cell division, and hence are very effective on fast-dividing cells such as tumour cells. But, this also means that fast-dividing cells such as those involved in hair growth, in the replacement of the intestinal epithelium, or in the production of white blood cells are also affected. The physical drawbacks include nausea, fatigue, nerve damage, anemia, hair loss, and a weaker resistance to infections.

The finding of the hormone responsiveness of ER+ breast cancer cases triggered development of antiestrogens, molecules which could compete with estradiol at its receptor and counterbalance its proliferative action. Thus, for the patients with ER+ tumours, an adjuvant treatment with antiestrogens [27, 32–35], or more recently with aromatase inhibitors, are currently available for their treatment [36,37]. This hormone therapy appears as a simple and safer

alternative to ablative surgery and to undiscriminating radio- and chemotherapy for patients having hormone-dependent breast cancer [27, 32, 38, 39].

1.2 Ligand-receptor relationship and hormone therapy

In the hormone induced pathway, when the natural ligand estradiol (E_2) binds to its intranuclear receptor, it induces a typical conformational change in the protein structure, involving Helix 12 [27, 40]. This enables the recruitment of co-activators and the dimerization of ERα and/or ERβ [24]. The homo/hetero-dimer can then bind to small palindromic ERE (Estradiol Response Element) sequences of DNA. The interaction allows the recruitment of transcriptional factors from the general transcription machinery around Polymerase II, and thus initiates gene transcription and specific protein synthesis leading finally to cell proliferation (Fig. 1-4) [41]. Therefore, in ER+ tumours, the increased concentration of estrogen receptors is associated with cell multiplication.

Transcription can also be regulated by estrogens through another pathway, the indirect AP-1 pathway. In this mechanism, the activated estrogen receptor associates with co-activator proteins (in particular the dimer jun/fos), and not directly with DNA. These co-activators then bind to another region of DNA (the AP-1 site), and enhance transcription activity [42, 43].

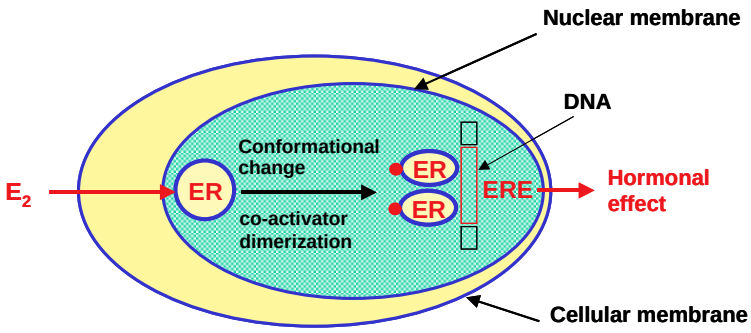

Figure 1-4: A proposed scheme for estradiol action on ER+ cells [41]

Since the binding of estradiol to its receptor promotes breast cancer cell proliferation (in the ER+ tumours), many molecules targeting this protein have been synthesized to counteract the estradiol action. Having no uterotrophic activity, the first non-steroidal antiestrogen was etamoxytriphetol **MER 25** (Fig. 1-5), discovered in 1958 by Lerner et *al.* [44]. Unfortunately, its very low affinity for ER, low potency and severe central nervous system (CNS) side-effects

hindered further development [27,32,39,45]. It was quickly discovered that to be able to compete with the natural hormone, the key feature lies in the presence of a phenol group analogous to phenol A of estradiol [46, 47], which is lacking in **MER 25**. Consequently, the structures of the synthetic anti-estrogens are mainly derived from known ligands, such as steroids or from diphenyl ethylene estrogens (like diethylstilbestrol, in Fig. 1-5).

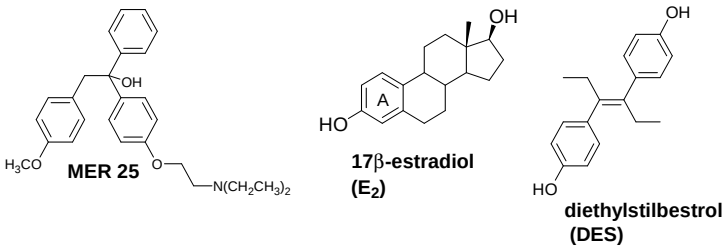

Figure 1-5: **MER 25** and the natural (E_2) and synthetic (DES) ligands of the estrogen receptor

1.2.1 Pure antiestrogens

To be a pure antiestrogen, the molecule must have an unique mechanism of action, independent of the cellular context. It should prevent the formation of a transcription complex at target genes, and/or enhance the ability of the ER complex to be destroyed, once the ligand is bound to the receptor. The steroidal pure antiestrogen ICI 182 780 (fulvestrant, Fig. 1-6) was one of the most effective in this series [32]. Prepared in the 1990s, it was approved by the FDA (Food and Drug Administration) in 2000 as a second-line drug (Faslodex®) for the treatment of advanced breast cancer [48, 49]. Its success stimulated the search for other potential agents, such as RU 58 668 (Fig. 1-6) [50]. This pure antiestrogen blocks ER nuclear localization, since it induces a protein synthesis-dependent clustering of ER in the cytoplasm. It has been proposed that the long hydrophobic side-chain of these antiestrogens significantly disrupts the ER protein structure. This results in cytoplasmic paralysis and rapid destruction of the ER.

Apart from the increased risks of osteoporosis and coronary heart disease, the other main problem associated with the pure antiestrogens described so far is bioavailibility and the route of administration. The steroidal molecules are highly hydrophobic, thus excluding oral administration. Patients have to pay monthly visits to the hospital, in order to receive a fulvestrant slow-release depot injection. This mode of administration may be considered highly inconvenient and could be improved.

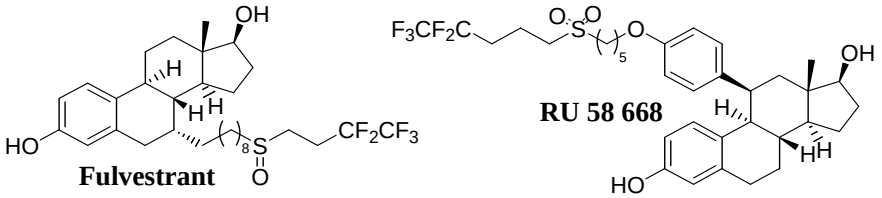

Figure 1-6: Some pure antiestrogens

In order to ameliorate the bioavailibility of RU 58 668, Renoir *et al.* have proposed an efficient drug delivery nanosystem for the antiestrogen. The long circulating, stealth drug carriers are polymeric nanoparticules, which are loaded with the bioactive compound. The ability of the molecule to arrest tumour growth has been strongly enhanced *in vitro* and *in vivo*, thanks to this encapsulation [51, 52].

1.2.2 SERMs

In the search for better estradiol antagonists, researchers noticed that some antiestrogens showed partial estrogen agonist activity, depending on the target tissue. These selective estrogen receptor modulators (SERMs) display an unusual tissue-selective pharmacology: agonists in some tissues (bone, liver, cardiovascular system), antagonists in others (brain, breast), and mixed agonists/antagonists in the uterus. The hope is that they would act as antiestrogens in the breast and uterus where they could limit estrogenic proliferative effects, but that they would retain estrogenic benefits for bones and the heart. The huge libraries of hormonal SERMs include families of triphenylethylenes (TPE), benzothiophenes, and indenes [27, 32, 38, 39].

Triphenylethylenes

Most SERMs share the stilbene-type common structural pattern of two aryl groups separated by two atoms (Fig. 1-5). The most popular and widely prescribed SERM for hormone-dependent breast cancer is tamoxifen (Novaldex®). The molecule possesses an additional phenyl group, and thus belongs to the triphenylethylene family. Its active metabolite, hydroxytamoxifen (OH-Tam), acts as an antagonist to estradiol in breast tumours (Fig. 1-7) [33].

The dimethylaminoethoxy side chain interaction with Asp351 of the binding site of the ER is held responsible for the observed antiestrogenic effect of hydroxytamoxifen [45,53,54]. This side-chain induces Helix 12 to undergo a conformational change different from that observed with

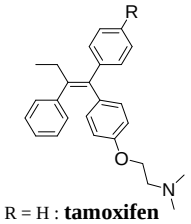

R = H : **tamoxifen**
R = OH : **4-hydroxytamoxifen or OH-Tam**

Figure 1-7: Tamoxifen and its active metabolite

estradiol (Fig. 1-8). This prevents the recruitment of co-activators, and favours the binding of co-repressors instead. However, depending on the nature of the gene promoter to which hydroxytamoxifen binds and the cellular context (e.g. the major type of ER (α or β) present in the tissue and the co-activator/co-repressor ratio in the cell) this SERM can also act as an agonist. Thus, just like estradiol, OH-Tam can induce beneficial effects such as maintaining bone density, but unfortunately it also slightly enhances endometrial tumour growth.

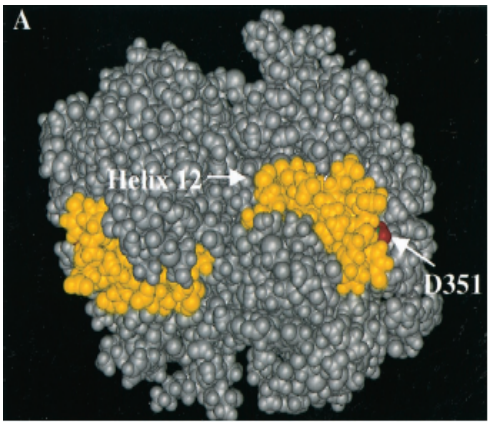

ERα liganded with 17β-estradiol | ERα liganded with OH-Tam

Figure 1-8: E_2 and OH-Tam docked in dimerized ERα
External surface of the ERα ligand binding domain complex liganded with 17β-estradiol (A) and with 4-hydroxytamoxifen (B). Helix 12 (shown in yellow) seals the ligand into hydrophobic binding pocket to activate the coactivator binding site. Aspartate 351 (Asp 351 or D351) interacts with the underside of Helix 12. Its carbon and oxygen atoms are in green and red, respectively; the remaining ER residues are in gray. OH-Tam side-chain atoms are shown in blue. [55]

The tamoxifen analogue **GW5638** (Fig. 1-9), discovered by Willson *et al.* at Glaxo Wellcome in 1994, presents the interesting feature of changing the usual tertiary amino antiestrogenic

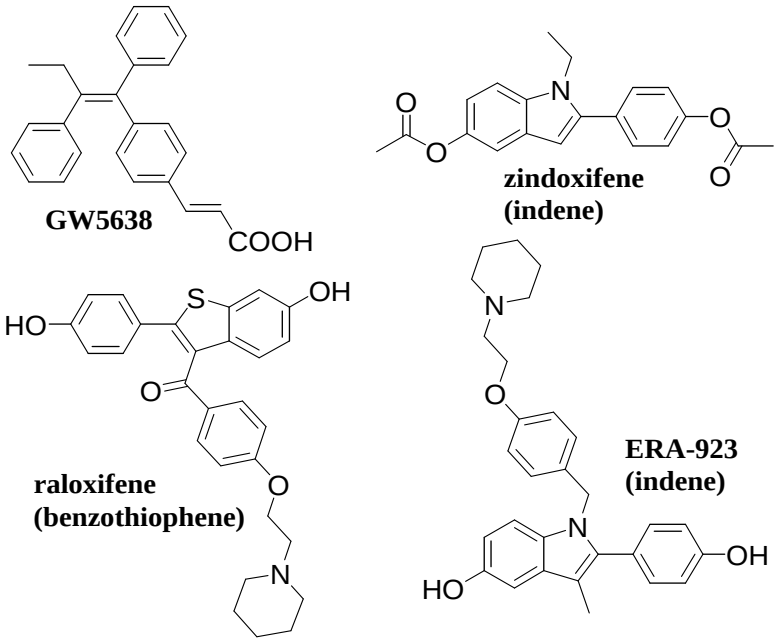

Figure 1-9: Chemical structures of some SERMs

side-chain of tamoxifen to an allylcarboxylic group [56, 57]. Ligand-receptor structure studies disclosed that the carboxylate side-chain has an unusual interaction with Asp351 of ER LBD, and therefore produces a subtle, but significant change in protein folding [58, 59]. The change in coregulator binding classifies this molecule as a new SERM, which could even reduce ER levels and has no uterotropic activity.

Other SERMs

Raloxifene is a benzothiophene SERM (Fig. 1-9). Like tamoxifen, it acts as an estrogen antagonist in breast tissue through competitive binding to ER. Formally known as LY 156,758 or keoxifene, it was first developed in the early 1980s as a breast cancer drug [60], along with tamoxifen. However, it performed poorly compared to tamoxifen in laboratory models and in tamoxifen-resistant patients. No further development followed, until its ability to maintain bone density in postmenopausal women was recognized, resulting in the approval of raloxifene for the treatment and prevention of osteoporosis (drug Evista®) [45].

Early studies of 2-hydroxyphenylindoles by von Angerer [61, 62] demonstrated their antitumour activity. Although zindoxifene (Fig. 1-9) looked promising, it proved to be an inactive antitumour agent in phase II clinical trials. However, deacetylation and substitution of the indole

nitrogen with long aminoalkyl side-chains gave birth to potent antiestrogens (e.g. ERA-923 in Fig. 1-9), which are currently in phase II clinical trials for the treatment of hormone-dependent breast cancer [63].

Problems of resistance

Unfortunately, the successful treatment of breast cancer by hydroxytamoxifen is also overshadowed by the fact that a third of hormone-dependent breast tumours do not respond to endocrine therapy, and some of those that initially respond to antihormonal treatment acquire resistance in the long term [35, 64, 65]. To those cases of intrinsic and acquired resistance, the class of insensitive ER- tumour cells have to be added to point out the limitation of hydroxytamoxifen. These cases highlight the dire need for new active molecules with broader therapeutic scope.

1.3 Development of metal-based bioactive molecules

Metals are often considered as toxic for living systems. However, any toxicity of metal ions depends on their actual concentration present in the organism, because "*allein die Dosis macht das ein Ding kein Gift ist*",* as already stated by Paracelsus in the Renaissance. In fact, many metal-based proteins, such as nitrogenase and the class of cytochrome oxidase enzymes, are required in important biological processes. Furthermore, some metal containing molecules are necessary for life, such as cobalt-containing Vitamin B_{12}, where early signs of its deficiency include anemia and macrocytosis. Vitamin B_{12}, its coenzyme B_{12}, and methylcobalamin were the first natural compounds with a carbon-metal bond to be described. Thanks to their role in biology, the use of metals in medicine could hold great promise [66].

The first successful bioactive organometallic compound was the famous anti-syphilis drug Salvarsan, discovered by Paul Ehrlich, who introduced at the same time the notion of receptors and chemotherapy ("magic bullets"). By the end of the twentieth century, another major breakthrough renewed interest in biomedical metal-based chemistry. It was the discovery of the coordination metal complex *cis*-platin by Rosenberg [67–69]. This inorganic complex (**Pt-1**) showed highly toxic effects, especially on some cancer cells. This therapeutic advance came together with a better theoretical understanding and control of new types of metal bonds, which enabled the discovery of a broad range of new complexes [70]. This is particularly important as

**only the dose determines a thing not to be a poison*, in "Sieben Defensiones, Verantwortung über etliche Verunglimpfungen seiner Mißgönner" or "Seven defenses, the reply to certain calumniations of his enemies"

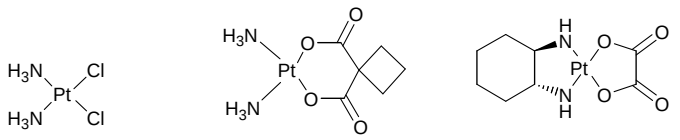

Pt-1 (*cis*-platin) **Pt-2** (carboplatin) **Pt-3** (oxaliplatin)

Figure 1-10: Platinum complexes used for cancer treatment

cis-platin possesses serious limitations such as a narrow therapeutic window and drug resistance problems [71]. It is worthwhile to note that *cis*-platin is *not* used for treatment of breast cancer, whereas it is widely prescribed for other types of cancer such as testes carcinoma.

Currently, two most widely used *cis*-platin analogues are carboplatin (Paraplatin®) and oxaliplatin (Eloxatin®), **Pt-2** and **Pt-3** (Fig. 1-10) [72]. The first drug is similar to *cis*-platin, in terms of activity, but has a lower systemic toxicity. The second one is a third generation drug. When associated with 5-fluorouracil, it is effective against some *cis*-platin-resistant cancers, such as metastatic colorectal cancer [73].

Many researchers consequently proposed a variety of complexes in which steroidal or non-steroidal ligands were attached to platinum, in order to add selectivity to the transport of Pt, to overcome the problem of resistance, and to smoothen undesirable side-effects observed in *cis*-platin therapy. Moreover, if the bioligand is an antiestrogen, this single drug could combine antiestrogenic and cytotoxic properties, and thus brings forth a new therapeutic spectrum.

1.3.1 Platinum complex SERMs

Due to their historical primacy, platinum complexes have been the first metal moieties to be coupled to estradiol [74–80], or later, to hydroxytamoxifen (Fig. 1-11) [81, 82]. Although **Pt-4** showed antiproliferative effects on breast cancer cells at high concentrations (around 5 μM), the effects are similar to those observed for the corresponding platinum complex alone, without the bioligand vector [74]. On the other hand, **Pt-5** did recognize the estrogen receptor (RBA = 6.4%), but its antiproliferative effects on MCF-7 breast cancer cells seemed to be mostly anti-hormonal, the Pt fragment showing only slight cytotoxicity on these cells [81]. Surprising biological behaviour was observed for cationic platinum estradiol complexes **Pt-6** and **Pt-7**. Compound **Pt-6** did show a cytostatic effect on MCF-7 breast cancer cell line at 5 μM, but direct hormonal activity of this complex seems unlikely [78]. An unprecedented higher binding affinity for the ER was noticed for the cationic complex **Pt-7** than for its metal-free ligand [79].

But more importantly, despite its cationic character, the compound was able to cross the cellular membrane. It seems that the hydrophobicity and size of the complex is more important than the charge.

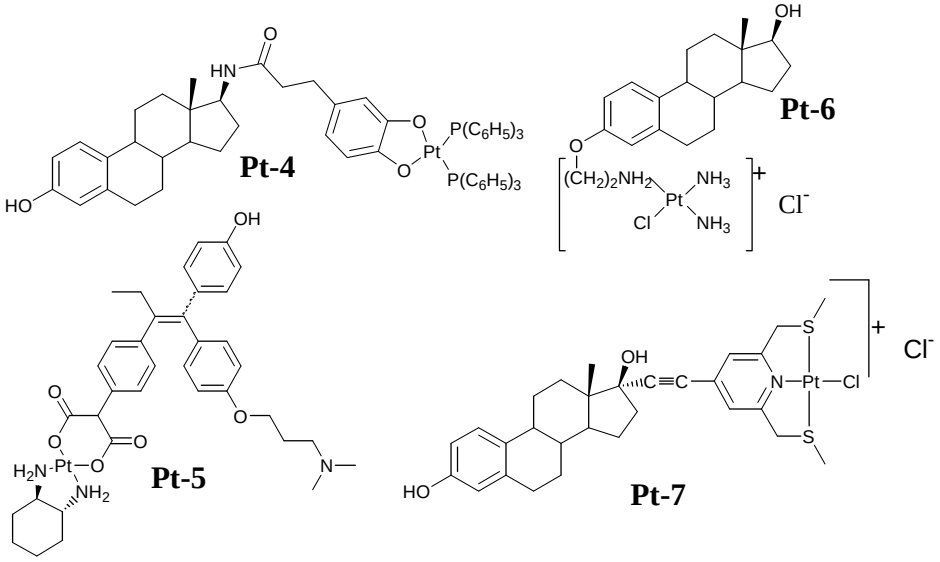

Figure 1-11: Platinum complexes for breast cancer

It should be mentioned that **Pt-4** to **Pt-7** are coordination compounds. The coordinating character of the metal-ligand bonds make these compounds susceptible to solvolysis. While the hydrolysis of the chloride ligands is necessary for the activity of *cis*-platin, in the case of biovector-platinum combinations, loss of the biovector may explain their lower (or even lost) biological potency in physiological media. Thus, other metal systems are sought.

1.3.2 Organometallic bioactive compounds

Organometallic chemistry refers to the chemistry of metal complexes bearing at least one metal-carbon bond. Organometallic compounds, having metal-ligand bonds with a strong covalent character, are often more stable than inorganic metal coordination complexes [83]. For instance, ferrocene has been thoroughly studied thanks to its robustness [84]. More generally, metallocenes are small, rigid, and lipophilic molecules which can easily cross cellular membranes. Therefore, the idea to use targeted organometallic bioligands for medical purposes naturally sprang to the mind of some researchers about 30 years ago. The sandwich structure formed by two cyclopentadienyl ligands in metallocenes resembles that of an aromatic nucleus,

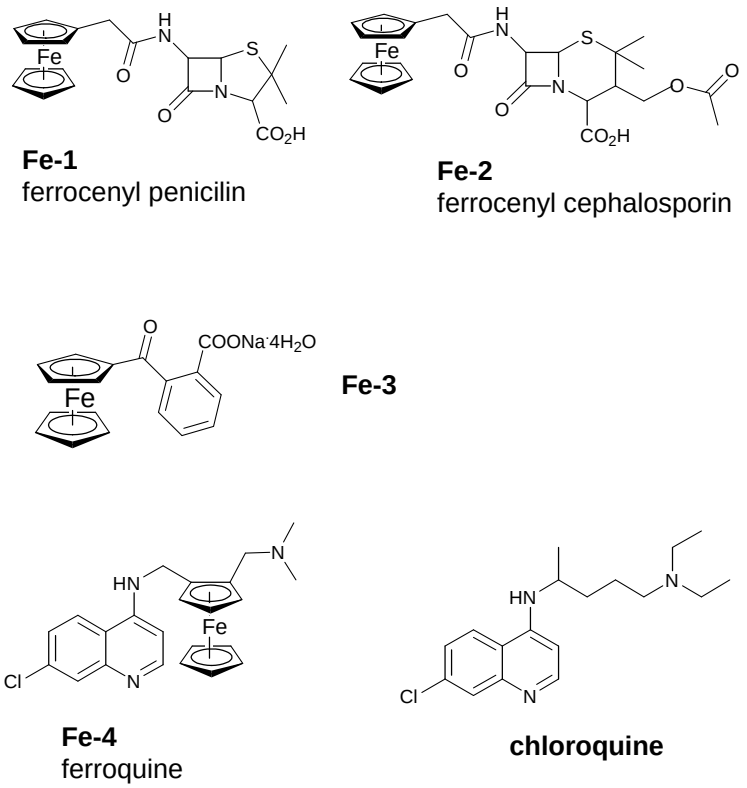

Figure 1-12: Some ferrocenyl derivatives with therapeutic applications

both in terms of geometry and aromatic properties. The relative stability of metallocenes in biological media is another argument to encourage their applications as tracers or vectorised bioactive compounds.

This approach was used by Edwards *et al.* in the 1970s to produce ferrocenyl antibiotics against penicillin resistant bacteria (**Fe-1** and **Fe-2** in Fig. 1-12) [85, 86]. *In vivo* toxicology studies on ferrocene derivatives disclosed low levels of toxicity, despite liver-related problems. Developed in the former USSR for the treatment of iron-deficiency anemia, a sodium salt of *o*-carboxybenzoyl ferrocene (**Fe-3**) is well tolerated for oral administration, and can also be prescribed for gum diseases [87]. The idea to modify the structure of organic bioactive compounds was taken up by Brocard *et al.* to produce ferroquine in 1997 (**Fe-4**) [88, 89]. This compound is a ferrocenyl analogue of chloroquine, a well-known antimalarial drug (Fig. 1-12). Thanks to the additional ferrocenyl moiety (Fc or -$C_{10}H_9Fe$), ferroquine is not only active against chloroquine-sensitive bacteria, but also against chloroquine-resistant strains. The active molecule is now in phase II clinical development by Sanofi-Aventis.

1.3.3 Hydroxyferrocifens

In 1996, a little earlier than the advent of ferroquine, Jaouen *et al.* published a paper on the coupling of the ferrocene functionality to an antiestrogenic vector [90, 91]. The resulting "hydroxyferrocifens" (differentiated by the length of the dimethyl amino chain, n = 2-5, 8) were designed to combine the antiestrogenic properties of tamoxifen with the potentially cytotoxic effect of ferrocene to possibly reach new therapeutic advantages [92–94]. To create the hydroxyferrocifens, a phenyl group of 4-hydroxytamoxifen is replaced by ferrocene. Since ferrocene is intrinsically aromatic, its presence in lieu of the phenyl group should not cause serious deterioration of recognition by the estrogen receptor. The most efficient synthetic path to substituted butenes relies on the key step of a McMurry cross-coupling reaction between a ferrocenyl ketone and the 4,4'-dihydroxybenzophenone (Fig. 1-13).

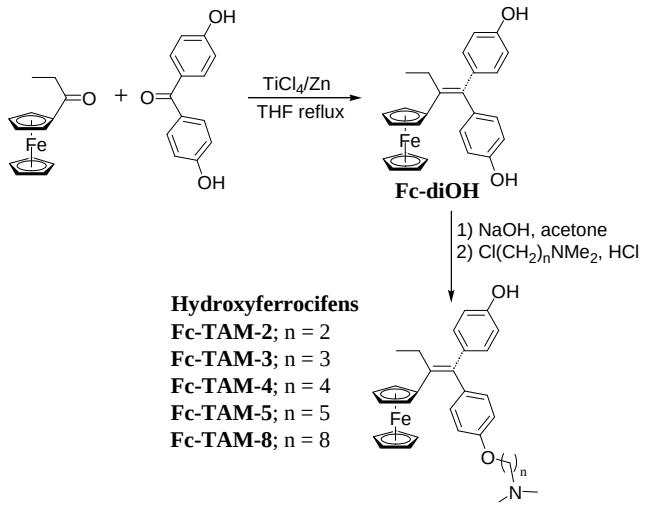

Figure 1-13: Synthetic pathway to hydroxytamoxifens

Although displaying less affinity for the estrogen receptor than hydroxytamoxifen, the hydroxyferrocifens were nonetheless satisfactorily recognised by the ER (n = 2 - 5). The values were lower probably because of the steric effect of the ferrocenyl group which is slightly bigger than the phenyl moiety. Also, the longer the amino side-chain, the lower the receptor affinity, because of steric reasons.

Antiproliferative activity of these ferrocenyl derivatives was evaluated on MCF-7 cells, which are hormone-dependent breast cancer cells having an important concentration of ERα, and on MDA-MB-231 cells, which are classified as hormone-independent breast cancer cells because

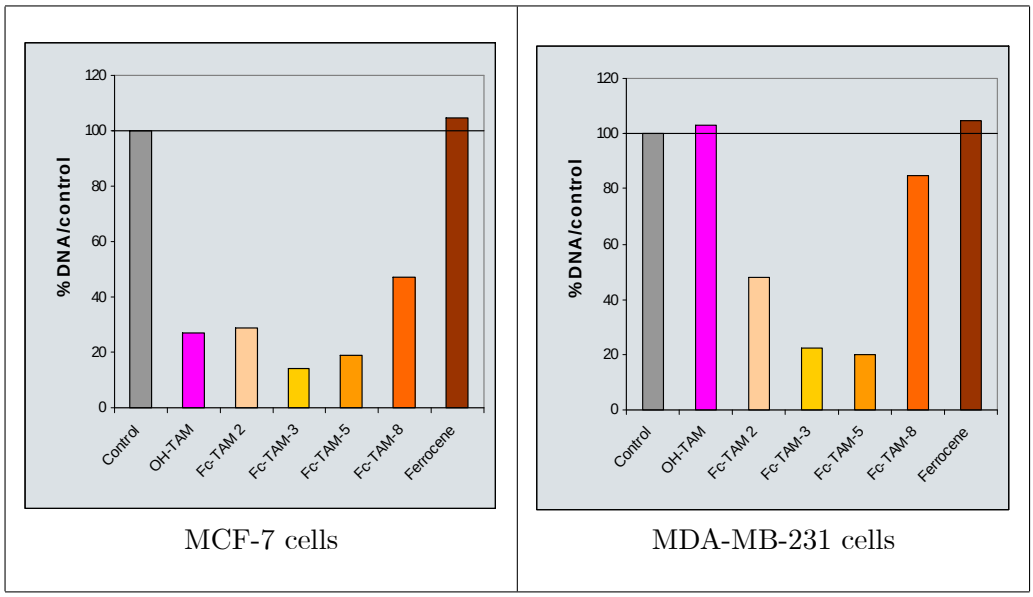

Figure 1-14: Antiproliferative effects of ferrocifens on MCF-7 and MDA-MB231 cells
The effects on breast cancer cells of 1μM hydroxyferrocifens (Fc-TAM-2 for n=2, Fc-TAM-3 for n=3, Fc-TAM-5 for n=5, Fc-TAM-8 for n=8), were compared to OH-Tam and ferrocene, after 6 days of culture.

devoid of ERα. It was found that on MCF-7 cells, the effects of hydroxyferrocifens are quite similar to that of hydroxytamoxifen, slightly more potent at a concentration of 0.1 μM, and definitely superior at 1 μM (Fig. 1-14).

Molecular modeling of **Fc-TAM-3**, the most potent compound of this series with an IC_{50} value of 0.5 μM [95], has confirmed that the molecule can be accommodated by the binding site of ERα in its antagonist configuration. The interaction between Asp 351 of ERα and the nitrogen of the amino side-chain, important for the antiproliferative activity of hydroxytamoxifen, provided the correct positioning of the organometallic molecule. This interaction supports the observation that the antiestrogenic effect is comparable to that of hydroxytamoxifen.

But the remarkable behavior of these compounds is with the MDA-MB-231 cells. While hydroxytamoxifen was completely inactive on the hormone-independent cells, the hydroxyferrocifens displayed a strong antiproliferative effect on the cells (Fig. 1-14). To understand this antiproliferative activity, two kinds of behavior could be put forward: one which is similar to the antiestrogenic role of hydroxytamoxifen on the estrogen receptor, and one which involves *in situ* activation of the ferrocenyl function. It is interesting to note that the organic compound hydroxytamoxifen is not effective on the hormone-independent MDA-MB-231 breast cancer cells, and that ferrocene alone has no cytotoxic effect [93]. However, by combining these two

entities, the hydroxytamoxifen and ferrocene, Jaouen *et al.* have created a new molecule which is strongly cytotoxic.

1.3.4 Target-specific Re and Tc radiopharmaceuticals

As pointed out earlier in this chapter, diagnosis and radiotherapy of breast cancer still need further improvements. The use of metallic radionuclides for medical imaging and radiotherapy is of particular interest because of their wide range of nuclear properties: type of radiation, γ ray or α/β particle energy, and half-life. Diagnostic radiopharmaceuticals provide simultaneous and non-invasive information on all tumour sites. They are molecules labeled with γ emitting isotopes such as ^{99m}Tc for SPECT or PET. On the contrary, therapeutic radiopharmaceuticals are molecules designed to deliver small doses of ionizing radiation (such as β particles with ^{186}Re and ^{188}Re) to specific diseased sites. Systemic administration of site-targeted therapeutic radiopharmaceuticals provides the opportunity to treat widely disseminated diseases, even when the location of the cancerous foci is unknown. This treatment comes as a complementary procedure to conventional or external beam radiotherapy, which is not effective on secondary or metastatic cancer sites outside of the treatment area [96].

Both metals (Tc and Re) are interesting because they are inexpensively and readily available from ^{99}Mo/^{99m}Tc and ^{188}W/^{186}Re generators. Ever since the milestone created by the invention of the ^{99}Mo/^{99m}Tc generator by Brookhaven National Laboratory in 1959, potential ^{99m}Tc radiopharmaceuticals have been closely scrutinized [96–100]. One of the successful results is the robust organometallic cation ^{99m}Tc-Sestamibi $[^{99m}\text{Tc(MIBI)}_6]^+$ (Fig. 1-15), which has been routinely used as a myocardial perfusion imaging agent (Cardiolite®, DuPont) since 1990 [101]. However, it has been recently discovered to also be a good imaging agent for breast cancer, and thus has been (re-)branded as Miraluma® [14, 102, 103]. ^{18}F-FDG (2-[^{18}F] fluoro-2-deoxy glucose) with PET imaging for breast cancer is also available, and other ^{18}F PET imaging agents still attract investigation [104, 105]. However, in comparison to SPECT, the PET method gives similar accuracy, but is expensive, and its usefulness is limited by the longer operation time necessary to acquire images [106].

In search of radiopharmaceuticals with specific ER binding properties, Katzenellenbogen and co-workers have proposed many rhenium and technetium derivatives. However, those compounds failed to show a good enough affinity with the estrogen receptor and exhibited high level of non-specific binding, and/or low stability [99, 107, 108]. In contrast, Jaouen *et al.* have

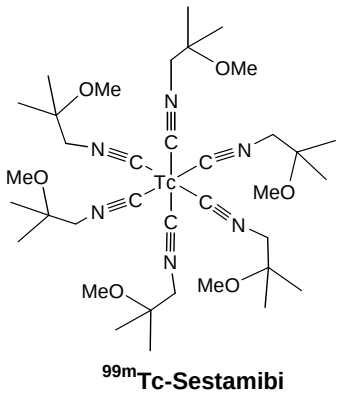

Figure 1-15: ^{99m}Tc-Sestamibi used as diagnostic radiopharmaceutical

found rhenium estradiol derivatives with high affinity with the receptor [109]. However, the synthetic route is not appropriate for routine clinical use in nuclear medecine. Indeed, the incorporation of the radionuclide must be introduced in the clinic, immediately prior to its use. Moreover, since the radiopharmaceuticals should not be active for too long in the patient's body, the half-life of the chosen radionuclide must be short, hence reducing the timeframe available for its manipulation. Therefore, its synthesis, ideally from a stable highly pure precursor, should be easy and rapid ("kit form"). Alberto *et al.* have proposed a water-stable and soluble ^{99m}Tc reagent $[^{99m}Tc(H_2O)_3(CO)_3]^+$, which can be prepared quantitatively (yield >98%) from a kit (Isolink®, Mallinckrodt Med B.V.). Since all three water molecules are very labile ligands, this technetium complex can be a convenient ^{99m}Tc source for the radiolabeling of biomolecules [110, 111].

1.4 Aim of the thesis

I have shown earlier that robust and lipophilic ferrocenyl moieties could bring forth interesting therapeutic applications. The aim of this thesis work is to develop new non-steroidal organometallic compounds for the diagnosis and treatment of breast cancer. With the same scaffold, according to the metal introduced, the organometallic compound could be used as a cytotoxic agent (Fe), a site-specific radiotherapeutic agent (^{186}Re and ^{188}Re), or an imaging agent (^{99m}Tc).

Always in the search of broader therapeutic scope, **Chapter 2** addresses the synthesis, characterization and biological assessment of new ferrocenyl derivatives of hydroxytamoxifen [112].

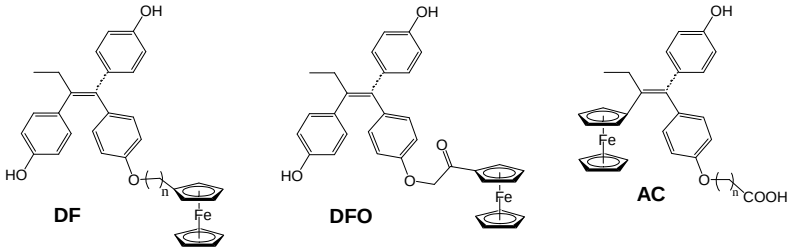

Figure 1-16: Ferrocenyl derivatives proposed for study

Since modification of substituents on the alkyl amine of the key side-chain -$O(CH_2)_2N(CH_3)_2$ has demonstrated the importance of the nitrogen atom for the antiestrogenic potency, only a few researchers have attempted to replace this functional group. The substitution of the key amino side-chain by a carboxylic acid moiety on the hydroxytamoxifen scaffold by both Willson's and Ruenitz's research groups has been the only important efficacious estrogen antagonist examples found so far [56, 113, 114]. In addition to the chemical alteration from a basic amino side-chain to a carboxylic acid side-chain, elongation of the chain length is also a crucial factor to observe a potent antiproliferative effect on hormone-dependent MCF-7 breast cancer cells. Bearing all these elements in mind, we have proposed to replace the amino side-chain of tamoxifen by a chain bearing the ferrocenyl group. Variations of the chemical structure such as the length of the new ferrocenyl side-chain and chemical function modifications were explored in order to test for their importance (**DF** and **DFO** in Fig. 1-16). Then, we extended the study by combining both the characteristics of the hydroxyferrocifens with those of the carboxylic acid antiestrogens. This resulted in a carboxylic ferrocenyl series, again, with a variable chain length (**AC** in Fig. 1-16). Finally, we evaluated their binding affinity with ERα and ERβ, and their ability to inhibit the proliferation of hormone-dependent breast cancer cells (MCF-7), hormone-independent breast cancer cells (MDA-MB-231), and prostate cancer cells (PC-3, devoid of ERα but with ERβ). In order to gain better insights on their biological behaviour, some electrochemical tests and molecular modelling studies were performed.

Chapter 3 tackles the issue of radiopharmaceuticals, for SPECT imaging (^{99m}Tc) or targeted radiotherapy (^{186}Re and ^{188}Re). Since the radioactive nuclide has to be incorporated easily and rapidly, this should be done at the very last step of the synthesis to produce the final radiopharmaceutical. Therefore, the appropriate ferrocenyl derivatives from those presented in **Chapter 2** could be used as stable precursors for rhenium and technetium analogues. The

non-radioactive rhenium derivatives were directly synthesized first, to evaluate their biological characteristics. Then the conversion of the ferrocenyl derivative into the non-radioactive rhenium counter-part was attempted, to test the success of the "double ligand transfer" reaction. Finally, since rhenium derivatives often serve as models for their technetium analogues, the transmetallation reaction was performed with technetium.

For the most promising antiproliferative agents, the problem of their bioavailibily is investigated in **Chapter 4**. Bioactive compounds, once introduced in the body, are often degraded and cleared from the bloodstream by macrophages of the reticulo-endothelial system. To prevent that, organometallic triphenylethylene compounds, with strong antiproliferative activity in breast cancer cells, but insoluble in biological fluids, were incorporated for the first time in two types of stealth nanoparticles: PEG/PLA nanospheres (NS) and nanocapsules (NC) (Fig. 1-17). Their physico-chemical parameters were measured (size, zeta potential, encapsulation and loading efficiency), and their biological activity assessed [115].

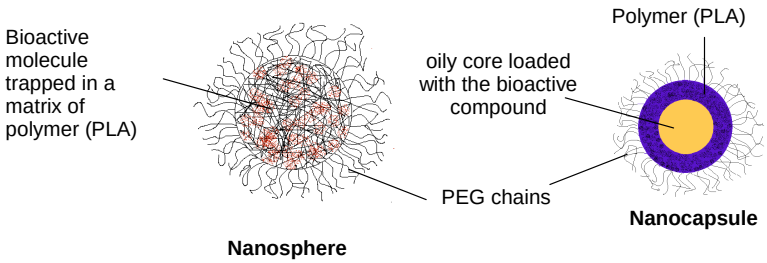

Figure 1-17: Structures of nanoparticles

The final part of this thesis summarizes the research described in this work. A general conclusion is given and future prospects of development in bioorganometallic chemistry applied to breast cancer are discussed.

Chapter 2

Effect of the amino side-chain replacement by a ferrocenyl unit in hydroxytamoxifen

The sandwich structure of orange crystalline ferrocene, Cp_2Fe, was uncovered simultaneously by Wilkinson and Woodward *et al.* and by Fischer *et al.* in 1952. In a metallocene, all the carbon atoms of the cyclopentadienyl ligands (Cp) are firmly bound to the metal, and the Cp ring is described as η^5-$C_5H_5^-$. Since all its bonding and non-bonding orbitals are exactly filled, ferrocene is the most stable compound in the metallocene series, particularly in various non-oxidizing media.

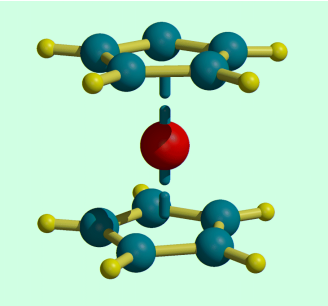

Figure 2-1: 3D representation of ferrocene, from the Crystallography Centre, NIU at Galway.

2.1 Molecule design

2.1.1 Tamoxifen analogues with modified amino side-chains

Widely prescribed for ER+ breast cancer cases [33], the SERM tamoxifen can behave as an estradiol antagonist or agonist depending on the cellular context. Thus, it appears that the tamoxifen-ER complex is not recognised similarly in all cells, suggesting that tamoxifen resistance and estrogen-like activity in some tissues are closely related to the ligand-ER structure [27, 32, 33, 45, 65]. The different conformational states of this complex are believed to modulate the cellular response, by regulating the interaction of ER with co-activators and co-repressors. Therefore, modifying the tamoxifen-ER structure may also lead to novel antiestrogenic properties, especially on tamoxifen-resistant cancer cells. Manipulation of the tamoxifen scaffold has been explored [27,32,38,39,116], but very few researchers have attempted to change the key side-chain -$O(CH_2)_2N(CH_3)_2$. Modification of substituents on the alkyl amine has always led to a decrease of antiestrogenicity, hence demonstrating the importance of the nitrogen atom [38,39,117–120]. Substitutions to diminish the basicity of the amine have been attempted, by replacing the alkylamino side-chain with N-oxides, quaternary salts, or by adding fluorinated tethers (Fig. 2-2) [118–120]. They always resulted in a weakened antiproliferative potency, because the ability of the nitrogen atom to form hydrogen bonds is reduced. In particular, when the interaction of the alkylamino chain of tamoxifen with Asp 351 of the ERα is diminished, the negative charge of the aspartate residue of the LBD is more exposed. Leclercq *et al.* postulated that the selective binding of co-activators may increase consequently, enhancing gene transcription, and thereby cell proliferation [55, 120].

The substitution of the amino side-chain by a carboxylic acid entity by Willson *et al.* and Ruenitz *et al.* has been the only important functional modification on the side-chain yielding strong antiestrogenic activity to date (Fig. 2-3) [56, 57, 59, 121, 122]. In particular, Ruenitz *et al.* noted that the elongation of the chain (to n=3) in **BA3** is crucial to observe a potent antiproliferative effect on hormone-dependent MCF-7 breast cancer cells [121]. Indeed the carboxylic acid may also interact with Asp 351 of ERα LBD as demonstrated with **GW7604**, and influence the antiproliferative activity of the carboxylic analogues of tamoxifen [58, 59]. A further reduced form, with an alcohol functionality, yielded molecule **BOH1**, which is in fact a minor metabolite of tamoxifen. However, it has a poor affinity with ER and weak antiestrogenic

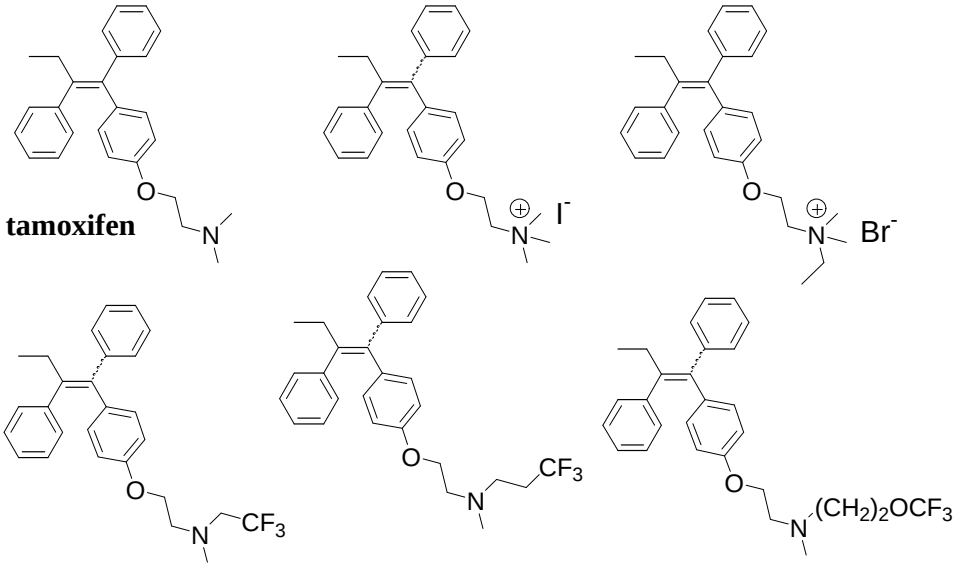

Figure 2-2: Tamoxifen analogues with various substituents on the amine

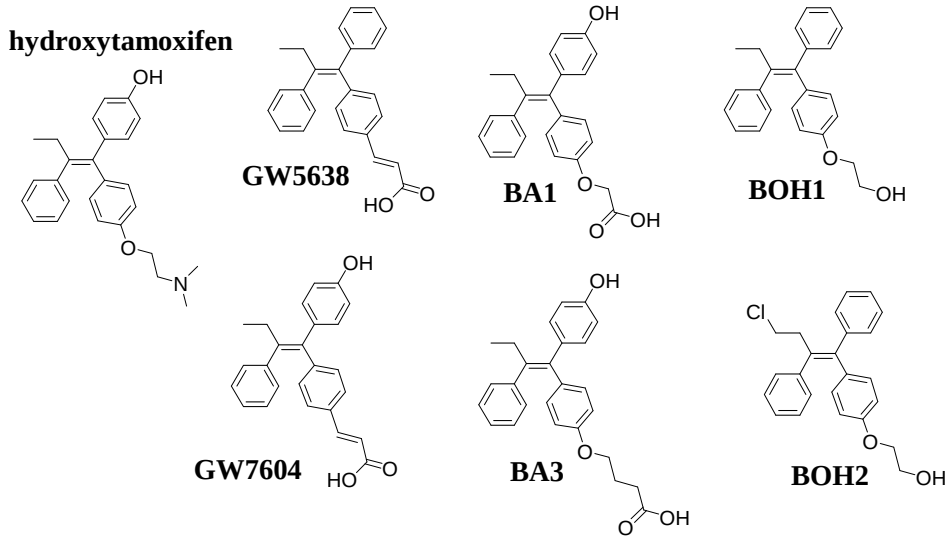

Figure 2-3: Carboxylic acid and alcohol analogues of tamoxifen

properties [123]. Only **BOH2**, a toremifene derivative, has additional benefits for the bones, and lowers cholesterol levels [124, 125].

2.1.2 Cytotoxicity of ferrocenyl derivatives

Although the anticancer potential of ferrocene derivatives had first been detected in the late 1970s, this field of investigation truly started after 1984, when Köpf-Meyer and Neuse disclosed the anti-tumour activity of ferrocenium salts (Fc^+) [126]. It has been proposed that ferrocenyl derivatives could be metabolically oxidized in the cell to ferrocenium salts, and that medicines bearing either Fc or Fc^+ could be responsible for anti-proliferative effects [127]. The Fenton pathway and DNA involvement have been suggested for their mechanism of action [128–130]. After the facile oxidation of ferrocene by the metabolism or ROS to the ferrocenium radical cation (Fenton reaction), the iron compound can catalyze the formation of $HO^\bullet$ (Haber-Weiss reaction). It has been shown that these radicals influence the apoptosis of cells and can damage the DNA [131].

Fenton reaction:
$$\begin{cases} Fe^{2+} + H_2O_2 \longrightarrow Fe^{3+} + HO^{\cdot} + HO^- \\ Fe^{3+} + O_2^{\cdot -} \longrightarrow Fe^{2+} + O_2 \end{cases}$$

Haber-Weiss reaction: $H_2O_2 + O_2{}^{\cdot -} \longrightarrow O_2 + HO^{\cdot} + HO^-$

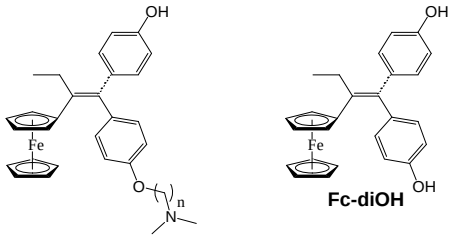

Figure 2-4: Series of hydroxyferrocifen

The series of hydroxyferrocifens (Fig. 2-4) have been designed to combine two properties: antiestogenic properties of the tamoxifen scaffold, and cytotoxic properties from the addition of the ferrocenyl group, thus resulting in compounds with a broad therapeutic spectra [93, 132]. However, one of the most promising compounds is **Fc-diOH**, which lacks the alkylamino side-chain (Fig. 2-4). It has a remarkable IC_{50} of 0.44 μM on MDA-MB-231 cells [133, 134]. Its

mechanism of action may involve the *in situ* generation of a quinone methide species, assisted by the ferrocenyl group via the "ferrocene-conjugated spacer-(*p*-phenol)" motif [133, 135].

Electrochemical experiments have suggested that the compounds possessing this structural motif can undergo two one-electron oxidations to yield a quinone methide-type structure [135]. Although it is well known that a variety of phenolic compounds, including hydroxytamoxifen [136], can be oxidized to the corresponding quinonoid, the presence of a ferrocene group seems to act as an oxidation catalyst, as shown in Figure 2-5. Fe(II) is oxidized, acidifying the proton, which could be easily abstracted by a base (e.g. pyridine). The abstraction appears to be coupled with electron transfer from the organic skeleton to the ferrocenium moiety. The resulting phenoxy radical species is stabilized by electron delocalization. This species is oxidized again, and after another proton abstraction from the ethyl group, a reactive quinone methide is produced. The reactive, electrophilic quinone methide species can then form adducts with DNA, GSH, or proteins [136–138]. The structure "ferrocene-conjugated spacer-phenol" is absolutely required for this mechanism, the π-system being necessary for electron delocalisation.

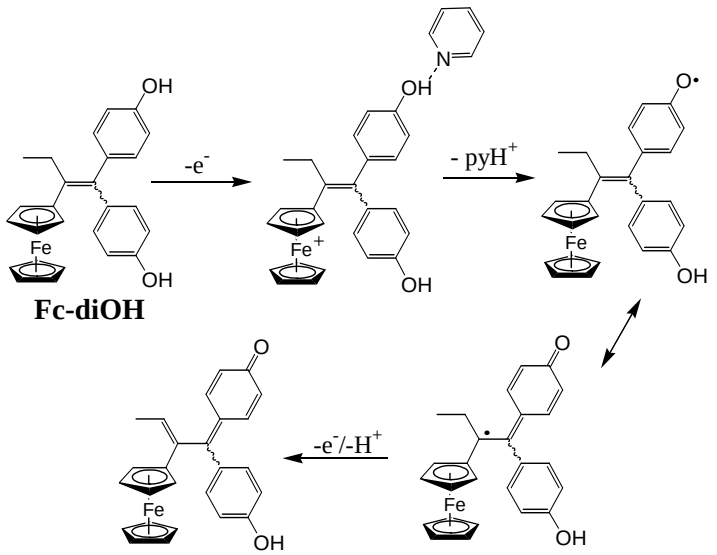

Figure 2-5: A proposed mechanism for the transformation of **Fc-diOH** into a quinone methide species

2.1.3 Amino side-chain replacement by a ferrocenyl moiety

In order to elucidate the mechanism of activity of ferrocenyl derivatives and to find new compounds with different activity, we have studied the **DF** series, which is characterized by

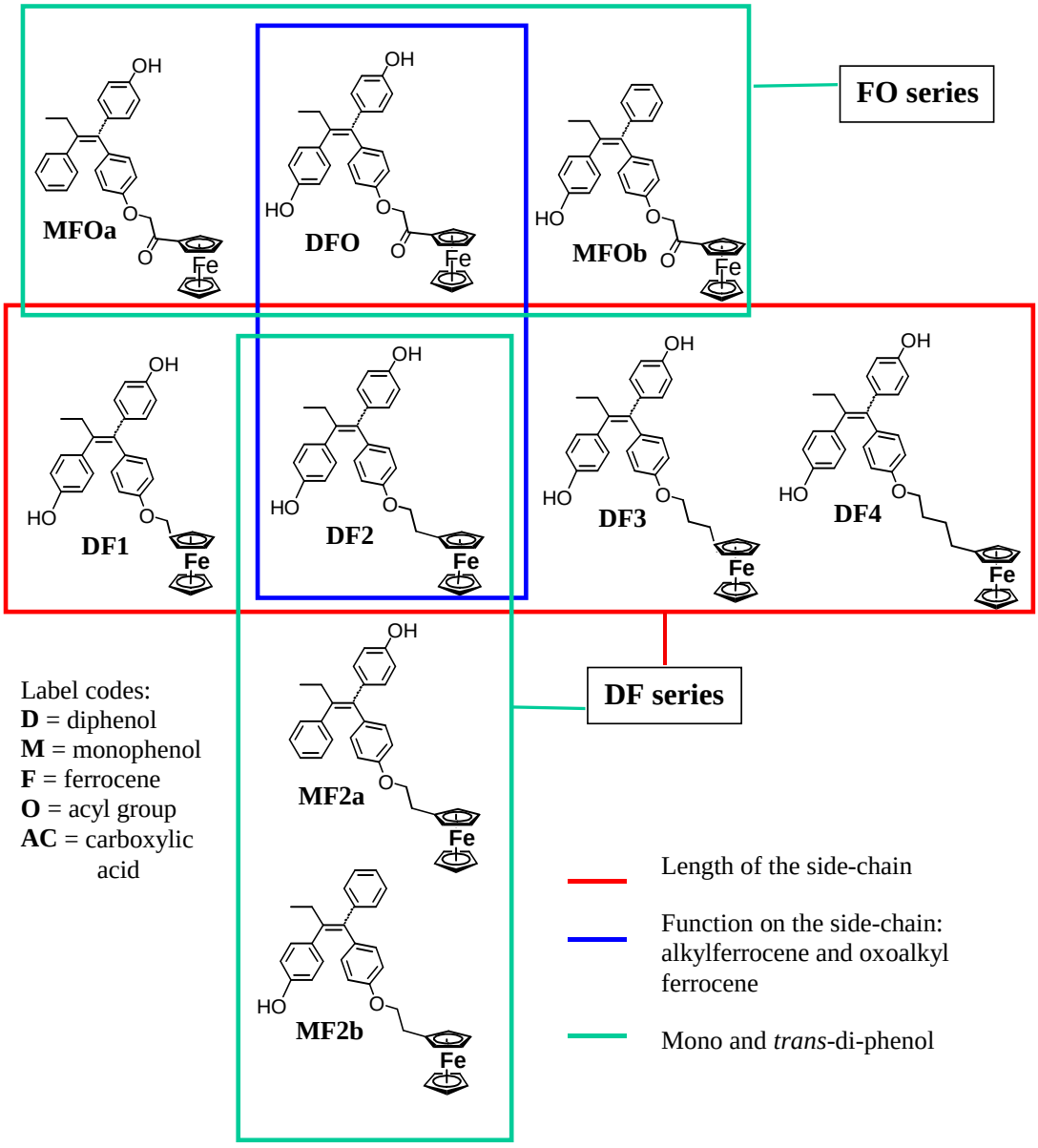

Figure 2-6: Tamoxifen analogues with ferrocenyl side-chains

the replacement of the -$O(CH_2)_2N(CH_3)_2$ side-chain by a ferrocenyl group –$O(CH_2)_n$-[(η^5-C_5H_4)FeCp] (Fig. 2-6). Its activity may be interesting because, in contrast to the hydroxyferrocifens and tamoxifen, **DF**s do not have the antiestrogenic amino side-chain, and the ferrocenyl group cannot assist in the production of the quinone methide. In addition, this ferrocenyl chain is a "neutral" group, in contrast to the basic nature of the amino chain in tamoxifen and to the acidic nature of carboxylate chain of **BA3** or **GW7604**. We hoped that the replacement of the antiestrogenic side-chain by a potentially cytotoxic moiety (which still fits in the LBD pocket) may give rise to new therapeutic properties.

Additionally, a ketone group has been placed next to the ferrocenyl entity to produce the **FO** series (Fig. 2-6), so that the influence of this electron-withdrawing moiety on the activity of Fc is probed. Indeed, as it has been shown previously for **GW5638** (Fig. 2-3), the presence of the acyl group on the side-chain enables the interaction of the chain with ERα Asp351, and thus probably is responsible for the antiproliferative activity of the compound. Therefore, by adding the ketone functionality, we wanted to favor this interaction of our ferrocenyl derivatives with ERα LBD, but it was also done with the perspective of exchanging the iron atom with rhenium or technetium (cf. **Chapter 3**). Lastly, to evaluate the influence of hydroxyl groups on the biological activity, mono and di-phenols of **DF** and **DFO** were synthesized (Fig. 2-6).

2.2 Synthesis

The synthesis of the **DF**s and **FO**s can be broken down into 4 main steps (Fig. 2-7):

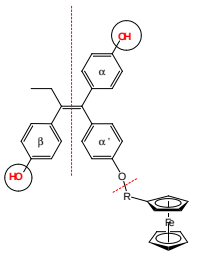

Figure 2-7: Retro-synthesis outline

- Synthesis of the **triphenylbut-1-ene** moiety
- **Coupling** of the ferrocenyl side-chain to the triphenylbut-1-ene scaffold

- **Protection** of the α and β phenol groups, because of the previous ferrocenyl chain coupling step
- **Deprotection** of the phenol groups, as the last step

From previous work both in the literature and by experience in the research group, the synthetic route based on McMurry coupling (Zn, $TiCl_4$) was deemed the most suitable to obtain tetra-substituted butene molecules. This strategy has been adopted for the synthesis of hydroxytamoxifen [139]. Starting from the appropriate ketones, it is short, easy to perform, and gives good yields of mixtures of Z and E isomers. Particularly, the McMurry coupling reaction has been found to be very effective for the synthesis of alkene organometallic derivatives [93].

Regarding the appropriate protecting group for the phenols, there are three main possibilities:

1. formation of an ether-oxide function
2. formation of a silyl ether function
3. formation of an ester function

The first solution does not seem suitable, because our compounds already bear an ether-oxide function, which is liable to be broken during the deprotection step. The advantage of using the silyl groups is that the deprotection step is rather mild, simple and quick. Thus, we first attempted to use the protecting group *tert*-butyldimethylsilane. The synthesis of the **FO** series is described first, being more straightforward.

2.2.1 FO series

An outline of the synthetic pathway of **DFO** is shown in Figure 2-8. The reaction starts from the McMurry cross-coupling between protected 4-hydroxypropiophenone **1** and 4,4'-dihydroxybenzophenone **2**, and is followed by a Williamson-type alkylation reaction. In this latter step, the proton of the α' phenol is abstracted by a base. The resulting phenolate then reacts with α-chloroacetylferrocene. Different bases have been tried for this reaction.

- The reaction with potassium carbonate used in the classical synthesis of hydroxytamoxifen [139] did not proceed at all, even after heating.

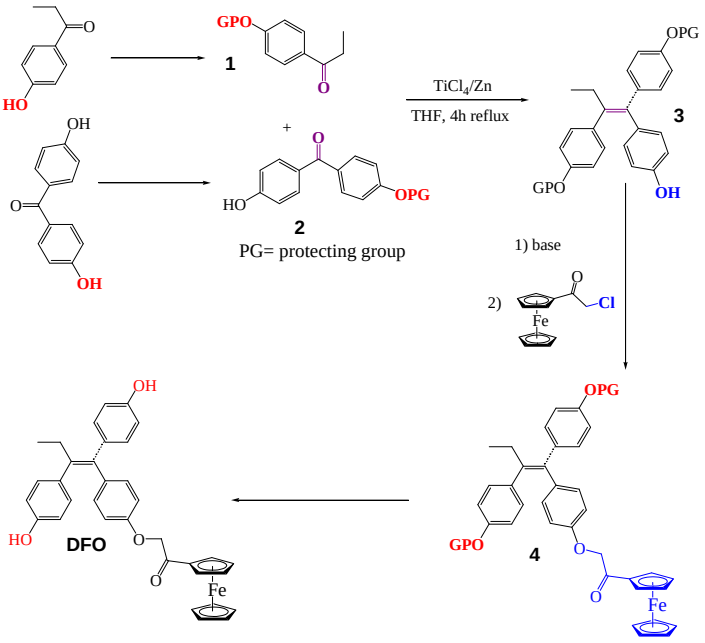

Figure 2-8: Synthesis outline of **DFO**

- When cesium carbonate was used, only a poor yield (14%) was obtained.

  Then stronger bases were tried:

- Sodium hydride was more successful, because the yield doubled (∼30%).

- With potassium hydride, the yield of 41% was the best obtained. Adding KI, to exchange the chloride with a better leaving group like iodide, did not increase the yield.

- Microwave techniques were attempted. However, the yield did not improve, although the time of reaction shrinked from 12h to 20 min.

Therefore, we chose to use KH as the base for the Williamson-type reaction. Since this strong base indiscriminately abstracts protons from all the three phenols, the α and β phenols, not involved in the alkylation reaction, must be protected as mentioned above. However, we found that the *tert*-butyldimethylsilane protecting group was not stable enough during the alkylation reaction, and that the silyl group was displaced to random sites of the molecule. Consequently, we used the pivaloate group instead (Fig. 2-9).

Gauthier *et al.* have shown that the protection of the phenol functionalities in the synthesis of hydroxytamoxifen can be achieved by using a pivaloate group [139]. Thus, 4-hydroxypropiophenone

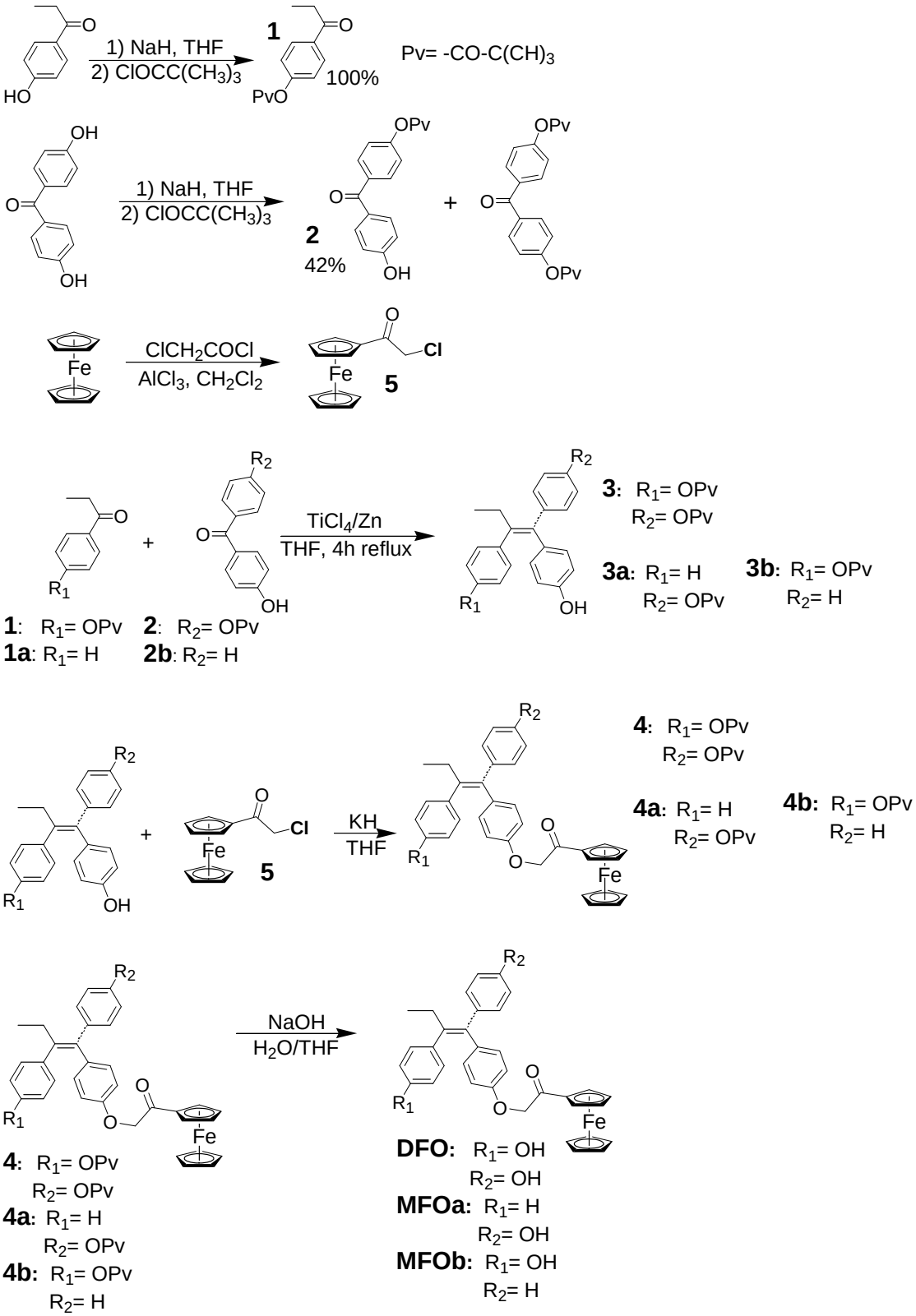

Figure 2-9: Synthesis of **DFO**, **MFOa**, and **MFOb**

and 4,4'-dihydroxybenzophenone were first transformed into their protected forms, **1** and **2** respectively (Fig. 2-9). McMurry coupling of **1** with **2**, using $TiCl_4$/Zn in dry THF, gave alkene **3** as a mixture of Z and E isomers in 67% yield. α-Chloroacetylferrocene **5** was prepared by the alkylation of ferrocene with chloroacetyl chloride using a Friedel-Crafts reaction [140]. Addition of **5** to the monopotassium salt of **3**, obtained from the reaction with KH, produced **4** in 41% yield. Finally, refluxing of **4** with NaOH in H_2O/THF for 6h gave **DFO** as a mixture of Z and E isomers in 72% yield [112].

The synthesis of **MFOa** and **MFOb** followed the same procedure starting with propiophenone and 4,4'-dihydroxybenzophenone, or 4-hydroxypropiophenone and 4-hydroxybenzophenone, respectively.

The separation of the Z isomer from the E isomer was achieved with preparative HPLC for **DFO** and **MFOb**. However, it was not possible to separate the signals of the Z and E isomers of **MFOa** by analytical HPLC.

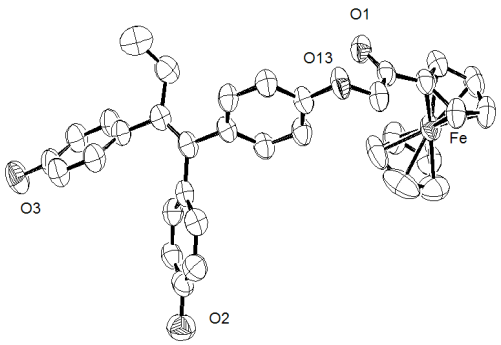

Figure 2-10: ORTEP diagram of (E)-**DFO.**
Thermal ellipsoids shown at 50% probability. Minor part of the disordered (unsubstituted) Cp ring, the diethyl ether solvent molecule, and hydrogen atoms omitted for clarity.

Only the **(E)-DFO** isomer gave crystals of sufficient quality to perform an X-ray crystal structure analysis. The crystals were grown from hexane/ether solution. Fig. 2-10 shows the molecular structure of (E)-**DFO**, and the crystal data and structure refinement are summarized in Table 2.1. The crystallographic characteristics found are similar to those of the classical hydroxytamoxifen-like structures [141, 142]. As in the case of the ferrocifens [93], the rate of isomerization of **DFO** depends on the nature of solvent. The molecules isomerize quickly in protic solvents, but neither isomer showed isomerization after a week in DMSO.

Table 2.1: Crystal data and structure refinement for compound (*E*)-**DFO**·0.5($C_4H_{10}O$).

Empirical formula	C_{36} H_{35} Fe $O_{4.5}$
Formula weight	595.49
Temperature	296(2) K
Wavelength	0.71073 $\AA$
Crystal system	Triclinic
space group	P-1
a [$\AA$]	10.69110(10)
b [$\AA$]	13.5700(3)
c [$\AA$]	13.71290(10)
α [°]	68.6640(10)
β [°]	84.4400(10)
γ [°]	68.5200(10)
Z	2
ρ [mg/m^3]	1.148
Absorption coefficient [mm^{-1}]	0.473
F(000)	626
Volume [$\AA^3$]	1722.87(4)
Crystal size [mm]	0.40 x 0.28 x 0.14
θ range for data collection [°]	1.60 - 22.50
Limiting indices	-11 $\leq$ h $\leq$ 11, -13 $\leq$ k $\leq$ 14, -14 $\leq$ l $\leq$ 14
Reflections collected / unique	57442 / 4482 [R(int) = 0.0279]
Completeness to $\theta = 22.50°$	99.2 %
Absorption correction	Semi-empirical from equivalents
Max. and min. transmission	0.9359 and 0.8276
Refinement method	Full-matrix least-squares on F^2
Data/restraints/parameters	4482/30/396
Goodness-of-fit on F^2	0.980
Final R indices [I >2 σ(I)]	R1 = 0.0615, wR2 = 0.1614
R indices (all data)	R1 = 0.0800, wR2 = 0.1737
Largest diff. peak and hole	0.733 and -0.300 e·$\AA^{-3}$

2.2.2 DF series

The same strategy of synthesis as described above was adopted for the **DF** series. The ferrocenyl alcohols were produced by reduction of the corresponding ferrocenyl carboxylic acids [143]. The alkylation step was achieved via the Mitsunobu reaction (Fig. 2-11).

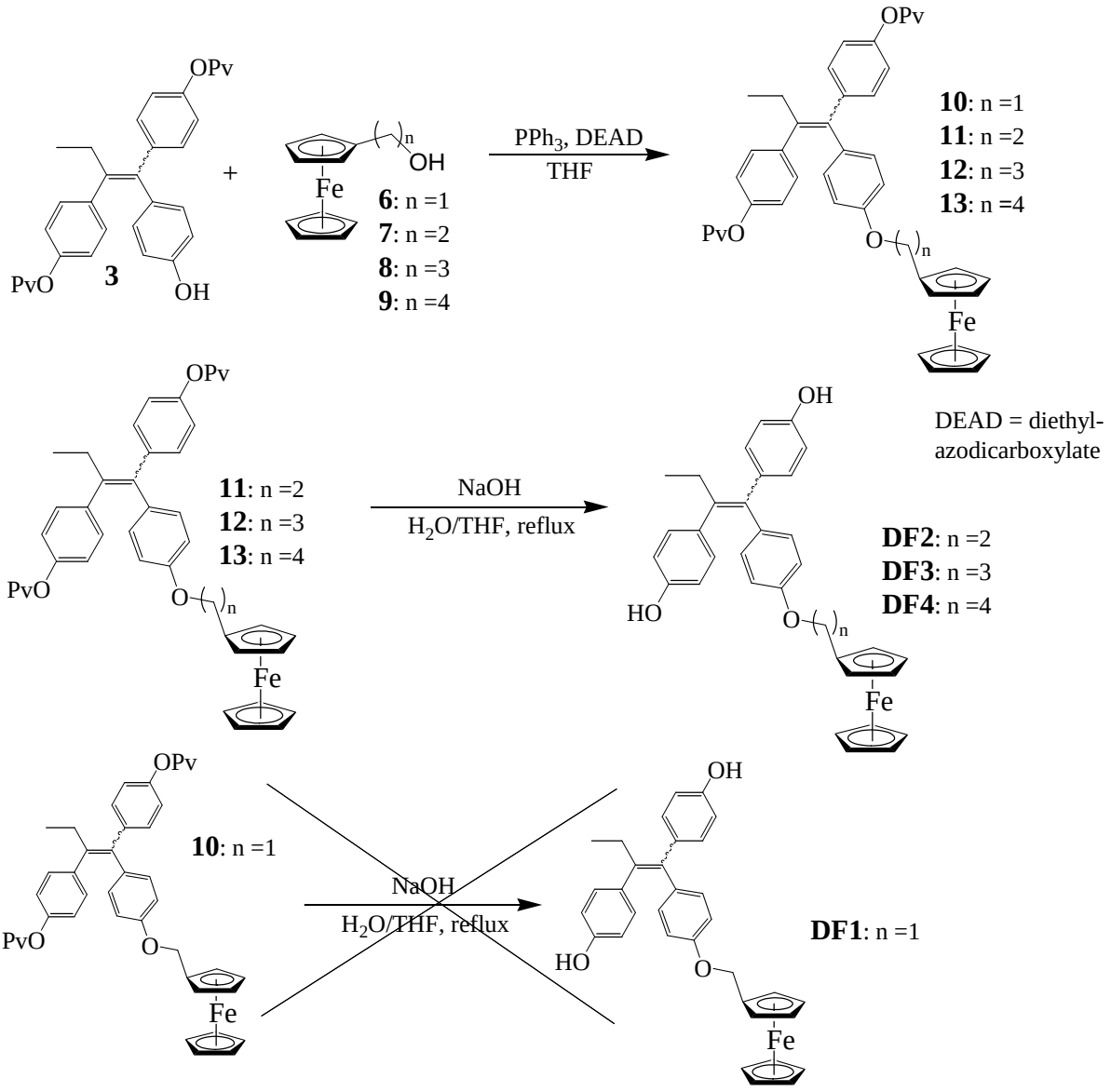

Figure 2-11: Synthesis of **DF2-4**

Similarly to **DFO**, the protected 4-hydroxypropiophenone and 4,4'-dihydroxybenzo-phenone cross-coupled to give **3**. This substituted butene **3** reacts with the ferrocenyl alcohols **6-9**, via the Mitsunobu reaction. The reactants were stirred with triphenylphosphine and DEAD

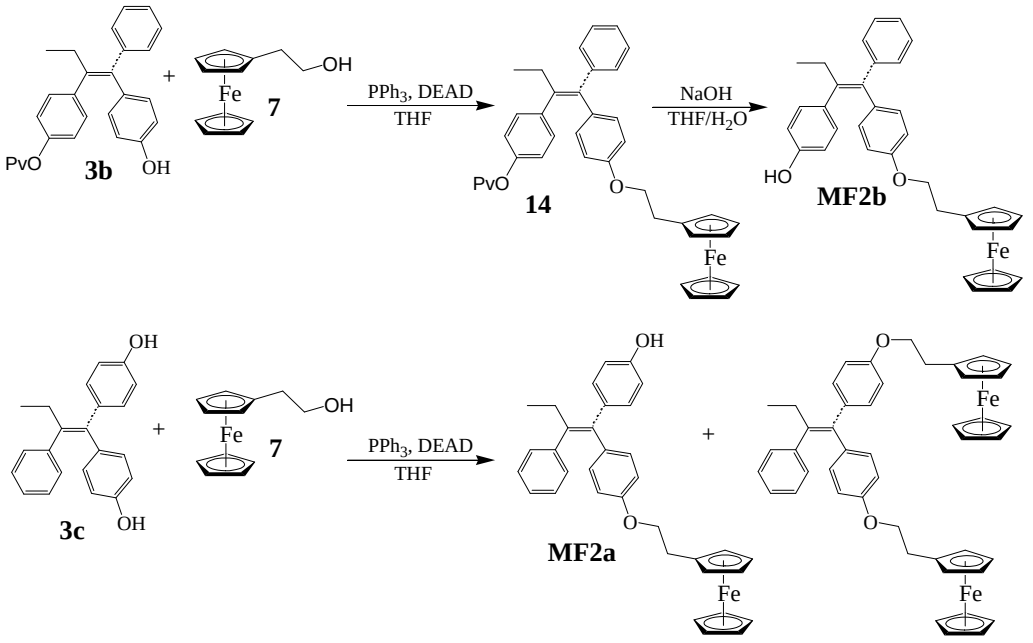

Figure 2-12: Synthesis of **MF2a** and **MF2b**

(diethyl azodicarboxylate) in THF for 2 days. The yield for **10-13** ranged from 70 to 80%. Deprotection was then performed by saponification of the pivaloate groups with sodium hydroxide in a THF/H_2O solution. **DF2-4** were obtained with 70-92% yield.

However, we failed to retrieve **DF1** (n = 1) after saponification. The action of sodium hydroxide on **10** immediately produced a deep purple color, and the work-up yielded a complex mixture of compounds, among which 1,1,2-*tris*-(4-hydroxyphenyl)but-1-ene was identified. This probably indicated a disruption of the ether function. Therefore we decided to use another protecting group for the phenols that allows milder conditions for deprotection: the *tert*-butyldimethylsilyl group.

Attempts to recrystallize the products at room temperature resulted in decomposition of **DF1**, whereas for all the compounds **DF2-4,** attempts to recrystallize at low temperature only gave oily mixtures. Compound **DF1** seems to be quite unstable in both acidic and basic media.

The monophenol **MF2b** was prepared in the same way as **DF2**, but the synthesis started with **1** and 4-hydroxybenzophenone to give **3b**. After alkylation with **7**, saponification of the protected ferrocenyl intermediate **14** finally gave **MF2b**. In contrast, we tried to obtain **MF2a** more rapidly, by skipping the protection/deprotection steps. The unprotected analogue of **3a**,

1,1-*bis*-(4-hydroxyphenyl)-2-phenylbut-1-ene or **3c**, reacted directly with ferrocenyl ethanol **7** to give a mixture of monoalkylated **MF2a** (31%) and dialkylated (32%) product.

All the compounds of the **DF** series were found to isomerize quite rapidly, roughly within one hour. Hence, *Z* and *E* isomers were not separated, and the biological tests were performed on a mixture of both isomers.

2.3 Biological studies

2.3.1 Relative Binding Affinity (RBA)

The ability of the ferrocenyl compounds to bind to the estrogen receptor is expressed by the relative binding affinity (RBA). This value was determined by competitive binding with radio-labeled [^{3}H]-estradiol on both isoforms of the estrogen receptor (ERα and ERβ), as previously described [93]. The RBA values for both ERα and ERβ were determined at 4°C, starting from solutions prepared in DMSO. Estradiol, the female hormone, is used as the reference, and therefore has a RBA value of 100%. The results are summarized in Table 2.2.

Following a general trend observed for previous ferrocenyl derivatives [93, 133, 144], the **DF**s and **FO**s have a better affinity with ERβ than ERα, except for (*Z*)-**DFO** and (*Z*)-**MFOb**, whose affinities for ERβ are slightly lower than for ERα. The affinity of the ferrocenyl derivatives with the ERs was not as good as that of hydroxytamoxifen, probably because of the greater steric hindrance of the ferrocenyl group as compared to a dimethylamine moiety.

The RBA tests were performed on mixtures of *Z* and *E* isomers of the ferrocenyl derivatives **DF1-4**, whose side-chain length varies (n=1, 2, 3, 4). With the shortest side-chain, compound **DF1** had the highest RBA values. With RBA values superior to 10%, **DF1** can be considered as being well recognized by the ERs. Nevertheless, when the chain length was increased by one carbon, the RBA value dropped by ten-fold for ERα, and six-fold for ERβ. Overall, as the side-chain lengthens, RBA values for both ERα and ERβ decrease.

The change in configuration of **DFO** from *Z* to *E* results in a dramatic drop in the affinity with both receptor isoforms (from 13.86% to 1.19% for ERα). In other words, the *Z*-isomer, which in this case is also the *trans*-isomer*, binds better to ER. This observation is in agreement with previous results on tamoxifen, hydroxyferrocifens and other triphenylethylenes: the estro-

*The terminology of *cis/trans* is used to designate the relative position of the ethyl group to the phenyl bearing the side-chain. It is noteworthy to bear in mind that the *trans* orientation is not always a *Z* configuration.

Table 2.2: Relative binding affinity (RBA) values for ERα and ERβ of the ferrocenyl compounds, in DMSO at 4°C. Mean of 2-3 experiments ± S.D.

Compound	RBA (%)	
	ERα	ERβ
17β-estradiol	100	100
(*Z*+*E*)-hydroxytamoxifen	38.5	24
(*Z*+*E*)-**DF1**	11.90 ± 0.25	16.4 ± 0.80
(*Z*+*E*)-**DF2**	0.93 ± 0.35	2.8 ± 0.96
(*Z*+*E*)-**DF3**	0.45 ± 0.05	1.84 ± 0.17
(*Z*+*E*)-**DF4**	0.24 ± 0.02	1.26
(*Z*)-**DFO**	13.86 ± 1.42	11.53 ± 1.27
(*E*)-**DFO**	1.19 ± 0.05	1.59 ± 0.02
(*Z*+*E*)-**MFOa**	4.06 ± 0.71	6.24 ± 1.65
(*Z*)-**MFOb**	2.30 ± 0.41	1.63 ± 0.74
(*E*)-**MFOb**	4.62 ± 0.44	6.49 ± 1.35
(*Z*+*E*)-**MF2a**	0.16 ± 0.02	0.83 ± 0.3
(*Z*+*E*)-**MF2b**	0.13	0.5 ± 0.2

gen receptor has a preference for the *trans*-isomer over the *cis*-isomer [39,93,121]. However, for these last compounds [93,121], there is always a hydroxyl group on the α phenyl. In the case of **MFOb**, the hydroxyl group has been transposed to the β phenyl. Surprisingly, the (E)-isomer of **MFOb** has a better affinity with ER than its Z analogue.

In addition, when a hydroxyl group is removed from the chemical structure of **DF2**, whether it was from the β phenyl (**MF2a**) or from the α phenyl (**MF2b**), it resulted in a reduced affinity with the receptor (from 0.93% to 0.16% and 0.13% respectively). The same trend is observed for (Z)-**DFO** and (Z)-**MFOb**. Drawing any conclusion with **MFOa** is more difficult, because the tests were performed on a mixture of Z and E isomers, and not on pure isomers as with **DFO** and **MFOb**.

As for the influence of a ketone group on the side-chain, **MFOa** binds with better affinity to the receptor than its counter-part without the ketone function **MF2a** (4.06% as compared to 0.16%). Again, it is difficult to compare **DFO** or **MFOb** to **DF2** and **MF2b** respectively, because the experiments were not performed under the same conditions (mixture vs. pure isomer).

2.3.2 Lipophilicity

Table 2.3: Lipophilicity of the **FO** series. Measured by $\log(P_{o/w})$

Compound	log(Po/w)
estradiol	3.5
(*Z*)-hydroxytamoxifen	3.2
(*E*)-hydroxytamoxifen	3.4
(*Z*)-**DFO**	4.6
(*E*)-**DFO**	5.1
(*Z*+*E*)-**MFOa**	5.8
(*Z*)-**MFOb**	3.6
(*E*)-**MFOb**	5.9

The degree of lipophilicity of the organometallic compounds is expressed as the octanol-water partitioning coefficient, $\log P_{o/w}$, determined by HPLC, according to a method described by Pomper *et al.* [104, 145]. $\text{Log}P_{o/w}$ of (Z)-**DFO** is 4.6, and is lower than that of (E)-**DFO**

(5.1). Analogously, for **MFOb**, the *Z* isomer also has a lower $\log P_{o/w}$ value than the *E* isomer. Table 2.3 shows that the organometallic compounds have higher $\log P_{o/w}$ values than estradiol and hydroxytamoxifen. This means that the ferrocenyl compounds are more lipophilic, and thus may more easily cross the cell membrane than hydroxytamoxifen. However, the amount of bioactive compound that can actually reach the target depends on other factors, and this problem will be addressed in **Chapter 4**.

2.3.3 Cell proliferation

The influence of the organometallic compounds on the proliferation of cancer cells have been tested on:

- hormone-dependent **MCF-7** breast cancer cells which present a high accumulation of ERα, qualified as ER+ cells.
- hormone-independent **MDA-MB-231** breast cancer cells which do not have ERα,qualified as ER- cells.
- hormone-independent **PC-3** prostate cancer cells which possess ERβ but no ERα, that we consider as ER- cells.

The results were obtained after 6 days of culture, and were expressed as percentages of cell proteins vs. control. Control experiments were conducted in the same conditions, but without any additional chemical compound. Reference proliferation experiments were conducted with estradiol (E_2), hydroxytamoxifen (OH-Tam) and **Fc-diOH**. The addition of estradiol caused as expected the hormone-dependent MCF-7 cells to proliferate faster than the control (Fig. 2-13), but did not influence the proliferation of the PC-3 prostate cancer cells, lacking ERα. If the antiestrogen hydroxytamoxifen was added instead, the MCF-7 cell proliferation was inhibited (Fig. 2-14). Furthermore, for the hormone-independent MDA-MB-231 cells, the previously studied ferrocene derivative **Fc-diOH** (Fig. 2-4) showed a potent cytotoxic effect (Fig. 2-14) [133].

Unexpectedly, the ferrocenyl derivatives of the **DF** series have a proliferative effect on the hormone-dependent MCF-7 breast cancer cells. However, they slightly inhibited the growth of the hormone-independent MDA-MB-231 breast cancer cells at 10 μM. The antiproliferative activity is more marked on the PC-3 prostate cancer cells. The experiments of **MF2a** and

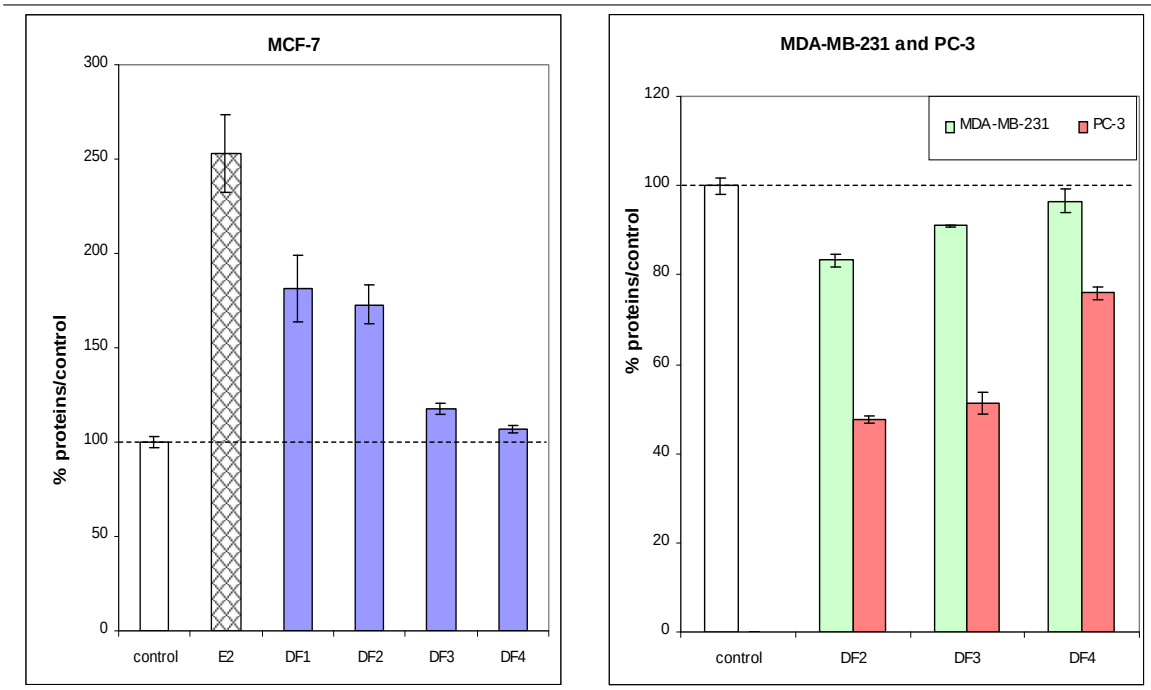

Figure 2-13: Effect of **DF1-4** on the growth of MCF-7, MDA-MB-231 and PC-3 cells. 1 μM of **DF1-4** and 1 nM of estradiol (E_2), respectively, were incubated with MCF-7 cells (medium with phenol red), and 10 μM of **DF2-4** incubated with MDA-MB-231 and PC-3 cells. After 6 days of culture. Mean of 2 experiments ± S.D.

MF2b, and those of **DF1** on ER- cells are underway. Anyhow, it can already be stated that the longer the ferrocenyl side-chain, the less biologically active the compounds, as it has been observed for the RBA experiments.

Unlike its analogues **DF1-4**, the ferrocenyl compound **DFO** inhibits the proliferation of the three cancer cell lines at 10 μM. However, like the **DF** series, the activity is less pronounced on the MDA-MB-231 cells as compared to PC-3 cells. Nevertheless, its activity on the ER- cancer cells (MDA-MB-231 and PC-3) is similar to its analogue **DF2**. However, the removal of one hydroxyl group completely changes the biological behaviour of the molecule on ER- cells. Indeed, **MFOa** and **MFOb** have nearly no effect on the proliferation of ER- cells. While **MFOa** still slightly inhibits the proliferation of MCF-7 cells, **MFOb** has clearly a proliferative effect. The configuration of the molecule does not seem to have any effect on the biological activity, because for **DFO** and **MFOb**, both Z and E isomers have similar effects on the proliferation of cancer cells. This, however, could be attributed to the isomerization of the compounds in protic solvents.

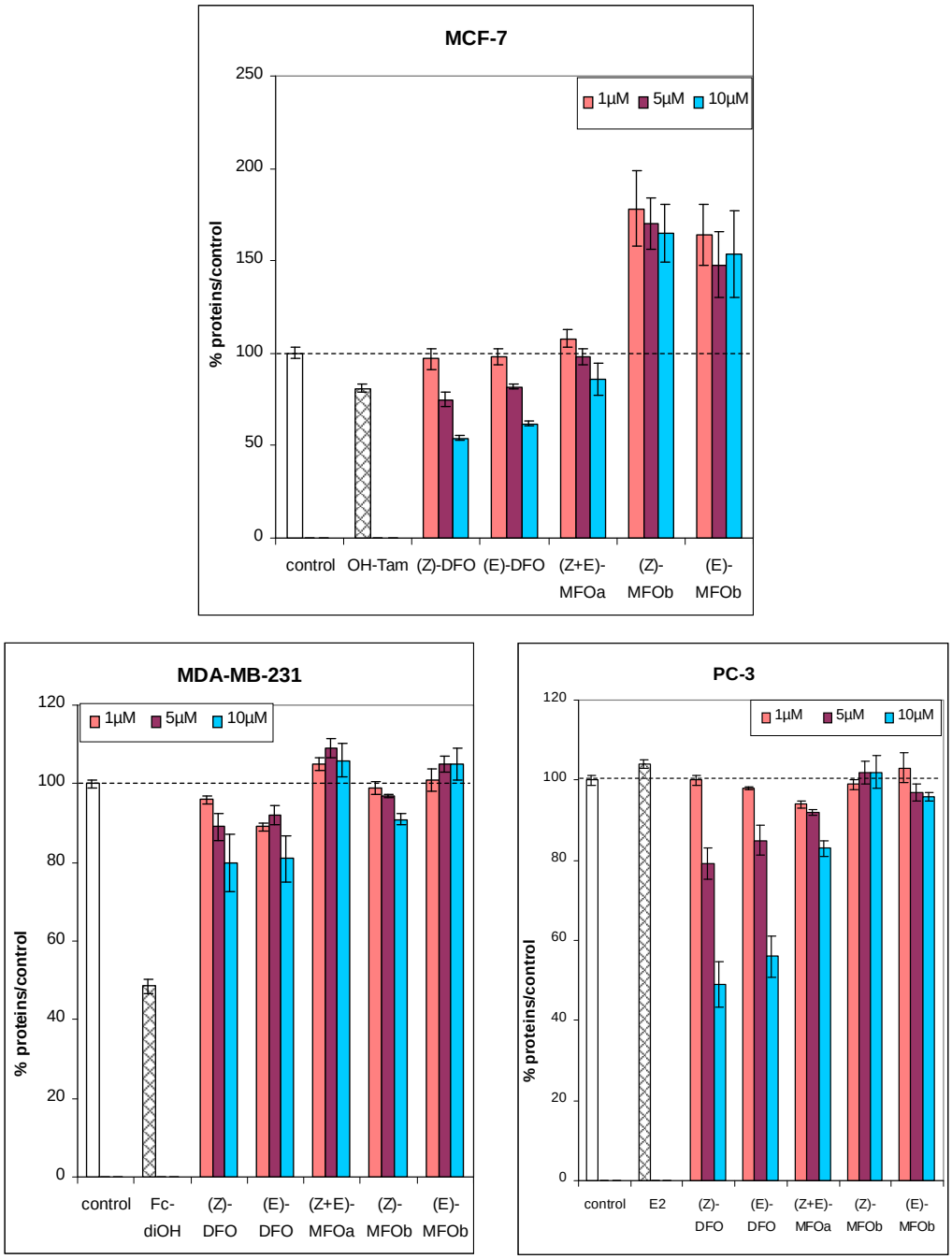

Figure 2-14: Effect of **FO**s on the growth of MCF-7, MDA-MB-231 and PC-3 cells. 1 μM, 5 μM, 10 μM of **FO**s, 1 nM of estradiol, 1 μM of hydroxytamoxifen (OH-Tam), and 1 μM of **Fc-diOH** were respectively incubated with MCF-7 (medium with phenol red), MDA-MB-231 and PC-3 cells. After 6 days of culture. Mean of 2 experiments ± S.D.

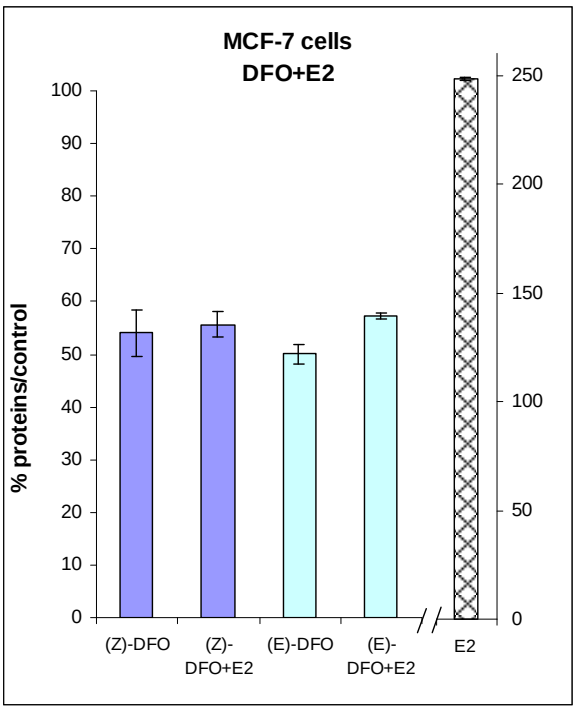

Figure 2-15: Effect of **DFO** on the growth of MCF-7 cells, in presence of estradiol.
10 μM of **DFO** and 10 nM of estradiol were incubated with MCF-7. After 5 days of culture. Mean of 2 experiments ± S.D.

In order to better understand the antiproliferative character of **DFO**, which seems to be the most active biomolecule in the series, another experiment was performed. The molecule was incubated with MCF-7 cancer cells, in the presence of estradiol (in 10 nM). If the antiproliferative effect of **DFO** is antiestrogenic (acting through ERα), then addition of estradiol should reverse to some extent the antiproliferative effect [93]. The results presented in Fig. 2-15 show that the inhibitory activity of **DFO** has very slightly decreased, in presence of estradiol. Therefore, the results are not conclusive enough to confer mainly an antiestrogenic character to the antiproliferative property of **DFO**. The cytotoxic character of the organometallic compound is very likely dominant over the antiestrogenic property in the antiproliferative activity of the molecule.

2.4 Electrochemical study

Since it has been suggested that the cytotoxic activity of the ferrocenyl derivatives may originate from its oxidized form [126–130], the ferrocenium ion, the electrochemical behaviour of our compounds was examined. Variable scan rate cyclic voltammograms (CVs) were obtained using a three electrode cell with a 0.5 mm platinum working electrode, gold-plated nickel mesh counter electrode, and saturated calomel reference electrode in DMF solutions. The compounds studied can be separated into two groups based on their electrochemical behaviour. The compounds possessing a ferrocenyl chain without the acyl group, **DF1**, **DF2**, **MF2a**, **MF2b**, **DF3** and **DF4** of the **DF** series belong to the first category, while the second category consists of those compounds carrying the ketone function, **MFOa**, **MFOb** and **DFO** from the **FO** series. The standard oxidation potentials of compounds belonging to the series of **DF** are given in Table 2.4.

Table 2.4: Oxidation potentials of **DF**s vs. SCE. In DMF. Scan rates = 0.5 and 20 V/s, 0.5 mm Pt electrode

Compound	$\mathbf{E}_{\frac{1}{2}}$**(V)**	$\mathbf{E}^{(o,p)}_{phenol}$**(V)**	**Compound**		$\mathbf{E}_{\frac{1}{2}}$**(V)**	$\mathbf{E}^{(o,p)}_{phenol}$**(V)**
DF1	0.506	0.867	**DF2**	2 phenols	0.447	0.880
DF2	0.447	0.880	**MF2a**	1 phenol	0.451	1.136
DF3	0.432	0.867	**MF2b**	1 phenol	0.442	1.050
DF4	0.454	0.867				

At all scan rates, **DF** compounds gave rise to a reversible ferrocene/ferrocenium (Fc/Fc^+) couple and a higher potential, irreversible phenol oxidation wave. The redox potentials ($E_{\frac{1}{2}}$) for the Fc/Fc^+ couple ranged from 0.432 (**DF3**) to 0.506 V (**DF1**) vs. SCE in DMF. There was no correlation between $E_{\frac{1}{2}}$ and the number of carbon atoms in the ferrocenyl chain.

Irreversible phenol oxidation potentials $E^{(o,p)}_{phenol}$ ranged between 0.867 and 1.136 V, and were bimodal in distribution. The compounds with the lowest phenol oxidation potentials, **DF1**, **DF2**, **DF3** and **DF4** (from 0.867 to 0.880 V) posess two phenol groups, while those with higher oxidation potentials, **MF2a** and **MF2b** (1.136 and 1.050 V respectively), have only one. The lowering of the phenol oxidation potential in the former case was probably due to the additional resonance stabilization that the second phenol imparts to the electrochemically

generated phenoxy radical. It is also noteworthy that the oxidation of the α phenol in **MF2a** occurred almost 100 mV higher in potential (1.136 V) than that of the β phenol in **MF2b** (1.050 V).

FO compounds exhibited a more complex behaviour. In DMF, at low scan rates the Fc/Fc^+ couple was irreversible, although a reduction wave begins to appear at higher scan rates, suggesting an EC* mechanism:

(1) $A \underset{+e^-}{\overset{-e^-}{\rightleftharpoons}} A^+$

(2) $A^+ \longrightarrow B$

When scan rates are low enough for reaction 2 to proceed, the electrochemically generated cation A^+ engages in irreversible follow-up chemistry. At higher scan rates, reaction 1 becomes reversible, as enough time does not elapse for reaction 2 to occur to a large extent. It is interesting to compare the ferrocene oxidation wave of the acyl-carrying compounds to that of their alkyloxy analogues (**MFOa/MF2a**; **MFOb/MF2b**; **DFO/DF2**, Fig. 2-16). We see that the Fc oxidation wave of the "acyls" is higher in intensity than that of the "alkyloxys" at low scan rates, but that the two waves are similar in intensity at high scan rates. We interpret this behaviour in the following way. The chemical reaction following the electrooxidation of ferrocene could regenerate Fc(II), thus enhancing the oxidation wave, as the Fc cycles from (II) to (III) back to (II) within the time scale of the experiment at low scan rates. As the scan rate increases, the chemical reaction hasn't time to proceed, Fc(II) is not generated, and the peak intensity approaches that of one electron. Thus we see that the chemical transformation occurs with rates **DFO**>**MFOb**>**MFOa**, and seems to be related to the number and position of the phenol substituents.

However, it should be pointed out that no phenol oxidation wave was observed for **DFO** at low scan rates. Therefore, the exceptionally large enhancement of the Fc oxidation wave may also be due to a phenol oxidation occurring at a similar potential. In the **DF** series, we saw that the phenol oxidation wave for a compound carrying two phenol groups occurs around 0.87 V, while the ferrocene oxidation wave for **DFO** occurs at 0.77 V. Thus it is possible to imagine that the ferrocene and phenol oxidation waves overlap, accounting for the high intensity of the **DFO** wave.

In order to gain more insight about the follow-up chemistry, we obtained cyclic voltammograms for the fragment **FRAG** pictured below (Fig. 2-17). The compound gave rise to an

*electrochemical-chemical

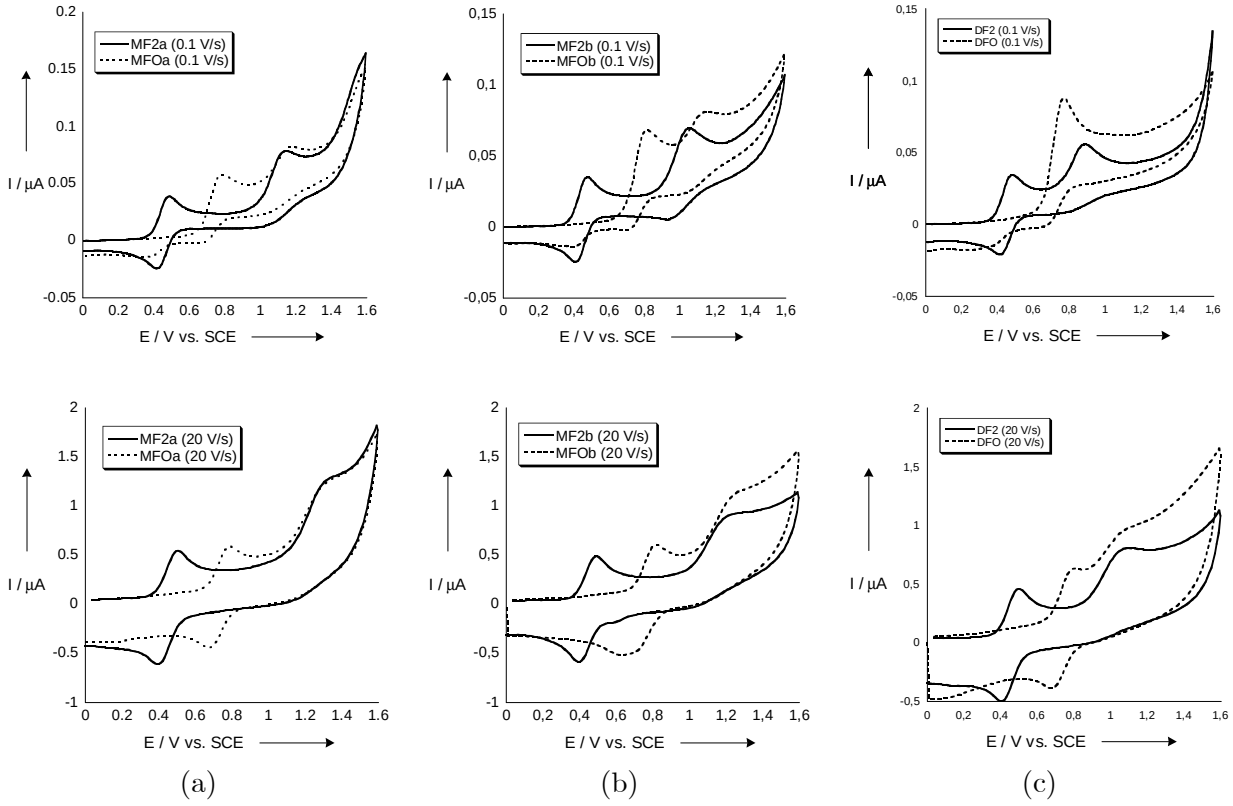

Figure 2-16: Cyclic voltammograms for the couple (a) **MFOa**/**MF2a**, (b) **MFOb**/**MF2b**, and (c) **DFO**/**DF2**.
Scan rates = 0.5 V/s and 20 V/s, 0.5 mm Pt electrode. Intensities have been normalized for concentration.

Table 2.5: Fc oxidation potential of **FO**s vs. SCE. In DMF. Scan rates = 0.5 and 20 V/s, 0.5 mm Pt electrode

Compound	**DFO**	**MFOa**	**MFOb**
$\mathbf{E}_{\frac{1}{2}}\mathbf{(V)}$	0.767	0.783	0.811

irreversible Fc oxidation wave at all scan rates (up to 2 V/s), suggesting that the decomposition after electrooxidation of compounds **MFOa**, **MFOb**, and **DFO** probably involves their ketone function.

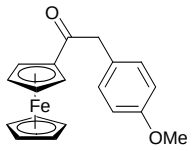

FRAG

Figure 2-17: Structure of the fragment **FRAG** studied in electrochemistry

The influence of the electron-withdrawing acyl group can be seen in the relatively high halfwave potentials ($E_{\frac{1}{2}}$) of the ferrocene group: 0.783, 0.811, and 0.767 V for **MFOa**, **MFOb**, and **DFO**, respectively (Table 2.5). When one compares the **FO**-compounds with their **DF** analogues, one finds that although the ferrocene oxidation potentials are uniformly shifted to higher energy, the phenol oxidation waves do not display uniform behaviour. For **MFOa**, the phenol oxidation wave occurs at approximately the same potential as for **MF2a**, Fig 2-16(a). On the other hand, the phenol oxidation wave is higher in energy for **MFOb** than for **MF2b**, Fig. 2-16(b). For **DFO**, only one wave is seen at low scan rates, and is associated with a multi-electron process. At higher scan rates, the ferrocene oxidation wave is similar in intensity to that of **DF2**, and a phenol oxidation wave is observed at a similar potential, Fig. 2-16(c).

2.5 Discussion

Three parameters of the organometallic compounds were studied: the ferrocenyl side-chain length (**DF1-4**), the presence of an acyl group (**DF2** vs. **DFO**), and the importance of the hydroxyl group and its position (**DFO**, **MFOa**, **MFOb**; **DF2**, **MF2a**, **MF2b**).

2.5.1 Ligand-receptor relationship

For the **DF** series, the longer the ferrocenyl side-chain, the bulkier is this hydrophobic group. Consequently, the more difficult the molecules are to fit in the LBD of ERα, the weaker their affinity with ER. This is consistent with the decrease of the RBA values, as we go from **DF1** (n=1) to **DF4** (n=4).

In order to better understand the relative binding affinity results, it may be helpful to have some theoretical docking insights of **DFO**. This molecule seems to have the most interesting biological behaviour, in terms of affinity as well as antiproliferative effect. That is why molecular modeling on (*E*)-**DFO** and (*Z*)-**DFO** in the anti-estrogenic form of the estrogen receptor was investigated. We used the LBD structure of ERα (Protein Data Bank (PDB) code: 3ERT), published by Shiau [53], and MacSpartan Pro Software [146]. 4-Hydroxytamoxifen (OH-Tam) was removed and replaced successively by the two isomers (*E*) and (*Z*)-**DFO** (Table 2-18). An energy minimization routine was carried out with all the heavy atoms immobilized, except for those of the ligand and the His 524 side chain, using the Merck Molecular Force Field (MMFF).

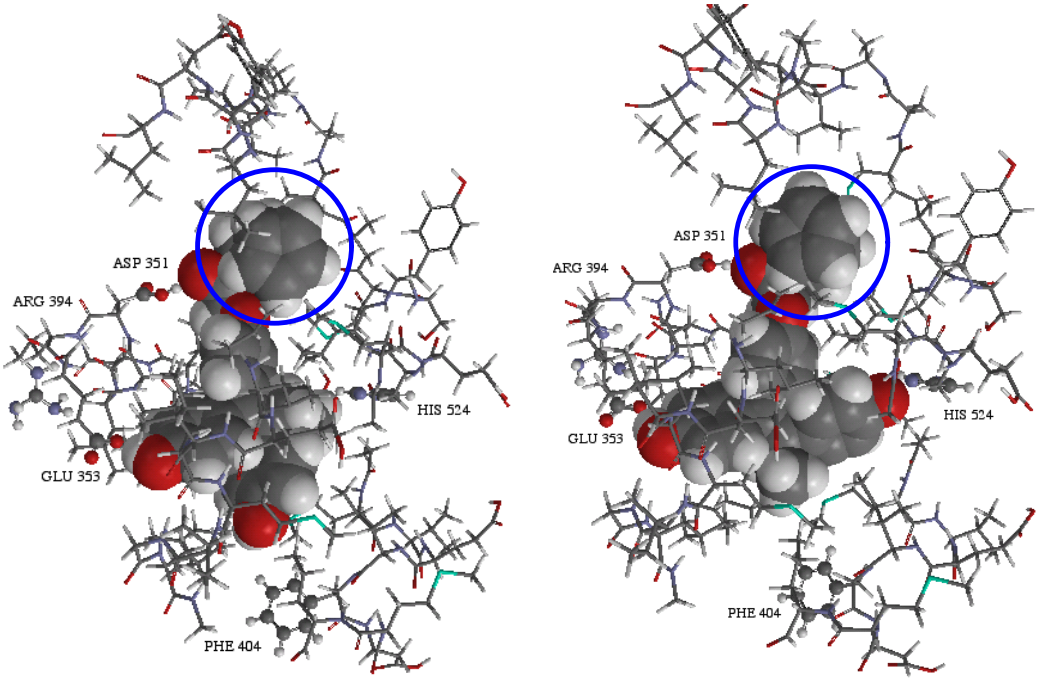

Figure 2-18: Representation of (left) *E*-**DFO** and (right) *Z*-**DFO** docked in ERα, assuming a direct interaction between the ketone group of **DFO** and Asp 351. The keto-ferrocenyl side-chain is circled in blue.

A conformational study in the cavity was also carried out to determine the best position for the organometallic moiety in relation to the rest of the molecule and by taking into account that there is possibly a hydrogen bonding interaction either between:

- Asp 351 and the iron atom, as Fe of the ferrocenyl side-chain bears a slight negative charge (Mulliken charge $\simeq$ -0.2)
- or between Asp 351 and the ketone group adjacent to the ferrocenyl moiety.

The affinity of the bioligand for the cavity was also determined using MMFF molecular mechanics, with calculations for the bioligand-ERα cavity combination, and for the ERα cavity and the bioligand done separately, each retaining the conformation previously determined for the molecular complex. This gives a value of the energy variation ΔE of the reaction: ligand + cavity $\rightarrow$ ligand-cavity complex. The cavity containing the amino side-chain is large enough to host the bulky keto-ferrocenyl group. The energy variation ΔE found for (Z)-**DFO** is -89 kcal·mol^{-1} with a direct interaction between Asp 351 and Fe, but -106 kcal·mol^{-1} if we consider a direct interaction between Asp 351 and C=O (Table 2.6). Either way, these exothermic values favor association. The [(Z)-**DFO**]-cavity complex is twice as stable as that of the [(E)-**DFO**]-cavity according to molecular modeling study, which yielded a value for [(E)-**DFO**]-cavity of -45 kcal·mol^{-1} (in case Asp 351 interacts with Fe) and -58 kcal·mol^{-1} (in case Asp 351 interacts with CO). Indeed, as shown in Fig. 2-18, because of its conformation, (E)-**DFO** has lost the interaction with His 524, unlike (Z)-**DFO**. This is consistent with the observed loss of affinity with the estrogen receptor of the (E)-isomer as compared to its (Z) counterpart.

Table 2.6: Energy variation ΔE values for the binding of the ferrocenyl ligands to ERα

Compound	**ΔE** (kcal·mol^{-1})	**ΔE** (kcal·mol^{-1})
	Asp 351 - Fc interaction	Asp 351 - C=O interaction
(Z)-**DFO**	-89	-106
(E)-**DFO**	-45	-58
(Z)-**MFOa**	-79.2	n.a.
(Z)-**MFOb**	-68.2	n.a.
(Z)-**DF2**	-11.7	

We now turn our attention towards the importance of the C=O group and the ligand-receptor relationship. Although the RBA experiments of **DFO** were performed on separate isomers, and that of **DF2** were done on the mixture of Z and E, the lowest RBA of **DFO** is still higher than that of **DF2**. Thus we may infer that **DF2** should have a weaker affinity with the receptor than **DFO**. This is consistent with the theoretical predictions. Since the docking experiments suggest that **DFO** can have two possible stabilizing interactions with Asp 351, the loss of one interaction by removing the ketone functionality should result in a weaker binding affinity with the receptor. And indeed, ΔE for (Z)-**DF2** is found to be -11.7 kcal·mol^{-1}, nearly ten-fold lower than the ΔE value for (Z)-**DFO**.

Then the importance of the phenol groups was probed. For that purpose, they were proposed for the chemical structure design of **DFO**, in the hope that they could both have interactions with the amino acids Glu 353 and His 524 of the LBD. When one of the hydroxyl groups is removed, only one stabilizing interaction remains, and consequently we expect a weaker binding affinity. ΔE for [(*Z*)-**MFOa**]-cavity and [(*Z*)-**MFOb**]-cavity are -79.2 and -68.2 kcal·mol^{-1}, respectively. They are indeed less exothermic than -89 kcal·mol^{-1} found for the [(*Z*)-**DFO**]-cavity complex (Table 2.6). The experimental results are consistent with this theoretical prediction, because (*Z*)-**MFOb** has a lower RBA value than (*Z*)-**DFO**.

2.5.2 Antiproliferative activity

We are going to examine how the three structural parameters mentioned above influence the biological activity of the ferrocenyl derivatives on cell proliferation, which is summarized in Table 2.7.

Table 2.7: Summary of the biological activity of the ferrocenyl derivatives.

Compound	proliferative effect (ER+ cells)	cytotoxic (ER- cells)
DF1	++	n.a.*
DF2	++	++
DF3	+	++
DF4	Ø	+
DFO	-**	++
MFOa	Ø	Ø
MFOb	++	Ø

"+" stands for the mentioned effect (++ is stronger)
"-" for the reverse effect
"Ø" for no significant effect
*experiments in progress,
addition of E_2 to MCF-7 cells incubated with **DFO
**did not significantly reverse the antiproliferative effect (cf. discussion below)

Antiestrogenic/cytotoxic effect?

As mentioned earlier, the antiproliferative activity of the ferrocenyl derivatives could originate either from an antiestrogenic character and/or from a cytotoxic property.

The antiestrogenic or ER-mediated pathway involves the binding to the receptor ER and a disruption of the transcription process. This could lead to a stabilisation of the receptor and a blockade of the transcription machinery, as observed with hydroxytamoxifen, or to the recruitment of ubiquitines, and the proteasomal degradation of ER, as for ICI 182 780 [147].

On the other hand, ferrocenyl derivatives have been shown to generate an antiproliferative effect on cancer cells which has been attributed to a "cytotoxic effect". Upon oxidation of iron(II) to iron(III), the ferrocenium ion(III) is very reactive and is likely to react with the chemicals in the biological environment, and maybe generate radicals. This kind of behaviour could be examplied by the Fenton reaction with requires the oxidation of iron(II) by hydrogen peroxide, and produces radicals. But the cytotoxic activity of ferrocenyl derivatives could also follow another pathway which involves the creation of a quinone methide species, as proposed for the ferrocifenol **Fc-diOH**.

All the described organometallic compounds have an antiproliferative activity on ER- cells. For each compound, the trends in their behaviour on PC-3 prostate cancer cells and MDA-MB-231 breast cancer cells are quite similar, although the effects were stronger with the PC-3 cells. Since ER- cells lack ERα, the ferrocenyl compounds could not inhibit cell proliferation by the ER-mediated pathway. These results suggest that their inhibition activity on ER- cells must follow the cytotoxic pathway.

As for **DFO**, this molecule inhibits the proliferation of both ER+ and ER- cells. Its antiproliferative effect on MCF-7 cells could be due to the binding of the ligand to ER, triggering the ER-mediated inhibition pathway. Indeed, it showed a good affinity with the estrogen receptor, which theoretically displays a stabilized antiestrogenic conformation when **DFO** binds to it. However, the favored antagonist conformation could not fully explain all the antiproliferative activities. In other words, if the ER-mediated pathway was the only one activated by the molecule, then when estradiol is added to the cell culture in the antiproliferation experiment, the natural ligand should be able compete easily with **DFO**, and reverse the inhibition effect. However the addition of estradiol did not reverse the effect notably in our experiments. Therefore, the antiproliferative activity of **DFO** is not mediated solely by ER, but might be due in good part to a cytotoxic pathway.

Influence of the ketone functionality

The cell proliferation experiments indicate that the loss of the ketone functionality changes completely the biological behaviour of the organometallic compound. By comparing the antiproliferative activity of **DFO** and **DF2**, we can see that they are both cytotoxic on ER- cells, and that they have similar activity on these cells. However, only **DFO** inhibited the proliferation of the ER+ MCF-7 cells, whereas **DF2** had a proliferative effect on those cells.

It has been shown that **DFO** has a good affinity with the receptor, unlike **DF2**. Moreover, molecular modeling experiments suggest that the estrogen receptor has a much more favorable antagonist conformation when the ligand is **DFO** instead of **DF2**, specifically thanks to the acyl group which interacts with Asp351. However, the different behaviours of both molecules on cell proliferation could not be explained satisfactorily by their difference in the binding affinities with ER, because their antiproliferative activities were not dominantly due to the ER-mediated inhibition pathway, as noted above.

The electrochemistry of **DFO** shows that the ferrocene oxidation wave is irreversible at low scan rates. Once incubated in the cancer cells, **DFO** probably does not interact with ER, but decomposes rapidly and produces reactive products, which destroy the cells. On the contrary, the cyclic voltammogram of **DF2** exhibited a reversible Fc/Fc^+ couple. Therefore, we might infer that the Fc cycles from (II) to (III) back to (II) without decomposition. Consequently, **DF2** could interact with the receptor, as an estrogenic diphenol compound [148], without being degraded. This proliferative effect arises from conformational activation of ERα.

It is worthy to note that the intensity of the estrogenic effect is not necessarily correlated to the RBA value [144]. A very small RBA is sometimes enough to trigger an estrogenic effect. For this reason, the fact that all the other compounds from the **DF** series have an estrogenic activity on ER+ cells was not unusual. In these latter cases, the organometallic moiety seems to behave simply as a spectator.

Mono/di-phenol

However, the presence of an acyl group next to the ferrocenyl entity is not enough to convey an efficacious cytotoxic effect. If the ketone function seems to be responsible for an irreversible Fc oxidation, suggesting a chemical reaction after the oxidation, the decomposition reaction does not occur in the same manner whether there is one or two phenols. At slow scan rates, **DFO** entirely decomposes, and no phenol oxidation is observed.

For **MFOa** and **MFOb**, at slow scan rates, the Fc oxidation is also irreversible, but reversibility was recovered rather quickly with higher scan rates. Thus, the decompostion is slower. And since the phenol oxidation signal is still present for **MFOa** and **MFOb**, but not for **DFO**, the decomposition must obviously occur in a different manner. This difference in stability and behaviour could be related to the weaker or even non-existant biological effects of **MFOa** and **MFOb** on the proliferation of cancer cells, as compared to **DFO**.

2.6 The prototype of an efficient biomolecule

In summary, we have described the first series of compounds where the amino side-chain of hydroxytamoxifen has been replaced by an organometallic moiety. Our molecular modeling studies predicted that the ferrocenyl side-chain would fit in the hydrophobic pocket in the LBD of the estrogen receptor α, despite its bulkiness. Overall, the ferrocenyl derivatives retained antiproliferative activity on ER- cancer cells: the MDA-MB-231 breast cancer line and PC-3 prostate cancer line. The intensity of the cytotoxic effect depended on the molecular structure.

The influence of the side-chain length, of the phenol groups (number and position), and of the electron withdrawing acyl group next to the ferrocenyl moiety was probed. It has been shown in the **DF** series that the longer the ferrocenyl side-chain, the less biologically active the molecules. This was verified for their binding affinities as well as for their activity on the proliferation of cancer cells. The tethering of a ketone function adjacent to the ferrocenyl entity conveyed an additional stabilizing interaction with Asp 351 of ERα. This could account for the good affinity of **DFO** with ERα and ERβ found experimentally. The acyl group is also responsible for unique irreversible Fc oxidation behaviour, which may explain the antiproliferative activity of **DFO** on the hormone-dependent MCF-7 breast cancer cells, unlike its other analogues. Indeed, this antiproliferative effect probably stems from a more dominant cytotoxic property of the compound, reflecting the primacy of this mechanism over the ER-mediated pathway. Although this ketone group contributed to the stronger cytotoxic activity of **DFO** as compared to its analogues, its mere presence is not sufficient. The loss of one hydroxyl group weakens this activity or even reverses it.

Therefore, it requires the presence of both the ketone function adjacent to the ferrocene group and the presence of two phenols to yield a bioactive molecule, with good binding affinity, and a noteworthy antiproliferative activity. This molecule **DFO**, presenting desirable cytotoxic properties, is an excellent prototype for further exploitation. Its particular chemical structure broadens the application scope of the compound to radioimaging and radiotherapy. Indeed, it has been shown that keto-ferrocenyl derivatives can be used as stable precursors of rhenium and technetium derivatives in the double ligand-transfer reaction. This will be further explored in the following chapter.

2.7 Sequel: the carboxylic acids

The previous study has demonstrated the importance of the ketone function in the triphenylethylene scaffold, and its role in the binding of the organometallic ligand to ERα, thanks to its interaction with Asp 351. Ruenitz *et al.*, and more particularly Willson *et al.* have also pointed out the dominant role of the carboxylate side-chain in the biological properties of their compounds [56, 121, 122]. Therefore, we wanted to further investigate this chemical functionality, and ultimately combine it with the ferrocenyl moiety.

2.7.1 Design

Of all the structural variations attempted by both research groups, compounds **BA1, BA3**, **GW5638**, and **GW7604** were found to be the most interesting (Fig. 2-19). Ruenitz *et al.* discovered that although **BA1** has an estrogenic activity, **BA3** with a longer side-chain has a better affinity with the receptor and a potent antiproliferative effect ($IC_{50} \simeq 20$ nM) [121]. More interestingly, they both exhibited beneficial effects as bone selective estrogen mimetics. Unfortunately, Ruenitz *et al.* have not yet proposed a molecular mechanism of action of their compounds.

In contrast, Willson *et al.* have done a thorough study to explain the behaviour of their compounds **GW5638** and **GW7604**, the active metabolite of **GW5638**. They have demonstrated that **GW5638/7604** is able to block the growth of breast cancer cells better than tamoxifen, and is efficacious even on tamoxifen-resistant breast cancer cells. Moreover, it has no uterotrophic nor endometrial behaviour. It functions as a full ER agonist in bone and the cardiovascular system [57]. A theoretical molecular modeling experiment has been performed to understand these features [58]. Jordan *et al.* proposed that the carboxylic acid side-chain repelled Asp 351, and therefore disrupted the surface charge. **GW5638/7604** loosely interacted with the aspartate [40]. The authors supposed that the resulting inappropriate surface charge should prevent the assembly of a transcription complex at the TGFα (transforming growth factor α) gene. Thus, the TGFα gene was not activated, and this could account for the observation that **GW5638/7604** silences the ER complex. In the case of OH-Tam, the amino side-chain interaction with Asp 351 probably enhanced TGFα gene activation instead, and could be responsible for some unwanted estrogenic properties of the (OH-Tam)-ER complex [149, 150].

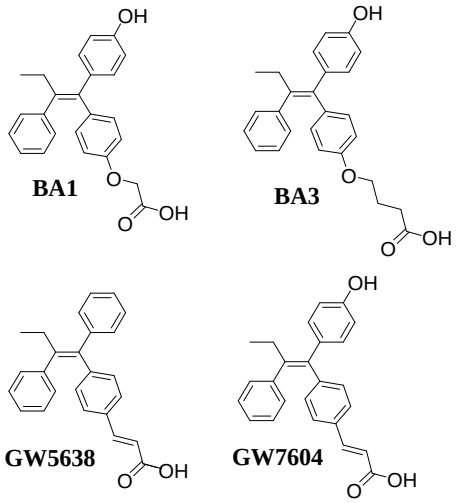

Figure 2-19: Carboxylic acid analogues of tamoxifen

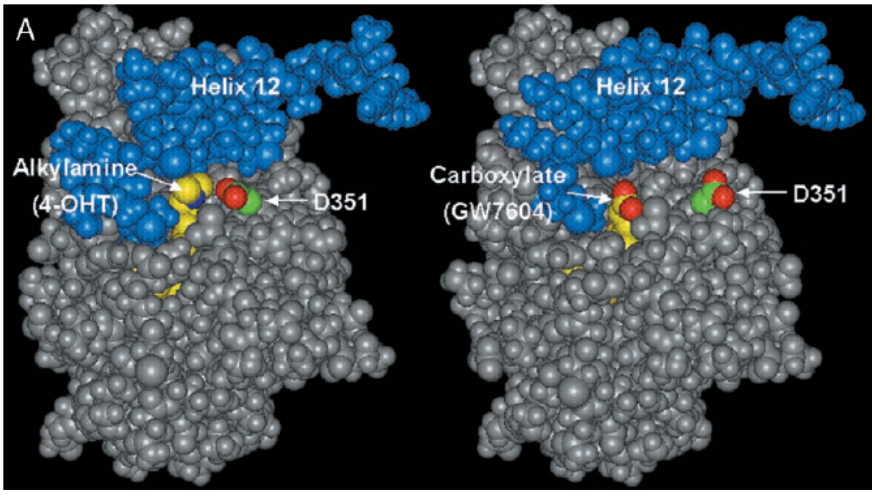

Figure 2-20: Molecular modeling of (left) **OH-Tam** and (right) **GW7604** in the LBD of ERα dimer.
Helix 12 is shown in blue. D351 stands for Aspartate 351.

However, the X-ray crystallographic structure of ERα LBD-**GW5638** indicated on the contrary a hydrogen bond between the acyl group and Asp 351, at crystallization pH of 5.6 [59]. The weakly acidic amino acid must have been protonated in the hydrophobic LBD pocket, allowing this hydrogen bonding. In fact, the acrylate carboxyl group also interacts with Leu 536 and Tyr 537 of ERα. This brings the N-terminal of Helix 12 closer to the ligand. The relocation of Helix 12 disrupts its exposed hydrophobic surface, which increases by 27%, as compared to the (OH-Tam)-ERα complex. This increase in hydrophobic surface could be correlated to a significant destabilization of ERα in MCF-7 cells. Thus **GW5638**-ER may be the target of proteins involved in ubiquitination. The new conformation of ERα might also facilitate the recruitment of co-repressors. This particular mechanism of action, different from tamoxifen, might explain the ability of **GW5638** to inhibit tamoxifen-resistant breast tumours.

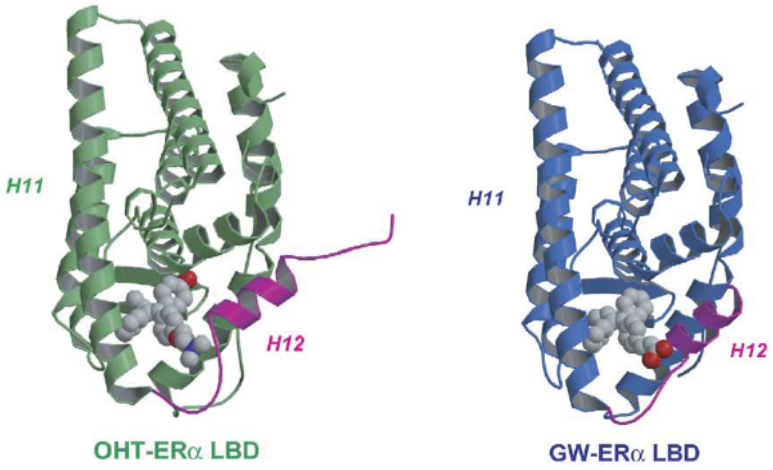

Figure 2-21: Structures of (left) (**OH-Tam**)-ERα LBD and (right) **GW5638**-ERα LBD obtained by crystallization. Helix 12 in the two structures is colored in magenta.

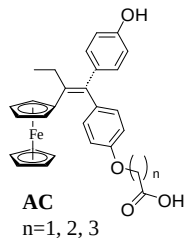

Figure 2-22: **AC** series

As a consequence, a combination of the ferrocifen structure and the carboxylic acid side-chain could produce molecules with interesting antiproliferative effects on tamoxifen-resistant

breast cancer cells (Fig. 2-22). The "ferrocene-conjugated spacer-phenol" scaffold necessary for the cytotoxicity of the ferrocifens and ferrocifenols (**Fc-diOH**) [132] is kept, and we also vary the length of the carboxylate side-chain, to produce the **AC** series.

2.7.2 Synthesis

The synthesis was similar to the **DF** and **FO** series. For **AC1** (n=1), **Fc-diOH** was directly reacted with ethyl bromoacetate, to avoid the protection/deprotection steps. It gave the mono (**15**) and di-alkylated (**16**) esters (Fig. 2-23). However, for **AC3** (n=3), the dialkylated compound was obtained directly, without allowing for the isolation of the mono-alkylated product. Hence, it was necessary to protect the phenol by a pivaloate group (yielding **17**) prior to reaction with ethyl 4-bromobutyrate (Fig. 2-24). The final carboxylic acids (**AC1** and **AC3**) were then obtained by saponification of their corresponding esters **15** and **18**. It was not possible to separate the *Z* and *E* isomers of either product, even by analytical HPLC.

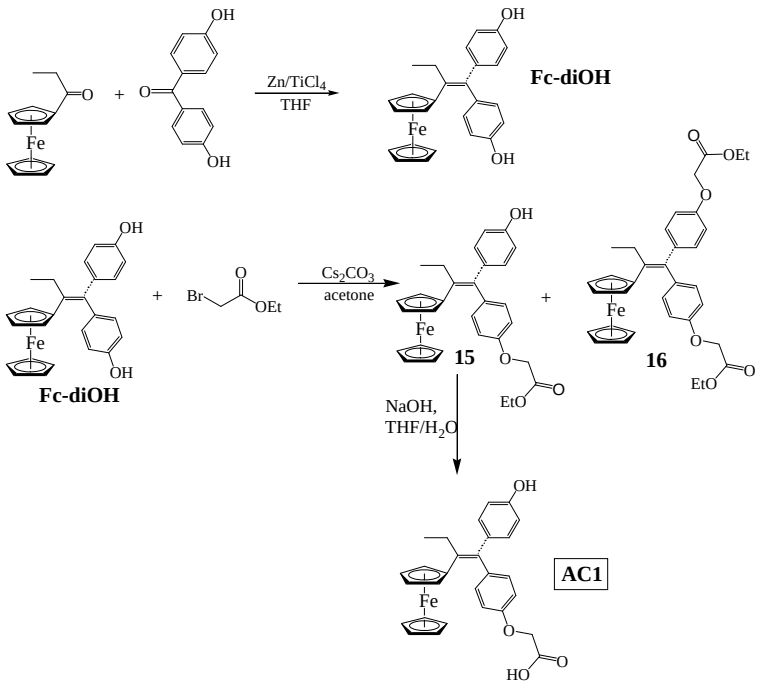

Figure 2-23: Synthetic pathway to **AC1**

The synthesis of **AC2** (n=2) was more difficult. For instance, Ruenitz *et al.* did not manage to obtain the carboxylic acid with a side-chain of 2 carbons between the phenoxy and the carboxylate functionalities [121]. The procedure used for **AC1** and **AC3** did not work at

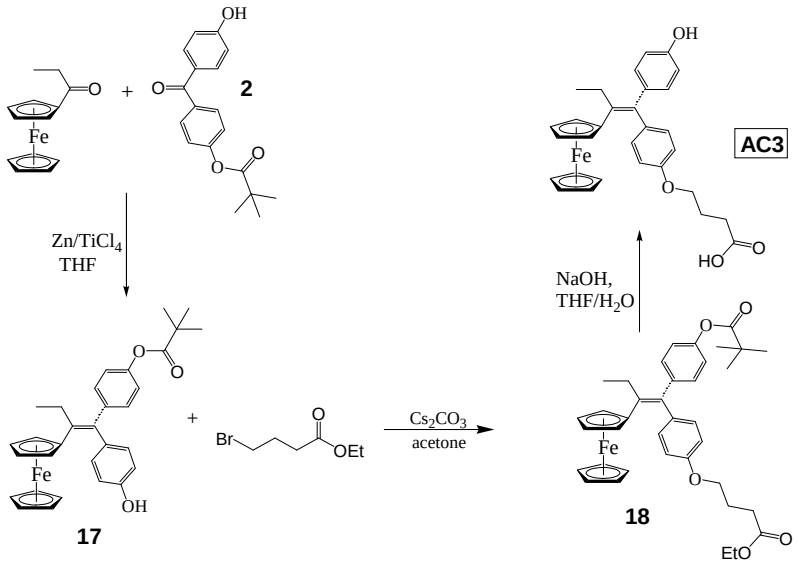

Figure 2-24: Synthetic pathway to **AC3**

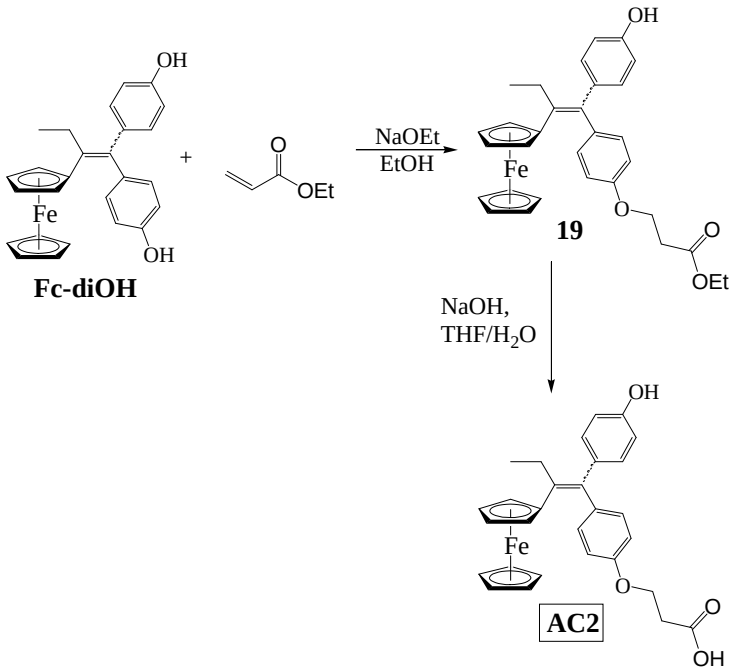

Figure 2-25: Synthetic pathway to **AC2**

all, as expected. Instead, we did succeed by another synthetic method, using an 1,4-addition on ethyl acrylate (Fig. 2-25) [151]. After stirring for two days **Fc-diOH** and ethyl acrylate together in an EtONa/EtOH solution, **19** was obtained in low yield (16%). **AC2** was then produced after saponification.

2.7.3 Biological experiments

Biological tests were performed in the same conditions as for the **DF** and **FO** series, in order to evaluate the biological interest of these new ferrocenyl carboxylic acids (Table 2.8 and Fig. 2-27). Because of the synthetic difficulties, tests on **AC2** could not be performed at the same time as those on **AC1** and **AC3**, but are underway. Preliminary results suggest that **AC1** and **AC3** have similar behaviour compared to the **BA** compounds proposed by Ruenitz *et al.* **AC1** has a lower affinity with ERα than **AC3** (0.33 and 1.2, respectively, in Table 2.8), in the same way that the **BA1** affinity value is about half that of **BA3** (1.2 and 2.5, respectively) [121]. Although **BA1** has a clear proliferative effect on MCF-7 cells (Fig. 2-27), **AC1** does not seem to influence the proliferation of the ER+ breast cancer cells. The very low affinity of **AC1** with ERα might be a reason for this lack of effect.

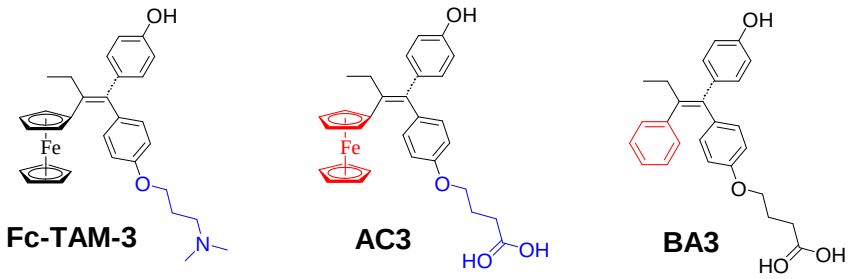

Figure 2-26: **AC3** and its analogues **Fc-TAM-3** and **BA3**

It could be interesting to compare **AC3** to two analogues: **Fc-TAM-3** and **BA3** (Fig. 2-26). The first one has the same chemical structure, but bears the classical amino side-chain instead of the carboxylate side-chain as in **AC3**. For the second one, we evaluate the effects of the substitution of its β phenyl group by a ferrocenyl unit in **AC3** (Fig. 2-26). Like **BA3**, **AC3** had also an antiproliferative effect on MCF-7 cells, though the activity was less strong. Indeed, the IC_{50} of **BA3** is approximated at 20 nM, while at 1 μM **AC3** only inhibited the growth of the MCF-7 cells by 30%. The ferrocenyl moiety did not seem to bring any additional cytotoxicity to the molecule. When compared to its other analogue **Fc-TAM-3**, its inhibition

Table 2.8: Relative binding affinity (RBA) values for ERα of the ferrocenyl compounds **AC1** and **AC3**, in DMSO at 4°C. Mean of 2 experiments ± range

Compound	**RBA with ERα**
AC1	0.33 ± 0.02
AC3	1.2 ± 0.1

activity is also weaker. At 1 μM, **Fc-TAM-3** inhibited the proliferation of MCF-7 cells by 86%. Therefore, the carboxylate side-chain seemed to induce a weaker antiproliferative effect than the amino side-chain. This is in contrast with the results obtained for **Fc-TAM-2** (n=2, in Fig 2-4). Indeed, for this ferrocenyl derivative, the substitution of the β phenyl group in OH-Tam by Fc resulted in an improved antiproliferative activity [93, 132]. In particular, **Fc-TAM-2** showed a potent cytotoxic activity on the ER- MDA-MB-231 cells, on which OH-Tam was not active.

However, like the **BA**s, the elongation of the side-chain of the **AC**s was crucial to observe an antiproliferative activity. This could look contradictory to the results found for the **DF** series. Precisely, we have found previously that the longer the side-chain of **DF**, the less biologically active is the compound, regarding the affinity as well as the influence on cancer cell growth. However, the ferrocenyl side-chain of **DF** is definitely much bulkier than the carboxylate side-chain of **AC**. Therefore, the sterical hindrance brought by the elongation of the side-chain should be more important for **DF** than **AC**. Besides, the acyl functionality on the side-chain of **AC** is very likely to interact with the Asp 351 of ERα, as it has been seen for **GW7604** and **DFO**. This stabilizing interaction is not possible for the **DF**s, since the compounds do not have the acyl function. Hence, we may infer that the side-chain of **AC1** is not long enough for the acyl group to interact with Asp 351, and this could explain its poor affinity and the lack of activity on the proliferation of the ER+ cancer cells. On the other hand, the acyl group of **AC3** might be brought close enough to Asp 351 to engage in hydrogen bonding. Consequently, this could account for the better affinity of **AC3** and its antiproliferative effect.

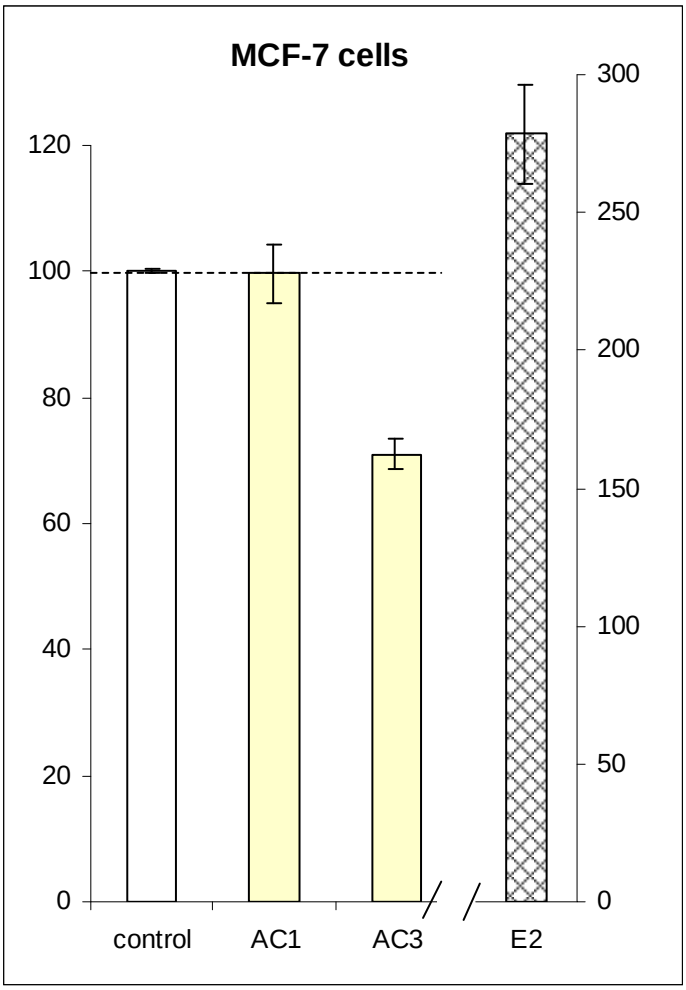

Figure 2-27: Effect of **AC**s on the growth of MCF-7 cells.
1 μM of **AC**s and 1 nM of estradiol (E_2) were incubated with MCF-7 cells (medium with phenol red). After 6 days of culture. Mean of 2 experiments ± S.D.

2.7.4 Conclusion

While further exploring the influence of the acyl functionality on the side-chain of tamoxifen-like molecules, we have found that again it may play a role in the biological behaviour of the **AC** molecules. The side-chain of **AC1** (n=1) may not be long enough for the acyl to interact with Asp 351 of ER, unlike **AC3** (n=3). Thus, its affinity is lower than for **AC3**, and **AC1** did not show an influence on the proliferation of MCF-7 breast cancer cells. Though weaker than **BA3**, the ferrocenyl carboxylic acid **AC3** did have an antiproliferative effect on these cancer cells at 1 μM. Curiously, **BA1** and **BA3** have opposite biological behaviours, though chemically similar. This needs further investigation, and maybe re-checking of the published results. Given the available information to date, the combination of two moieties known to induce an antiproliferative activity (the "ferrocene-conjugated spacer-phenol" motif and the carboxylate side-chain) did not seem to contribute any additional inhibition potency to the compounds, and the effect was even weaker. Some biological experiments are still underway to determine more precisely the phenomenon, but this unexpected behaviour needs further studies, both in molecular modeling studies and in electrochemistry.

2.8 Experimental section

2.8.1 Synthesis

General remarks:

All air-sensitive reactions were carried out under argon atmosphere, using standard Schlenk and vacuum-line techniques. "Standard work-up" refers to extraction of the reaction mixture with dichloromethane, washing of the organic phase with water, drying over $Mg(SO_4)$, filtering, and removal of the solvent under reduced pressure. The product was then purified by flash chromatography. Anhydrous THF and diethyl-ether were obtained by distillation from sodium/benzophenone. Preparative TLC chromatography was performed on silica gel 60 GF254. Flash chromatography was performed on silica gel Merck 60 (0.040-0.060 mm), or when necessary on aluminium oxide. HPLC were measured by a Shimadzu instrument. HPLC system: Kromasil C18 columns (analytical: 4.6x250, preparative: 20x250), eluent: water/acetonitrile mixture. Infrared spectra were obtained on a IR-FT BOMEM Michelson-100 spectrometer equipped with a DTGS detector. ^{1}H and ^{13}C NMR spectra were recorded on 300 MHz Bruker spectrometer and the results δ given in ppm. Mass spectrometry was performed with a Nermag R 10-10C spectrometer. High Resolution Mass Spectrometry was done with a MStation 700 (JEOL) spectrometer. Melting points were measured with a Kofler device. Elemental analyses were performed by the Microanalysis Service of ICSN (Institut de Chimie des Substances Naturelles), Gif-sur-Yvette. Pivaloate ketones **1**, **2** were prepared by the procedure described in the literature. [139] The synthesis of compounds **Fc-diOH** [93], **3a** [139], **5**, **6**, **7**, **8**, **9** [143] and ferrocenyl-*p*-methoxybenzylketone (**FRAG**) [152] were already described in literature. Compounds **DF1** and **MF2a** were prepared according to a procedure proposed by Dr. Clara Rigamonti, University of Milan. Compound **DF2** has also been attempted by her, but by a different route.

1-(4-hydroxyphenyl)-1,2-*bis*-(4-trimethyacetoxyphenyl)but-1-ene (3)

To a suspension of Zn (5.36 g, 82 mmol) in 100 mL of anhydrous THF, $TiCl_4$ (5.3 mL, 48 mmol) was added drop-wise under inert atmosphere. After being under reflux for 2h, (*p*-trimethylacetoxy)propiophenone (**1**) (2.3 g, 10 mmol) and 4,4'-hydroxy(trimethylacetoxy) benzophenone (**2**) (3.58 g, 12 mmol) dissolved in 50 mL of anhydrous THF were added.

The mixture was left under reflux for another 2h. After cooling, the mixture was hydrolysed by 200 mL of acidified water, and went under standard work-up. The crude product was recrystallised in ethanol, yielding a white powder (3.36 g, 67% yield) of a (*Z*+*E*)-**3** mixture.

^{1}H *NMR* (300 MHz, $CDCl_3$): δ 0.91 (t, J = 7.3 Hz, 3H, CH_3 of Et); 1.34 and 1.37 (s, 18H, CH_3 of $C(CH_3)_3$); 2.45 (q, J = 7.3 Hz, 2H, CH_2); 6.47, 6.71, 6.87, 7.05, 7.09, 7.22 (6 d, J = 8.6 Hz, 6×2H, CH_{arom}). ^{13}C *NMR* (75 MHz, $CDCl_3$): δ 13.5 (CH_3 of Et); 27.1 (CH_3 of $C(CH_3)_3$); 28.9 (CH_3 of Et); 39.0 ($C(Me)_3$); 114.5, 120.9, 121.1, 130.4, 130.5, 132.1 (CH_{arom}); 135.1, 137.8, 139.7 (Cq_{arom}); 140.8 and 141.0 (C=C); 149.2, 149.7, 153.8 (Cq_{arom}); 177.3 (C=O). *IR* (KBr, cm^{-1}): 3407 ν(O-H), 2977 ν(C-H_{arom}), 1749 and 1726 ν(C=O), 1610 ν(C=C), 1504 ν(C=C arom). *MS* (EI): m/z = 500 $[M]^{\cdot+}$, 57 $[^{t}Bu]^{+}$. *HRMS* (EI, 70 eV, $C_{32}H_{36}O_5$: $[M]^{\cdot+}$) calcd: 500.2563, found: 500.2574.

1-(4-hydroxyphenyl)-1-(4-trimethylacetoxyphenyl)-2-phenylbut-1-ene (3b)

The same procedure as for **3** was used, with 4-hydroxybenzophenone (4 g, 20 mmol) and (4-trimethyl-acetoxy)propiophenone (4.69 g, 20 mmol) to give 1-(4-hydroxyphenyl)-1-(4-trimethylacetoxyphenyl)-2-phenyl but-1-ene (**3b**) in 70% yield, as a mixture of both isomers (ratio = 1/1):

^{1}H *NMR* (300 MHz, $CDCl_3$): δ 0.90 (m, 3H, CH_3 of Et), 1.33 and 1.34 (s, 9H, CH_3 of $C(CH_3)_3$), 2.41 (m, 2H, CH_2), 4.74 and 4.99 (s, 1H, OH), 6.46 - 7.30 (m, 13H, CH_{arom}). ^{13}C *NMR* (75 MHz, $CDCl_3$): δ 13.6 (CH_3 of Et); 27.1 (CH_3 of $C(CH_3)_3$); 28.9 (CH_2); 39.1 (Cq of ^{t}Bu); 114.4, 115.0, 120.8, 120.9, 125.8, 125.6, 126.6, 127.4, 128.1, 129.4, 130.6, 130.7, 130.8, 132.1 (CH_{arom}); 135.4, 136.0, 138.6, 138.7, 139.7, 139.8 (Cq_{arom}); 140.5, 141.0, 143.1, 143.6 (C=C); 149.2, 153.6, 154.4 (Cq_{arom}); 177.2 (C=O). *MS* (EI): m/z = 400 $[M]^{\cdot+}$, 57 $[^{t}Bu]^{+}$. *Anal.* Calcd for $C_{27}H_{28}O_3$: C, 80.90; H, 6.99. Found: C, 80.77; H, 6.96

General procedure for the preparation of 4, 4a, and 4b

In a Schlenk tube, under inert atmosphere, KH at 25-35% in oil (0.03 mL, 1.2 mmol; 1.2 eq) was dispersed in 10 mL of anhydrous THF. After stirring for 10 min, a red solution of **3**, **3a**, **3b** (1 mmol) respectively, in 10 mL of anhydrous THF, was added. The mixture was stirred under reflux for 15 min. α-chloroacetylferrocene (**5**) (443 mg, 1.5 mmol) in 10

mL of anhydrous THF was finally added. The solution was heated under reflux overnight. After hydrolysis and standard work-up, orange solids of **4**, **4a**, **4b** were obtained.

1-[4-(2-ferrocenyl-2-oxoethoxy)phenyl]-1,2-*bis*-(4-trimethylacetoxyphenyl)but-1-ene (4)

300 mg of **4** were isolated as a mixture of both isomers (ratio = 1/1) in 41% yield.

^{1}H NMR (300 MHz, $CDCl_3$): δ 0.89 (t, J = 7.3 Hz, 3H, CH_3 of Et), 1.33 and 1.36 (s, 18H, CH_3 of $C(CH_3)_3$), 2.42 (q, J = 7.2 Hz, 2H, CH_2), 4.16 (s, 5H, Cp), 4.54 (t, J = 1.9 Hz, 2H, C_5H_4), 4.82 (s, 2H, O-CH_2-CO), 4.87 (t, J = 7.2 Hz, 2H, C_5H_4), 6.65-7.23 (m, 12H, CH_{arom}). *^{13}C NMR* (75 MHz, $CDCl_3$): δ 13.6 (CH_3 of Et); 27.1 (CH_3 of $C(CH_3)_3$); 29.0 (CH_2); 39.0 and 39.1 (Cq of ^{t}Bu); 69.3, 72.3, 72.5, 72.6 (C_5H_4); 70.0 (Cp); 71.4 (O-CH_2-CO), 77.2 (Cip of C_5H_4); 113.9, 121.0, 121.1, 130.4, 130.5, 132.1 (CH_{arom}); 136.0, 137.6, 139.5 (Cq_{arom}); 140.9 and 141.1 (C=C); 149.3, 149.8, 156.4 (Cq_{arom}); 177.0 (O-C=O); 199.3 (-(C=O)-(η^5-C_5H_4)). *IR* (KBr, cm^{-1}) : 2972 ν(C-H Ph), 1751 ν(C=O), 1685 ν(FcC=O), 1507 ν(C=C arom). *MS* (EI): m/z = 726 $[M]^+$, 121 $[CpFe]^+$, 57 $[^tBu]^+$. *MS* (CI, NH_3): m/z = 744 $[M+NH_4]^+$, 727 $[M+H]^+$. *Anal.* Calcd for $C_{44}H_{46}O_6Fe$: C, 72.66; H, 6.33. Found: C, 72.38; H, 6.36.

1-[4-(2-ferrocenyl-2-oxoethoxy)phenyl]-1- (4-trimethylacetoxyphenyl)-2-phenylbut-1-ene (4a)

4a was obtained as a mixture of both isomers (ratio = 1/1) in 50% yield.

^{1}H NMR (300 MHz, $CDCl_3$): δ 0.88 (m, 3H, CH_3 of Et), 1.36 (s, 9H, CH_3 of $C(CH_3)_3$) 2.42 (m, 2H, CH_2), 4.16 (s, 5H, Cp), 4.54 (t, 2H, C_5H_4), 4.86 (t, 2H, C_5H_4), 4.80 (s, 2H, O-CH_2-CO), 6.61-7.25 (m, 13H, CH_{arom}). *^{13}C NMR* (75 MHz, $CDCl_3$): δ 13.5 (CH_3 of Et); 27.1 (CH_3 of $C(CH_3)_3$); 29.1 (CH_2); 39.1 (Cq of ^{t}Bu); 69.4 and 72.5 (C_5H_4); 70.0 (Cp); 71.5 (O-CH_2-CO); 77.2 (Cip of C_5H_4); 113.7, 121.1, 126.1, 127.9, 129.6, 130.4 and 132.0 (CH_{arom}); 136.1, 136.2, 137.2, 140.8, 141.0, 142.0, 142.2, 149.7 and 156.3 (C=C and Cq_{arom}); 177.1 (O-C=O); 199.3 (-(C=O)-(η^5-C_5H_4)). *MS* (EI): m/z = 626 $[M]^{\cdot+}$, 121 $[FeCp]^+$, 57 $[^tBu]^+$. *HRMS* (EI, $C_{39}H_{38}O_4Fe$: $[M]^{\cdot+}$) calcd: 626.2120, found: 626.2117.

1-[4-(2-ferrocenyl-2-oxoethoxy)phenyl]-2- (4-trimethylacetoxyphenyl)-1-phenylbut-1-ene (4b)

4b was obtained as a mixture of both isomers (ratio = 2/3) in 45% yield.

^1H NMR (300 MHz, $CDCl_3$): δ 0.90 (m, 3H, CH_3 of Et), 1.32 and 1.34 (s, 9H, CH_3 of $C(CH_3)_3$), 2.41 (m, 4H, CH_2), 4.16 and 4.23 (s, 5H, Cp), 4.54 and 4.55 (t, J = 1.9 Hz, 2H, C_5H_4), 4.82 and 4.97 (s, 2H, O-CH_2-CO), 4.88 and 4.94 (t, J = 1.9 Hz, 2H, C_5H_4), 6.66-7.36 (m, 13H, CH_{arom}). *^{13}C NMR* (75 MHz, $CDCl_3$) : δ 13.6 (CH_3 of Et); 27.1 (CH_3 of $C(CH_3)_3$); 29.0 (CH_2); 39.0 (Cq of ^{t}Bu); 69.4, 72.5, 72.6 (C_5H_4); 70.0 (Cp); 71.5 (O-CH_2-CO); 77.2 (Cip of C_5H_4); 113.9, 114.5, 120.8, 121.0, 126.6, 127.4, 128.1, 129.4, 130.5, 130.7, 130.8, 132.0 (CH_{arom}); 138.5, 138.6, 139.6 (Cq_{arom}); 140.8 and 141.2 (C=C); 149.3, 156.3, 157.1 (Cq_{arom}); 177.0 (O-C=O); 199.4 (-CO-(η^5-C_5H_4)). *MS* (EI): m/z = 626 $[M]^{\cdot+}$, 121 $[FeCp]^+$, 57 $[^tBu]^+$. *HRMS* (EI, $C_{39}H_{38}O_4Fe$: $[M]^{\cdot+}$) calcd: 626.2120, found: 626.2120.

General procedure for the preparation of DFO, MFOa, and MFOb

4, **4a**, and **4b** (0.3 mmol) were respectively dissolved in 5 mL of THF. NaOH (220 mg, excess) in 5 mL of water was added. The mixture was allowed to stir under reflux for 6h. The reaction mixture was extracted with dichloromethane, the organic phase was washed with water, dried over $MgSO_4$, filtered, and the solvent removed under reduced pressure. By flash chromatography, orange-red solids of **DFO**, **MFOa**, and **MFOb** were isolated as a mixture of *Z* and *E* isomers.

1-(2-ferrocenyl-2-oxoethoxyphenyl)-1,2-*bis*-(4-hydroxyphenyl)but-1-ene (DFO)

83% yield.

MS (EI): m/z = 558 $[M]^{\cdot+}$, 121 $[CpFe]^+$.

The two isomers were separated by preparative HPLC (Kromasil C18, MeCN:H_2O 70:30).

(Z)-isomer: *^1H NMR* (400 MHz, DMSO-d_6): δ 0.83 (t, J = 7.2 Hz, 3H, CH_3), 2.34 (q, J = 7.2 Hz, 2H, CH_2), 4.23 (s, 5H, Cp), 4.62 (t, 2H, H_β of C_5H_4), 4.88 (t, H_α of C_5H_4), 5.04 (s, 2H, O-CH_2-CO), 6.55 (d, J = 8.2 Hz, 2H, C*H*-COH of β-C_6H_4), 6.65 (d, J = 8.4 Hz, 2H, C*H*-C-O- of α'-C_6H_4), 6.72 (d, J = 8.7 Hz, 4H, C*H*-C-OH of α-C_6H_4 and C*H*-C-C- of α'-C_6H_4), 6.88 (d, J = 8.2 Hz, 2H, β-C_6H_4), 6.94 (d, J = 8.4 Hz, 2H, α-C_6H_4), 9.14 (s, 1H, OH), 9.20 (s, 1H, OH). *^{13}C NMR* (75 MHz, DMSO-d_6): δ 13.5 (CH_3 of Et); 28.5 (CH_2); 68.8 (C_5H_4); 69.7 (Cp); 70.0 (O-CH_2-CO); 72.3 (C_5H_4); 75.9 (Cip of C_5H_4); 113.6, 114.8, 114.9, 130.1, 130.3, 131.3 (CH_{arom}); 132.3, 134.2, 136.3, 136.7, 139.9 (Cq_{arom} and

C=C); 155.4, 155.7, 155.9 (Cq_{arom}); 198.4 (C=O). *IR* (KBr, cm^{-1}): 3423 ν(OH), 1663 ν(C=O), 1609 ν(C=C), 1509 ν(C=C arom). *Anal.* Calcd for $C_{34}H_{30}O_4Fe$: C, 72.54; H, 5.88. Found: C, 72.71; H, 5.58. The (*Z*) isomer was identified by 2D-NMR.

(E)-isomer: *^{1}H NMR* (400 MHz, DMSO-d_6): δ 0.81 (t, J = 7.2 Hz, 3H, CH_3), 2.33 (q, J = 7.2 Hz, 2H, CH_2), 4.28 (s, 5H, Cp), 4.65 (t, 2H, H_β of C_5H_4), 4.94 (t, H_α of C_5H_4), 5.19 (s, 2H, O-CH_2-CO), 6.40 (d, J = 8.4 Hz, 2H, α'-C_6H_4), 6.54 (d, J = 8.2 Hz, 2H, β-C_6H_4), 6.59 (d, J = 8.4 Hz, 2H, α'-C_6H_4), 6.87 (d, J = 8.2 Hz, 2H, β-C_6H_4), 6.95 (d, J = 8.4 Hz, 2H, α-C_6H_4), 7.06 (d, J = 8.4 Hz, 2H, α-C_6H_4), 9.14 (s, 1H, OH), 9.20 (s, 1H, OH). *^{13}C NMR* (75.4 MHz, DMSO-d_6): δ 13.5 (CH_3); 28.3 (CH_2); 68.8 (C_5H_4); 69.8 (Cp); 70.2 (O-CH_2-CO); 72.3 (C_5H_4); 75.9 (Cip of C_5H_4); 114.4, 114.7, 130.0, 130.3, 131.3 (CH_{arom}); 132.5, 133.9, 136.6, 140.0 (Cq_{arom} and C=C); 155.0, 155.2, 156.6 (Cq_{arom}); 198.5 (C=O). *mp* = 114°C. *IR* (KBr, cm^{-1}) : 3429 ν(OH), 1665 ν(C=O), 1608 ν(C=C), 1509 ν(C=C arom.). *Anal.* Calcd for $C_{34}H_{30}O_4Fe$: C, 72.54; H, 5.88. Found: C, 72.48; H, 5.53. The (*E*) isomer was identified by 2D-NMR and X-ray crystal structure.

1-(2-ferrocenyl-2-oxoethoxyphenyl)-1-(4-hydroxyphenyl)-2- phenylbut-1-ene (MFOa)

MFOa was obtained in 75% yield.

^{1}H NMR (300 MHz, $CDCl_3$): δ 0.90 (t, 3H, CH_3), 2.45 (m, 2H, CH_2), 4.16 and 4.23 (s, 5H, Cp), 4.55 and 4.60 (t, J = 1.9 Hz, 2H, C_5H_4), 4.81 and 4.98 (s, 2H, O-CH_2-CO), 4.87 and 4.95 (t, J = 1.9 Hz, 2H, C_5H_4), 6.47-7.19 (m, 13H, CH_{arom}). *^{13}C NMR* (75 MHz, $CDCl_3$): 13.6 (CH_3); 29.1 (CH_2); 69.4, 72.7, 72.8 (C_5H_4); 70.0 and 70.2 (Cp); 71.3 and 71.4 (O-CH_2-CO); 113.7, 114.4, 115.1, 126.0, 127.8, 127.9, 129.7, 130.7, 132.1 (CH_{arom}); 135.6, 136.0, 136.8, 137.3, 137.7 (Cq_{arom}); 141.2, 141.3, 142.6 (C=C); 153.8, 154.7, 156.1, 156.9 (Cq_{arom}); 199.9 (C=O). *MS* (ESI): m/z = 565 $[M+Na]^+$, 541 $[M+H]^-$. *IR* (KBr, cm^{-1}) : 1665 ν(C=O), 1608 ν(C=C), 1508 ν(C=C arom.). *HRMS* (EI, $C_{34}H_{30}O_3Fe$: $[M]^{\cdot+}$) calcd: 542.1545, found: 542.1549.

1-(2-ferrocenyl-2-oxoethoxyphenyl)-2-(4-hydroxyphenyl)-1- phenylbut-1-ene (MFOb)

MFOb was obtained in 73% yield, as a mixture of both isomers (Z/E 45/55).

(Z)-isomer: ^{1}H NMR (400 MHz, DMSO-d_6): δ 0.83 (t, 3H, CH_3), 2.30 (q, J = 7.44 Hz, 2H, CH_2), 4.23 (s, 5H, Cp), 4.61 (t, 2H, H_β of C_5H_4), 4.88 (t, H_α of C_5H_4), 5.04 (s, 2H, O-CH_2-CO), 6.56 (d, J = 8.3 Hz, 2H, C*H*-COH of β-C_6H_4), 6.66 (d, J = 8.7

Hz, 2H, C*H*-CO of α'-C_6H_4), 6.74 (d, J = 8.7 Hz, 2H, α'-C_6H_4), 6.91 (d, J = 8.3 Hz, 2H, β-C_6H_4), 7.16 (d, J = 7.2 Hz, 2H, *ortho*-CH of α-C_6H_4), 7.26 (d, 2H, *para*-CH of α-C_6H_4), 7.34 (d, J = 7.5 Hz, 2H, *meta*-CH of α-C_6H_4), 9.25 (s, 1H, OH). The (*Z*) isomer was identified by 2D-NMR.

(E)-isomer: ^{1}H *NMR* (400 MHz, DMSO-d_6): δ 0.93 (t, 3H, CH_3), 2.45 (q, 2H, CH_2), 4.16 (s, 5H, Cp), 4.55 and 4.94 (t, t, J = 1.9 Hz, 2H, 2H, C_5H_4), 4.81 (s, 2H, O-CH_2-CO), 6.61-7.33 (m, 13H, CH_{arom}).

(Z+E)-mixture: ^{13}C *NMR* (100.61 MHz, $CDCl_3$): δ 13.6 (CH_3); 28.9 (CH_2); 69.4, 72.6 (C_5H_4); 70.1 (Cp); 71.5 (O-CH_2-CO); 77.2 (Cip of C_5H_4); 113.8, 114.5, 114.8, 114.9, 125.6, 125.7, 126.5, 127.4, 127.6, 128.1, 129.5, 130.8, 130.9, 132.0 (CH_{arom}); 137.6, 138.4, 139.5, 141.6, 143.4 (C=C and Cq_{arom}); 153.9, 160.6 (Cq_{arom}); 200.5 (C=O). *MS* (CI, NH_3): m/z = 560 $[M+NH_4]^+$, 543 $[M+H]^+$. *IR* (CH_2Cl_2, cm^{-1}) : 3595 ν(OH), 1686 ν(C=O), 1606 ν(C=C), 1509 ν(C=C arom.). *Anal* Calcd for $C_{34}H_{30}O_3Fe$: C, 75.22; H, 5.53. Found: C, 75.35; H, 5.57.

General procedure for the preparation of 10, 11, 12, and 13

A solution of diethyl azodicarboxylate (DEAD) (0.42 g, 2.4 mmol) in dry THF (3 mL) was added drop-wise at 0°C into a solution of ferrocenyl alcohol **6**, **7**, **8**, or **9** (2.4 mmol) respectively. **3** (1 g, 2 mmol) and triphenylphosphine (0.74 g, 2.8 mmol) in dry THF (12 mL) were then introduced into the reaction mixture. The reaction was stirred at room temperature for 48 h. The solvent was evaporated under vacuum and the residue was purified by aluminium oxide column chromatography (petroleum ether) to obtain **10**, **11**, **12**, **13** (E/Z ratio = 1/1) as yellow solids. These compounds were recrystallized from a ether/pentane solution.

1-[4-(ferrocenylmethoxy)phenyl]-1,2-*bis*-[4-(trimethylacetoxy)phenyl]but-1-ene (10)

The reaction was done with 0.519 g (2.4 mmol) of ferrocenylmethanol **6**. Yield 83%.

^{1}H *NMR* (300 MHz, $CDCl_3$) : δ 0.92 (t, J = 7.4 Hz, 3H, CH_3), 1.30, 1.34, 1.35, 1.37 (s, 18H, ^{t}Bu), 2.46 (q, J = 7.4 Hz, 2H, CH_2), 4.15 and 4.20 (s, 5H, Cp), 4.16 and 4.21 (t, J = 1.8 Hz, 2H, C_5H_4), 4.26 and 4.34 (t, J = 1.8 Hz, 2H, C_5H_4), 4.67 and 4.81 (s, 2H, OCH_2), 6.50-7.25 (m, 12H, H_{arom}). ^{13}C *NMR* (75 MHz, $CDCl_3$): δ 13.5 (CH_3); 27.1 (CH_3 of ^{t}Bu); 29.0 and 29.1 (CH_2); 39.0 and 39.1 (Cq of ^{t}Bu); 66.3 and 66.6 (OCH_2); 68.5

(Cp); 68.6 (C_5H_4), 69.2 (C_5H_4); 82.6 (Cip of C_5H_4); 113.8 and 114.3 (CH_{arom}); 120.4 and 120.9 (CH_{arom}); 120.9 and 121.1 (CH_{arom}); 130.4 and 130.5 (CH_{arom}); 131.7 and 131.9 (CH_{arom}); 135.1 and 135.8; 137.8 and 137.9, 139.5, 139.7, 140.5, 140.7, 141.1, 141.2, 149.0, 149.3, 149.3, 149.8, 157.0, 157.8 (C=C and C_{arom}); 177.0, 177.1 (C=O). *MS* (EI): m/z = 698 $[M]^{\cdot+}$, 199 $[CpFe(\eta^5\text{-}C_5H_4)CH_2]^+$. *IR* (KBr, cm^{-1}): 1752 ν(C=O). *Anal.* Calcd for $C_{43}H_{46}FeO_5$: C, 73.92; H, 6.63. Found: C, 73.58; H, 6.66.

1-[4-(2-ferrocenylethoxy)phenyl]-1,2-*bis*-(4-trimethylacetoxyphenyl)but-1-ene (11)

The reaction was done with 0.552 g (2.4 mmol) of ferrocenylethanol **7**. Yield 85%.

^{1}H NMR (300 MHz, $CDCl_3$): δ 0.84 and 0.86 (t, J = 7.4 Hz, 3H, CH_3), 1.22, 1.25, 1.26, 1.29 (s, 18H, ^{t}Bu), 2.38 and 2.41 (q, J = 7.4 Hz, 2H, CH_2), 2.66 and 2.76 (t, J = 7.0 Hz, 2H, CH_2), 3.89 and 4.01 (t, J = 7.0 Hz, 2H, OCH_2), 3.90-4.20 (m, 9H, (η^5-C_5H_4)FeCp), 6.49 and 6.66 (d, J = 8.8 Hz, 2H, H_{arom}), 6.65-7.20 (m, 10H, H_{arom}). *^{13}C NMR* (75 MHz, $CDCl_3$): δ 13.6 (CH_3); 27.1 (CH_3 of ^{t}Bu); 29.0 and 29.5 (CH_2); 39.0 (Cq of ^{t}Bu); 67.4 and 67.5 (C_5H_4); 68.2 and 68.4 (OCH_2); 68.6 (Cp + (η^5-C_5H_4)); 84.8 (Cip of C_5H_4); 113.5 and 114.1 (CH_{arom}); 120.4 and 120.9 (CH_{arom}); 121.0 and 121.1 (CH_{arom}); 130.4 and 130.5 (CH_{arom}); 130.5 and 130.6 (CH_{arom}); 131.7 and 132.0 (CH_{arom}); 135.0, 135.7, 137.8, 137.9, 139.5, 139.6, 140.5, 140.7, 141.1, 141.2, 149.0, 149.2, 149.3, 149.7, 156.9, 157.7 (C=C and C_{arom}); 177.0 (C=O). *MS* (CI, NH_3) m/z : 712 $[M+H]^+$, 730 $[M+NH_4]^+$. *IR* (KBr, cm^{-1}): 1752 ν(C=O). *Anal.* Calcd for $C_{44}H_{48}FeO_5$: C, 74.15; H, 6.78. Found: C, 74.03; H, 6.84.

1-[4-(3-ferrocenylpropoxy)phenyl]-1,2-*bis*-(4-trimethylacetoxyphenyl)but-1-ene (12)

The reaction was done with 0.586 g (2.4 mmol) of ferrocenylpropanol **8**. Yield 70%.

^{1}H NMR (300 MHz, $CDCl_3$): δ 0.90 and 0.91 (t, J = 7.4 Hz, 3H, CH_3), 1.30 and 1.34 (s, 9H, ^{t}Bu), 1.34 and 1.37 (s, 9H, ^{t}Bu), 1.86-2.09 (m, 2H, CH_2), 2.39-2.59 (m, 4H, 2 CH_2), 3.86 and 3.99 (t, J = 6.3 Hz, 2H, OCH_2), 4.02-4.14 (m, 9 H, (η^5-C_5H_4)FeCp), 6.57 and 6.73 (d, J = 8.8 Hz, 2H, H_{arom}), 6.74-7.24 (m, 10H, H_{arom}). *^{13}C NMR* (75 MHz, $CDCl_3$): δ 12.7 (CH_3); 25.0 (CH_2); 26.3 (CH_3 of ^{t}Bu); 28.1 and 28.8 (CH_2); 29.6 (CH_2 of Et); 38.2 (Cq of ^{t}Bu), 66.2 (OCH_2); 66.3 and 66.4 (C_5H_4), 67.2 (C_5H_4), 67.6 (Cp), 87.4 (Cq, Cp), 112.6 and 113.2 (CH_{arom}), 119.5 and 120.2 (CH_{arom}), 120.0 (CH_{arom}), 129.5 (CH_{arom}), 129.6 (CH_{arom}), 130.9 and 131.1 (CH_{arom}), 134.1, 136.9, 138.7, 139.8, 140.2, 148.4, 148.8, 151.6, 152.5, 156.2, 157.1 (C=C and C_{arom}); 176.2 (C=O). *MS* (EI) m/z :

726 $[M]^{\cdot+}$, 661 $[M\text{-}Cp]^+$, 199 $[CpFe(\eta^5\text{-}C_5H_4)CH_2]^+$, 121 $[CpFe]^+$, 57 $[^tBu]^+$. *IR* (KBr, cm^{-1}): 1752 ν(C=O). *Anal.* Calcd for $C_{45}H_{50}FeO_5$: C, 74.37; H, 6.93. Found: C, 74.28; H, 6.99.

1-[4-(4-ferrocenylbutoxy)phenyl]-1,2-*bis*-(4-trimethylacetoxyphenyl)but-1-ene (13)

The reaction was done with 0.620 g (2.4 mmol) of ferrocenylbutanol **9**. Yield 74%.

^1H NMR (300 MHz, $CDCl_3$): δ 0.92 and 0.94 (t, J = 7.0 Hz, 3H, CH_3), 1.27, 1.30, 1.35, 1.38 (s, 18H, ^{t}Bu), 1.52-1.90 (m, 4H, CH_2-CH_2), 2.30-2.55 (m, 4H, CH_2), 3.85 and 3.99 (t, J = 6.2 Hz, 2H, OCH_2), 4.03 and 4.04 (s, 2H, C_5H_4), 4.05 and 4.06 (s, 2H, C_5H_4), 4.09 and 4.12 (s, 5H, Cp), 6.50-7.30 (m, 12H, H_{arom}). *^{13}C NMR* (75 MHz, $CDCl_3$): δ 13.6 (CH_3); 27.2 (CH_3 of ^{t}Bu); 27.5 (CH_2); 29.0 and 29.7 (CH_2); 29.2 (CH_2); 29.3 (CH_2); 39.0 (Cq of ^{t}Bu); 39.1 (Cq of ^{t}Bu); 67.1 (C_5H_4); 67.4 and 67.7 (OCH_2); 68.1 (C_5H_4); 68.5 (Cp); 89.0 (Cq of C_5H_4); 113.4 and 114.0 (CH_{arom}); 120.4 and 120.9 (CH_{arom}); 120.9 and 121.1 (CH_{arom}); 130.4 and 130.5 (CH_{arom}); 130.5 (CH_{arom}); 131.7 and 132.0 (CH_{arom}); 134.9, 135.6, 137.8, 137.9, 139.6, 140.5, 140.6, 141.1, 149.2, 149.7, 155.0, 157.2 (C=C and C_{arom}); 176.9, 177.0 and 177.1 (C=O); 177.2 (C=O). *MS* (EI) m/z : 740 $[M]^{\cdot+}$, 199 $[CpFe(\eta^5\text{-}C_5H_4)CH_2]^+$, 121 $[CpFe]^+$. *IR* (KBr, cm^{-1}): 1754 ν(CO). *Anal.* Calcd for $C_{46}H_{52}FeO_5$: C, 74.58; H, 7.07. Found: C, 74.51; H, 7.36.

1-[4-(2-ferrocenylethoxy)phenyl]-1-phenyl-2-(4-trimethylacetoxyphenyl)but-1-ene (14)

The same procedure as for compound **10** was used to synthesize **14**. The substituted butene **3** was replaced by **3b** (0.801 g, 2 mmol). Yield 96%.

^1H NMR (300 MHz, $CDCl_3$) : δ 0.94 and 0.96 (t, J = 7.4 Hz, 3H, CH_3), 1.34 and 1.35 (s, 9H, ^{t}Bu), 2.45 and 2.51 (q, J = 7.4 Hz, 2H, CH_2), 2.75 and 2.85 (t, J = 7.0 Hz, 2H, CH_2), 3.97 and 4.11 (t, J = 7.0 Hz, 2H, OCH_2), 4.00-4.25 (m, 9 H, (η^5-C_5H_4)FeCp), 6.58 and 6.87 (d, J = 8.5 Hz, 2H, H_{arom}), 6.75-7.40 (m, 11H, H_{arom}). *^{13}C NMR* (75 MHz, $CDCl_3$) : δ 13.6 (CH_3); 27.1 (CH_3 of ^{t}Bu); 29.0 (CH_2); 29.5 and 29.6 (CH_2); 39.0 (Cq of ^{t}Bu); 67.4 and 67.5 (C_5H_4); 68.2 and 68.4 (OCH_2); 68.5 (Cp + (η^5-C_5H_4)), 84.7 (Cip of C_5H_4); 113.5 and 114.1 (CH_{arom}); 120.8 and 120.9 (CH_{arom}); 125.8 and 126.6 (CH_{arom}); 127.4 and 128.1 (CH_{arom}); 129.4 and 130.6 (CH_{arom}); 130.6 (CH_{arom}); 130.8 and 131.9 (CH_{arom}); 135.0, 135.7, 138.7, 138.8, 139.7, 140.4, 141.0, 143.2, 143.7, 149.2, 156.9, 157.7 (C=C and C_{arom}); 177.0 (C=O). *MS* (CI, NH_3) m/z : 612 $[M+H]^+$, 630 $[M+NH_4]^+$. *IR*

(KBr, cm^{-1}): 1756, 1747 ν(CO). *Anal.* Calcd for $C_{39}H_{40}FeO_3$: C, 76.46; H, 6.58. Found: C, 76.56; H, 6.61.

General procedure for the preparation of DF2, DF3, DF4, and MF2b

A mixture of sodium hydroxide (0.80 g, 20 mmol) were added to a solution of **11**, **12**, **13**, and **14** respectively (2 mmol) dissolved in tetrahydrofuran (30 mL) and water (40 mL). The reaction mixture was heated under reflux for 24 hours. The solution was hydrolyzed, acidified to pH = 1. Standard work-up was performed. However, the crude products were isolated on an aluminium oxide column (eluent: dichloromethane/acetone 95/5). The products were further purified by preparative HPLC with a solution of acetonitrile and water or pure acetonitrile. The isomers (distinctly separate on TLC plates, eluent = dichloromethane, in approximatively 1/1 ratio), could be easily separated but re-isomerize rapidly, before the solvents could be removed. Recrystallization failed to occur because the solutions became oily at low temperature and at room temperature, the compounds degrade in a few days.

1-[4-(2-ferrocenylethoxy)phenyl]-1,2-*bis*-(4-hydroxyphenyl)but-1-ene (DF2)

The reaction was performed with 1.425 g (2 mmol) of compound **11**. The product was purified by preparative HPLC with acetonitrile/water 90/10 as eluent. **DF2** was retrieved as a yellow solid. Yield 92%.

^{1}H NMR (300 MHz, $CDCl_3$): δ 0.90 (t, J = 7.3 Hz, 3H, CH_3), 2.42 (q, J = 7.3 Hz, 2H, CH_2), 2.69 and 2.80 (t, J = 7.0 Hz, 2H, CH_2), 3.93 and 4.08 (t, J = 7.0 Hz, 2H, OCH_2), 4.02-4.25 (m, 9H, (η^5-C_5H_4)FeCp), 6.45 and 6.53 (d, J = 8.6 Hz, 2H, H_{arom}), 6.59 and 6.60 (d, J = 8.6 Hz, 2H, H_{arom}), 6.70 and 6.75 (d, J = 8.6 Hz, 2H, H_{arom}), 6.76 and 6.85 (d, J = 8.6 Hz, 2H, H_{arom}), 6.94 (d, J = 8.6 Hz, 2H, H_{arom}), 7.05 and 7.11 (d, J = 8.6 Hz, 2 H, H_{arom}). *^{13}C NMR* (75 MHz, $CDCl_3$) : δ 15.1 (CH_3); 30.3 (CH_2); 30.9 and 31.0 (CH_2); 69.0 and 69.1 (C_5H_4); 69.7 and 69.9 (OCH_2); 70.2 (Cp + (η^5-C_5H_4)); 86.3 (Cq of Cp), 114.8 and 115.5 (CH_{arom}); 115.8 and 116.4 (CH_{arom}); 116.3 (CH_{arom}); 132.0 and 132.2 (CH_{arom}); 132.3 (CH_{arom}); 133.4 and 133.5 (CH_{arom}); 136.1, 137.4, 137.6, 137.8, 138.0, 138.7, 141.9, 154.9, 155.8, 155.3, 158.0, 158.8 (C=C and C_{arom}). *MS* (CI, NH_3) m/z : 712 $[M+H]^+$, 730 $[M+NH_4]^+$. *HRMS* (CI, CH_4, $C_{34}H_{33}FeO_3$: $[MH]^+$) calcd: 545.1780, found: 545.1786.

1-[4-(3-ferrocenylpropoxy)phenyl]-1,2-*bis*-(4-hydroxyphenyl)but-1-ene (DF3)

The reaction was performed with 1.453 g (2 mmol) of compound **12**. The product was purified by preparative HPLC with acetonitrile/water 90/10 as eluent. **DF3** was retrieved as a yellow solid. 70% yield.

^{1}H NMR (300 MHz, $CDCl_3$): δ 0.90 and 0.91 (t, J = 7.3 Hz, 3H, CH_3), 1.75-2.06 (m, 2H, CH_2), 2.36-2.55 (m, 4H, CH_2), 3.85 and 3.97 (t, J = 6.3 Hz, 2H, OCH_2), 4.01-4.14 (m, 9H, (η^5-C_5H_4)FeCp), 6.45 and 6.55 (d, J = 8.7 Hz, 2H, H_{arom}), 6.60 (d, J = 8.7 Hz, 2H, H_{arom}), 6.71 and 6.75 (d, J = 8.7 Hz, 2H, H_{arom}), 6.76 and 6.86 (d, J = 8.7 Hz, 2H, H_{arom}), 6.94 (d, J = 8.7 Hz, 4H, H_{arom}), 7.06 and 7.11 (d, J = 8.7 Hz, 2H, H_{arom}). *^{13}C NMR* (75 MHz, $CDCl_3$): δ 13.7 (CH_3); 25.9 and 26.0 (CH_2); 28.9 (CH_2); 30.4 and 30.6 (CH_2); 67.2 and 67.4 (OCH_2); 67.3 (C_5H_4); 68.2 (C_5H_4); 68.6 and 68.7 (Cp); 88.4 and 88.6 (Cip of C_5H_4); 113.4 and 114.1 (CH_{arom}); 114.3 and 115.0 (CH_{arom}); 114.8 (CH_{arom}); 130.6 and 130.8 (CH_{arom}); 130.9 (CH_{arom}); 132.0 and 132.2 (CH_{arom}); 134.9, 136.0, 136.2, 136.4, 136.6, 137.3, 140.5, 153.3, 154.2, 153.7, 156.7, 157.6 (C=C and C_{arom}). *HRMS* (CI, CH_4, $C_{35}H_{35}FeO_3$: $[MH]^+$) calcd: 559.1936, found: 559.1926. *IR* (KBr, cm^{-1}): 3407 ν(OH).

1-[4-(4-ferrocenylbutoxy)phenyl]-1,2-*bis*-(4-hydroxyphenyl)but-1-ene (DF4)

The reaction was performed with 1.481 g (2 mmol) of compound **13**. The product was purified by preparative HPLC with acetonitrile/water 90/10 as eluent. **DF4** was retrieved as a yellow solid. 83% yield.

^{1}H NMR (300 MHz, $CDCl_3$) : δ 0.93 (t, J = 7.3 Hz, 3H, CH_3), 1.54-1.93 (m, 4H, CH_2-CH_2), 2.30-2.52 (m, 4H, CH_2), 3.85 and 3.99 (t, J = 6.3 Hz, 2H, OCH_2), 4.03-4.19 (m, 9H, (η^5-C_5H_4)FeCp), 6.48 and 6.56 (d, J = 8.7 Hz, 2H, H_{arom}), 6.60 and 6.61 (d, J = 8.7 Hz, 2H, H_{arom}), 6.73 and 6.77 (d, J = 8.7 Hz, 2H, H_{arom}), 6.79 and 6.87 (d, J = 8.7 Hz, 2H, H_{arom}), 6.96 (d, J = 8.7 Hz, 2H, H_{arom}), 7.08 and 7.13 (d, J = 8.7 Hz, 2H, H_{arom}). *^{13}C NMR* (75 MHz, $CDCl_3$): δ 13.7 (CH_3); 27.4 and 27.5 (CH_2); 28.9 (CH_2), 29.1 and 29.3 (CH_2), 29.2 (CH_2), 67.2 and 67.3 (C_5H_4), 67.5 and 67.7 (OCH_2), 68.1 and 68.2 (C_5H_4), 68.6 and 68.7 (Cp), 89.1 (Cip of C_5H_4), 113.3 and 114.0 (CH_{arom}), 114.3 and 114.9 (CH_{arom}); 114.8 (CH_{arom}); 130.6 and 130.8 (CH_{arom}); 130.9 (CH_{arom}); 131.9 and 132.1 (CH_{arom}); 134.9, 135.9, 136.2, 136.3, 136.5, 137.3, 140.4, 153.4, 153.7, 153.7, 154.3,

156.8, 157.7 (C=C and C_{arom}). *HRMS* (CI, NH_3, $C_{36}H_{37}FeO_3$: $[MH]^+$) calcd: 573.2093, found: 573.2089. *IR* (KBr, cm^{-1}): 3422 ν(OH).

1-[4-(2-ferrocenylethoxy)phenyl]-1-phenyl-2-(4-hydroxyphenyl)but-1-ene (MF2b)

The reaction was done with 1.225 g (2 mmol) of compound **14**. The product was purified by preparative HPLC with pure acetonitrile. **MF2b** was retrieved as a yellow solid. Yield 79%.

^{1}H NMR (300 MHz, $CDCl_3$): δ 0.85 and 0.87 (t, J = 7.4 Hz, 3H, CH_3), 2.36 and 2.37 (q, J = 7.4 Hz, 2H, CH_2), 2.66 and 2.76 (t, J = 7.0 Hz, 2H, CH_2), 3.89 and 4.04 (t, J = 7.0 Hz, 2H, OCH_2), 3.95-4.15 (m, 9H, (η^5-C_5H_4)FeCp), 4.54 and 4.56 (s, 1H, OH), 6.42-6.75 (m, 4H, H_{arom}), 6.75-7.35 (m, 9H, H_{arom}). *^{13}C NMR* (75 MHz, $CDCl_3$): δ 13.6 (CH_3); 28.9 (CH_2); 29.5 and 29.6 (CH_2); 67.4 and 67.5 (C_5H_4); 68.3 and 68.5 (OCH_2); 68.6 (Cp + (η^5-C_5H_4)); 84.8 (Cq of Cp); 113.4 and 114.0 (CH_{arom}); 114.8 and 114.9 (CH_{arom}); 125.5 and 126.4 (CH_{arom}); 127.3 and 128.1 (CH_{arom}); 129.5 and 130.6 (CH_{arom}); 130.8 and 130.9 (C=C and CH_{arom}); 130.9 and 131.9 (CH_{arom}); 134.8, 135.7, 136.2, 137.9, 138.0, 140.7, 141.3, 143.6, 144.0, 153.7, 156.7, 157.5 (C_{arom}). *HRMS* (CI, CH_4, $C_{34}H_{33}FeO_2$: $[MH]^+$) calcd: 529.1830, found: 529.1829. *IR* (KBr, cm^{-1}): 3432 ν(OH).

Ethyl (4-{[1-(4-hydroxyphenyl)-2-ferrocenyl]but-1-en-1-yl}phenoxy)ethanoate (15)

Cs_2CO_3 (1.07 g, 3.3 mmol) and **Fc-diOH** (1.27 g, 3 mmol) were stirred in 20 mL of acetone. After stirring for 10 min, ethyl bromoacetate (0.33 mL, 3 mmol) was added, and the reaction mixture was left heating under reflux for 4h. After standard work-up, the product **15** (400 mg, 26% yield), a mixture of Z and E isomers, was separated by flash chromatography on silica gel column.

^{1}H NMR (300 MHz, $CDCl_3$): δ 1.01 (m, 3H, CH_3 of Et), 1.30 (m, 3H, CH_3 of OEt), 2.57 (m, 2H, CH_2 of Et), 3.88 and 3.90 (t, 2H, C_5H_4), 4.06 (m, 2H, C_5H_4), 4.10 (s, 5H, Cp), 4.28 (m, 2H, CH_2 of OEt), 4.58 and 4.62 (s, 2H, O-CH_2-CO), 6.68-7.12 (m, 8H, H_{arom}). *^{13}C NMR* (75 MHz, $CDCl_3$): δ 14.3 (CH_3 of OEt); 15.6 (CH_3 of Et); 28.1 (CH_2 of Et); 61.5 (CH_2 of OEt); 65.6 (O-CH_2); 68.2 (C_5H_4); 69.3 (C_5H_4); 69.4 (Cp); 87.1 (Cip of C_5H_4); 114.4, 114.6, 115.2, 115.3, 130.6, 130.7, 131.2 (CH_{arom}); 137.0, 137.2, 137.3, 138.5, 138.7 (C=C and Cq_{arom}); 154.1 and 156.3 (Cq_{arom}-O); 169.3 (C=O). *IR* (KBr, cm^{-1}): 1735 ν(C=O), 1606 ν(C=C), 1507 ν(C=C arom). *HRMS* (FAB, $C_{30}H_{30}O_4Fe$: $[M]^{\cdot+}$) calcd: 510.1494, found: 510.1498.

(4-{[1-(4-hydroxyphenyl)-2-ferrocenyl]but-1-en-1-yl}phenoxy)ethanoic acid (AC1)

Sodium hydroxide (200 mg, 5 mmol) and ester **15** (400 mg, 0.8 mmol) were dissolved in a solution of acetone (10 mL) and water (5 mL). After stirring for 1h, the solution was hydrolyzed and washed by diethyl ether. The aqueous layer was acidified until a precipitation was observed, and was then extracted with diethyl ether. The organic layer was dried over $MgSO_4$, and the solvent was evaporated under reduced pressure. The product was purified by preparative HPLC with acetonitrile/water + 0.1% TFA (trifluoroacetic acid) 90/10 as eluent. **AC1** was retrieved as a dark red solid (300 mg, 78%), a mixture of *Z* and *E* isomers.

^{1}H NMR (300 MHz, $CDCl_3$): δ 1.00 (m, 3H, CH_3), 2.56 (m, 2H, CH_2), 3.87 and 3.90 (t, J = 3Hz, 2H, C_5H_4), 4.05 (m, 2H, C_5H_4), 4.09 (s, 5H, Cp), 4.61 and 4.66 (s, 2H, O-CH_2-CO), 6.68-7.12 (m, 8H, H_{arom}). *^{13}C NMR* (75 MHz, $(CD_3)_2SO$): δ 15.4 and 15.5 (CH_3); 29.6 (CH_2); 64.5 (O-CH_2-(CO)); 67.8, 68.5, 68.7 and 69.0 (Cp + (η^5-C_5H_4)); 86.0 and 86.1 (Cip of C_5H_4); 114.1, 115.1, 129.8, 130.2 (CH_{arom}); 135.1, 135.3, 135.8, 135.9, 136.9, 137.5, 137.7 (C=C and Cq_{arom}); 155.6, 155.7, 155.9, 156.0 (Cq_{arom}-O); 170.2 (C=O). *IR* (KBr, cm^{-1}): 3428 ν(OH), 1605 ν(C=C), 1507 ν(C=C arom). *MS* (EI): m/z = 482 $[M]^{\cdot+}$, 121 $[CpFe]^+$. *HRMS* (EI, $C_{28}H_{26}O_4Fe$: $[M]^{\cdot+}$) calcd: 482.1181, found: 482.1187.

[1-(4-trimethylacetoxyphenyl)-1-(4-hydroxyphenyl)-2-ferrocenyl]but-1-ene (17)

To a suspension of Zn (3.9 g, 60 mmol) in 80 mL of anhydrous THF, $TiCl_4$ (3.6 mL, 33 mmol) was added drop-wise, under inert atmosphere. After being under reflux for 2h, 4,4'-hydroxy(trimethylacetoxy)benzophenone (**2**) (2.98 g, 10 mmol) and propionylferrocene (2.4 g, 10 mmol) dissolved in 20 mL of anhydrous THF were added to the three-neck round flask. The mixture was left under reflux for another 2h. After cooling, the mixture was hydrolysed by 200 mL of acidified water, and went under standard work-up. An orange-red solid (*Z* and *E* mixture in 53:47 ratio) was recovered (1.7 g, 33% yield).

^{1}H NMR (300 MHz, $CDCl_3$): δ 1.02 (t, 3H, CH_3), 1.34 and 1.36 (s, 9H, ^{t}Bu), 2.58 (m, 2H, CH_2), 3.91 (m, 2H, C_5H_4), 4.07 (t, 2H, C_5H_4), 4.10 (s, 5H, Cp), 6.66-7.20 (m, 8H, H_{arom}). *^{13}C NMR* (75 MHz, $CDCl_3$): δ 15.6 (CH_3); 27.3 (CH_3 of ^{t}Bu); 28.1 and 28.2 (CH_2); 39.2 (Cq of ^{t}Bu); 68.1, 68.2, 68.3, 69.3, 69.5 (Cp + (η^5-C_5H_4)); 86.9 (Cip of C_5H_4); 115.2, 115.3, 121.2, 121.3, 130.4, 130.8, 131.0, 131.4 (CH_{arom}); 136.7, 137.0, 137.2, 137.6, 137.9, 142.2 (C=C and Cq_{arom}); 149.5 and 154.2 (Cq_{arom}-O); 177.3 and 173.4 (C=O). *IR* (KBr,

cm^{-1}): 1751 ν(C=O), 1608 ν(C=C), 1509 ν(C=C arom). *HRMS* (FAB, $C_{31}H_{32}O_3FeNa$: $[MNa]^+$) calcd: 531.1599, found: 531.1613.

Ethyl (4-{[1-(4-trimethylacetoxyphenyl)-2-ferrocenyl]but-1-en-1-yl}phenoxy)butanoate (18)

Cs_2CO_3 (196 mg, 0.6 mmol) and **17** (310 mg, 0.6 mmol) were stirred in 10 mL of acetone. After stirring for 10 min, ethyl bromobutyrate (0.09 mL, 0.6 mmol) was added, and the reaction mixture was left heating under reflux for 24h. After standard work-up, the product **18** (190 mg, 50% yield), a mixture of *Z* and *E* isomers, was separated by flash chromatography on silica gel column.

^{1}H NMR (300 MHz, $CDCl_3$): δ 1.02 (t, J = 7.4 Hz, 3H, CH_3 of Et), 1.26 (m, 3H, CH_3 of OEt), 1.34 and 1.36 (s, 9H, CH_3 of ^{t}Bu), 2.10 (m, 2H, CH_2 of Et), 2.54 (m, 4H, $(CH_2)_2$-(CO)), 3.91 (m, 2H, C_5H_4), 3.94 (m, 2H, O-CH_2), 4.13 (m, 8H), 4.08 (s, 7H, Cp + (η^5-C_5H_4)), 4.13 (m, 2H, CH_2 of OEt), 6.72-6.89 (m, 4H, H_{arom}), 7.03 (m, 2H, H_{arom}), 7.10 and 7.19 (d, J = 8.6 Hz, 2H, H_{arom}). *^{13}C NMR* (75 MHz, $CDCl_3$): δ 14.4 (CH_3 of OEt); 15.6 (CH_3 of Et); 27.3 (CH_3 of ^{t}Bu); 24.9 (CH_2-CH_2-CH_2); 27.3 (CH_3 of ^{t}Bu); 28.1 and 28.2 (CH_2 of Et); 31.0 (CH_2-(CO)); 39.2 (Cq of ^{t}Bu); 60.5 (CH_2 of OEt); 66.8 (O-CH_2); 68.2, 68.3, 69.3, 69.5 (Cp + (η^5-C_5H_4)); 86.9 (Cip of C_5H_4); 114.5, 114.6, 115.4, 115.5, 130.7, 130.8, 131.2 (CH_{arom}); 136.8, 137.0, 137.1, 137.5, 137.8, 142.2, 142.4 (C=C and Cq_{arom}); 149.5 and 157.4 (Cq_{arom}-O); 173.4 (C=O). *MS* (EI, $C_{37}H_{42}O_5Fe$): m/z = 622 $[M]^{\cdot+}$, 121 $[CpFe]^+$, 57 $[^tBu]^+$.

(4-{[1-(4-hydroxyphenyl)-2-ferrocenyl]but-1-en-1-yl}phenoxy)butanoic acid (AC3)

Sodium hydroxide (200 mg, 5 mmol) and ester **18** (400 mg, 0.6 mmol) were dissolved in a solution of acetone (10 mL) and water (5 mL). After heating under reflux for 2h, the solution was cooled to room temperature, hydrolyzed and washed by dichloromethane. The aqueous layer was acidified until a precipitation was observed, and was then extracted with dichloromethane. The organic layer was dried over $MgSO_4$, and the solvent was evaporated under reduced pressure. The product was purified by preparative HPLC with acetonitrile/water + 0.1% TFA (trifluoroacetic acid) 80/20 as eluent. Recristallisation in a mixture of dichloromethane/hexane yielded **AC3** as an orange-red solid (200 mg, 65%), and as a mixture of *Z* and *E* isomers.

^{1}H NMR (300 MHz, $(CD_3)_2CO$): δ 1.02 (m, 3H, CH_3), 2.06 (m, 2H, CH_2), 2.51 and 2.62 (m, 4H, $(CH_2)_2$-(CO)), 3.92 (m, 2H, C_5H_4), 4.01 (m, 2H, O-CH_2), 4.06 (m, 2H, C_5H_4), 4.11 (s, 5H, Cp), 6.71-7.14 (m, 8H, H_{arom}). *^{13}C NMR* (75 MHz, $CDCl_3$): δ 15.4 (CH_3); 25.1 (CH_2-*C*H_2-CH_2); 28.0 and 28.1 (CH_2 of Et); 30.7 (*C*H_2-(CO)); 67.0 (O-CH_2); 68.3 (C_5H_4); 69.47 (Cp); 87.43 (Cip of C_5H_4); 114.26, 114.36, 121.18, 121.32, 130.37, 130.67, 130.98, 131.16 (CH_{arom}); 136.59, 136.75, 136.85, 137.86, 138.06, 138.13 (C=C and Cq_{arom}); 156.2 and 157.9 (Cq_{arom}-O); 174.0 and 179.3 (C=O). *MS* (EI): m/z = 510 $[M]^{\cdot+}$, 121 $[CpFe]^+$. *HRMS* (EI, $C_{30}H_{30}O_4Fe$: $[M]^{\cdot+}$) calcd: 510.1494, found: 510.1495.

Ethyl (4-{[1-(4-hydroxyphenyl)-2-ferrocenyl]but-1-en-1-yl}phenoxy)propanoate (19)

Compound **Fc-diOH** (4.24 g, 10 mmol) was added to a freshly prepared solution of NaOEt, obtained by dissolving Na (0.23 g, 10 mmol) in 20 mL of absolute EtOH. After 15 min, ethyl acrylate (10.88 mL, 0.1 mol) was added to the solution, and the reaction mixture was left stirring for 48h. The solvent was then evaporated under reduced pressure, and the residue was dissolved in ethyl acetate. Water was added, and the pH of the aqueous layer was adjusted to pH = 2.5 with dilute HCl. After extraction, the organic layers were collected, dried over MgSO4, and the solvent removed by evaporation under reduced pressure. After purification by preparative HPLC, the product **19** (800 mg, 16% yield) was obtained as a mixture of *Z* and *E* isomers.

^{1}H NMR (300 MHz, $CDCl_3$): δ 1.00 (t, J = 6.3 Hz, 3H, CH_3 of Et), 1.28 (m, 3H, CH_3 of OEt), 2.50 (m, 2H, CH_2 of Et), 2.78 (q, J = 6.5 Hz, 2H, CH_2-(CO)), 3.98 (m, 2H, C_5H_4), 4.15 (s, 7H, Cp + (η^5-C_5H_4)), 4.22 (m, 4H, O-CH_2 of $O(CH_2)_2COOEt$ + OEt), 4.88 and 4.90 (s, 1H, OH), 6.67-7.09 (m, 8H, H_{arom}). *^{13}C NMR* (75 MHz, $CDCl_3$): δ 14.3 (CH_3 of OEt); 15.6 (CH_3 of Et); 28.1 (CH_2 of Et); 34.9 (CH_2-(CO)); 60.9 (CH_2 of OEt); 63.5 (O-CH_2); 68.6 (C_5H_4); 69.6 (C_5H_4); 69.8 (Cp); 88.1 (Cip of C_5H_4); 114.4, 114.5, 115.2, 115.2, 130.6, 130.8, 131.2 and 131.4 (CH_{arom}); 136.8, 137.4, 137.5 and 137.8 (C=C and Cq_{arom}); 154.1 and 157.0 (Cq_{arom}-O); 171.4 (C=O). *MS* (EI): m/z = 524 $[M]^{\cdot+}$, 459 $[M\text{-}Cp]^+$, 121 $[CpFe]^+$. *Anal.* Calcd for $C_{31}H_{32}FeO_4$: C, 70.99; H, 6.15. Found: C, 70.95; H, 6.21.

(4-{[1-(4-hydroxyphenyl)-2-ferrocenyl]but-1-en-1-yl}phenoxy)propanoic acid (AC2)

Sodium hydroxide (600 mg, 15 mmol) and ester **19** (700 mg, 1.3 mmol) were dissolved in a solution of THF (10 mL) and water (5 mL). After heating under reflux for 4h, the solution was cooled to room temperature, hydrolyzed and washed by dichloromethane. The aqueous layer was acidified until a precipitation was observed, and was then extracted with dichloromethane. The organic layer was dried over $MgSO_4$, and the solvent was evaporated under reduced pressure. The product was purified by preparative HPLC with acetonitrile/water + 0.1% TFA (trifluoroacetic acid) 80/20 as eluent. **AC2** was retrieved as a red solid (480 mg, 75%), a mixture of *Z* and *E* isomers. Yield of 52%, which has not been optimized yet.

^{1}H NMR (300 MHz, $(CD_3)_2CO$): δ 1.00 (s, 3H, CH_3), 2.50 (m, 2H, CH_2 of Et), 2.84 (m, 2H, CH_2-(CO)), 3.98 (m, 2H, C_5H_4), 4.15 (s, 7H, Cp + (η^5-C_5H_4)), 4.22 (m, 2H, O-CH_2), 6.67-7.10 (m, 8H, H_{arom}). *^{13}C NMR* (75 MHz, $CDCl_3$): δ 15.5 (CH_3); 28.1 (CH_2 of Et); 34.5 and 35.3 (CH_2-(CO)); 63.1 (O-CH_2); 68.5, 69.6, 69.7 (Cp + (η^5-C_5H_4)); 88.0 (Cip of C_5H_4); 114.3, 114.4, 115.2, 115.2, 130.7, 130.8, 131.2, 131.4 (CH_{arom}); 136.8, 137.3, 137.5, 137.7, 138.0 (C=C and Cq_{arom}); 154.0 and 156.9 (Cq_{arom}-O); 176.7 (C=O). *HRMS* (EI, $C_{29}H_{28}O_4Fe$: $[M]^{\cdot+}$) calcd: 496.1337, found: 496.1326.

2.8.2 Crystal data for (E)-DFO·0.5 ($C_3H_{10}O$)

Single crystals were attached to a glass fiber mounted on the Bruker SMART system for data collection using Mo Kα radiation at 296 K. Cell parameters were obtained from the autoindexing routine SMART (SMART for Windows NT, Bruker AXS Inc, Madison, WI, 1997-2001) and were refined with 4301 reflections within a 2θ range of 3.20-59.72°. Data reduction and integration were performed with the software package SAINTPLUS (SAINTPLUS for Windows NT, Bruker AXS Inc, Madison, WI, 1997-2001). Absorption corrections were applied using the program SADABS (SADABS, V2.03, Bruker/Siemens Area Detector Absorption and Other Corrections, Bruker AXS Inc, Madison, WI, 1997-2001). Crystal and space group symmetries for all compounds were determined using the XPREP program (XPREP, Bruker AXS Inc, Madison, WI, 1997-2001). The positions of some of the non-hydrogen atoms were found by direct methods using the program SHELXS. [153] The positions of the remaining non-hydrogen atoms were located by use of a combination of least-squares refinement and difference Fourier maps in the SHELXL-97 program. [154] Non-hydrogen atoms were refined with anisotropic displacement parameters. The hydrogen atoms were included in the structure factor calcula-

tions at idealized positions. The diethylether solvent molecule was disordered over the inversion center, and thus the occupancy was fixed at 0.5. The unsubstituted cyclopentadienyl ring was disordered over two rotational positions. These were modeled as rigid pentagons with a major part occupancy of 80%.

CCDC 626320 contains the supplementary crystallographic data for this work. These data can be obtained free of charge from www.ccdc.cam.ac.uk/conts/retrieving.html, or from the Cambridge Crystallographic Data Centre, 12 Union Road, Cambridge CB2 1EZ, UK; fax: (+44) 1223-336-033; or email: deposit@ccdc.cam.ac.uk.

2.8.3 Electrochemistry

Cyclic voltammograms (CVs) were obtained using a three electrode cell with a 0.5 mm platinum working electrode, gold-plated nickel mesh counter electrode, and saturated calomel reference electrode, with an Autolab PGStat20 potentiostat driven by GPES software (General Purpose Electrochemical System, Version 4.8, EcoChemie B.V., Utrecht, the Netherlands). Solutions consisted of 6 mL DMF, 1 mM analyte, and 0.1 M tetrabutylammonium tetrafluoroborate supporting electrolyte. After variable scan rate CVs were obtained from 0.05 to 20 V/s. Between each scan, the working electrode was gently polished with a sheet of "kimwipe light" (®Kimberly-Clark Corporation).

2.8.4 Biological experiments

Stock solutions ($1{\cdot}10^{-3}$ M) of the compounds to be tested were prepared in DMSO and were kept at 4°C in the dark. Under these conditions they are stable for at least two months. Serial dilutions in DMSO were prepared just prior to use. Dulbecco's modified eagle medium (DMEM) was purchased from Gibco BRL, fetal calf serum from Dutscher, Brumath, France, glutamine, estradiol and protamine sulfate were from Sigma. MCF-7 and MDA-MB-231 cells were from the Human Tumor Cell Bank. Sheep uteri weighing approximately 7 g were obtained from the slaughterhouse at Mantes-la-Jolie, France. They were immediately frozen and kept in liquid nitrogen prior to use.

Determination of the relative binding affinity (RBA)

RBA values were measured on ERα from lamb uterine cytosol and on ERβ purchased from Pan Vera (Madison, WI, USA). Sheep uterine cytosol prepared in buffer A (0.05 M Tris–HCl,

0.25 M sucrose, 0.1% β-mercaptoethanol, pH 7.4 at 25°C) as described previously was used as a source of ERα. For ERβ, 10 μL of the solution containing 3500 pmol/mL were added to 16 mL of buffer B (10% glycerol, 50 mM Bis–Tris–propane pH = 9, 400 mM KCl, 2 mM DTT, 1 mM EDTA, 0.1% BSA) in a silanized flask. Aliquots (200 μL) of ERα in glass tubes or ERβ in polypropylene tubes were incubated for 3h at 0°C with [6,7-^{3}H]-estradiol ($2{\cdot}10^{-9}$ M, specific activity 1.62 TBq/mmol, NEN Life Science, Boston MA) in the presence of nine concentrations of the hormones to be tested. At the end of the incubation period, the free and bound fractions of the tracer were separated by protamine sulfate precipitation. The percentage reduction in binding of [^{3}H]-estradiol (Y) was calculated using the logit transformation of Y (logitY: $\ln(\frac{Y}{1-Y})$ versus the log of the mass of the competing steroid. The concentration of unlabeled steroid required to displace 50% of the bound [^{3}H]-estradiol was calculated for each steroid tested, and the results expressed as RBA. The RBA value of estradiol is by definition equal to 100%.

Measurement of octanol/water partition coefficient, log$\mathbf{P}_{o/w}$

The log$P_{o/w}$ values of the compounds were determined by reverse-phase HPLC on a C-8 column (Nucleosil 5.C8, from Macherey Nagel, France) according to the method previously described by Minick and Pomper. [104,145] Measurement of the chromatographic capacity factors (k') for each compounds was done at various concentrations in the range 85–60% methanol (containing 0.25% octanol) and an aqueous phase consisting of 0.15% n-decylamine in 0.02 M MOPS (3-morpholinopropanesulfonic acid) buffer, pH 7.4 (prepared in 1-octanol saturated water). These capacity factors (k') are extrapolated to 100% of the aqueous component given the value of k'$_w$. log$P_{o/w}$ (y) is then obtained by the formula: log$P_{o/w}$ = 0.13418 + 0.98452×log k'$_w$.

Culture conditions

Cells were maintained in monolayer in DMEM with phenol red (Gibco BRL) supplemented with 8-9% fetal calf serum (Gibco BRL) and glutamine 2 mM (Sigma) at 37°C in a 5% CO_2 air humidified incubator. For proliferation assays, cells were plated in 1 ml of DMEM medium with or without phenol red, supplemented with 10% decomplemented and hormone-depleted fetal calf serum and 2 mM glutamine and incubated. The following day (D0) 1 mL of the same medium containing the compounds to be tested was added to the plates (final volumes of DMSO: 0.1%; four wells for each conditions, one plate per day). After 3 days (D3), the incubation medium was removed and fresh medium containing the compounds was added. After 5 or 6 days (D5 or

D6), the total protein content of the plate was analyzed by methylene blue staining as follows. Cell monolayers were fixed for 1h in methanol, stained for 1h with methylene blue (1 mg/mL) in PBS, then washed thoroughly with water. 1 mL of HCl (0.1 M) was then added and the absorbance of each well was measured at $\lambda = 620$ nm with a Biorad spectrophotometer. The results are expressed as the percentage of proteins versus the control.

Chapter 3

Rhenium and Technetium tamoxifen derivatives: potential radiopharmaceuticals?

A radiopharmaceutical is a molecule tagged with a radionuclide and prepared in a suitable form for human use. Being in an excited state, a radionuclide tries to attain stability through decay, which could be in the forms of α, β, or γ decays. An α decay involves emission of a helium nucleus ^{2}He and is lowest in energy (4-10 MeV). An electron or a positron is emitted in a β decay, whereas a photon particle is released in a γ decay.

3.1 Re and Tc in Nuclear Medicine

Besides the easy, quick and low-cost preparation requirements, the perfect radiopharmaceutical should travel to target cells and interact efficiently with only the desired molecular pathway [155]. Radioimaging methods for diagnosis are attractive because they simultaneously and non-invasively provide information on all tumour sites. This procedure requires highly penetrating radiation that can traverse overlying body tissues and be detected by suitable instruments outside the body [96, 97, 156]. For radiotherapy, a non-penetrating radiation is needed. On one hand, the radiation should deposit as much energy as possible in the tissues of the target site in order to damage the cancerous cells. On the other hand, it should ideally have limited effects on the neighbouring normal tissues [97,155,157]. For both applications, the nature of the particle emission, its energy, its physical half-life time*, and the clearance time determine the appropriate radiopharmaceutical. The radionuclide should preferably emit a monochromatic γ-ray with energy between 100 and 300 keV for imaging applications [158], while therapeutic radionuclides should be β-emitters with a 0.5-2 MeV energy range [159].

3.1.1 Technetium

Technetium was the first artificially produced element, discovered in 1937 by Carlo Perrier and Emilio Segrè. All its isotopes are radioactive, and among them are ^{99}Tc, ^{99m}Tc and ^{94m}Tc. ^{99}Tc is a long lived and weak β-emitter radionuclide ($E_{\beta\,max^-} = 0.29$ MeV) whose $\tau_{\frac{1}{2}}$ is $2.1{\cdot}10^5$ years. It is produced in commercial quantities mainly as a by-product from nuclear reactors. On the contrary, ^{94m}Tc has nuclear characteristics ($\tau_{\frac{1}{2}} = 52$ min, $E_{\beta\,max^+} = 2.44$ MeV) suitable for imaging using positron emission tomography, with which more quantitative measurements of radiopharmaceutical uptake, biodistribution and clearance can be made.

With its 6h half-life and 140 keV γ-ray emission, ^{99m}Tc presents very favorable characteristics to be used in nuclear imaging medicine [96, 97, 156, 158, 159]. 6h is long enough for radiopharmaceutical preparation and *in vivo* accumulation in the target tissue, though short enough to minimize the radiation dose delivered to the patient. The γ emission is nearly pure, and close to optimal detection for commercial γ cameras. Alongside its ideal nuclear characteristics, the easy production in the laboratory of the isotope thanks to the ^{99}Mo/^{99m}Tc generator has also contributed to its success [96]. Nowadays, ^{99m}Tc is used in more than 80% of all nuclear

*$\tau_{\frac{1}{2}}$, time required for the population of a given isotope to decrease to half the initial value

medicine procedures [160]. Some are classified as perfusion agents (e.g. Cardiolite® [101]), which accumulate in specific organs by their biophysical properties [97]. Others are designed as target-specific radiopharmaceuticals, consisting of a radionuclide and an organic vector.

The generator system, by which ^{99m}Tc is produced, is based on the decay of a long-lived radionuclide ("parent") into the short-lived radionuclide ("daughter") of interest, on an alumina column (Fig. 3-1): $^{99}\text{Mo} \longrightarrow {}^{99m}\text{Tc}$

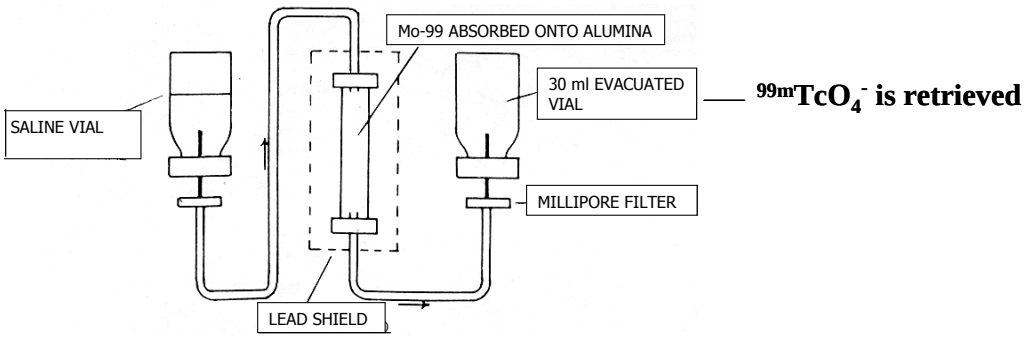

Figure 3-1: $^{99}\text{Mo}/^{99m}\text{Tc}$ generator

$[^{99}MoO_4]^-$, strongly bound to the alumina ion exchange column, is eluted with a physiological saline (NaCl at 0.15 M). $Na^{99m}TcO_4$ can be easily and repetitively collected at the end in 10^{-6} - 10^{-7} M concentration [96, 97], by negative pressure. This procedure is called "milking" [158]. Because of the very low concentrations, the main way to monitor the chemical transformations with ^{99m}Tc is by chromatographic methods (like HPLC) with γ detection [96, 155, 161]. The other consequence is that, since ^{99m}Tc is only available in aqueous solution, the chemistry must accomodate this solvent.

3.1.2 Rhenium

Just below technetium in the periodic table, rhenium has two radioactive isotopes suitable for therapeutic use: ^{186}Re (E_{β^-} = 1.07 MeV) and ^{188}Re (E_{β^-} = 2.1 MeV). The depths of penetration into tissue for these β-emitting radioelements are 5 mm and 11 mm, respectively [161]. Because of the short penetration range and the weaker irradiation energy, ^{186}Re is more appropriate to treat small tumours [157]. As for ^{188}Re, it has a shorter $\tau_{\frac{1}{2}}$ (17h vs. 90h) and can be used for larger masses. The ^{186}Re isotope is produced by neutron radiation of ^{185}Re, and hence is prone to contamination by non-radioactive ^{185}Re [96, 161]. Conversely, ^{188}Re is

commercially available in the form of perrhenate aqueous solutions produced from $^{188}W/^{188}Re$ generators, which are based on the same principles as the $^{99}Mo/^{99m}Tc$ generators.

In addition, rhenium presents the advantage of exhibiting comparable physical and chemical properties as technetium. It is often used as a model to predict the behaviour of technetium compounds [157, 162]. Since rhenium occurs naturally as a mixture of non-radioactive isotopes ^{185}Re and ^{187}Re, it is possible to work on the non-radioactive rhenium compounds first. Their interest could thus be evaluated, before tackling the radioactive $^{186/188}Re$ and ^{99m}Tc derivatives.

3.1.3 The [Cp-M-tricarbonyl] core

Their ultimate use *in vivo* and their availability in aqueous solutions make it necessary to find water-stable rhenium and technetium compounds. The stable piano stool $CpM(CO)_3$ core (M = Re, Tc) is one of the most promising moieties for this purpose [97, 98, 163]. Indeed, the formal oxidation state of the metal is +I, and the CO ligands can stabilize low-valent metal centers by π-backbonding. Therefore, the metal is less susceptible to oxidation. As for the cyclopentadiene ligand, it is small, with low molecular weight, and presents the additional possibility of being coupled to targeting vectors [97, 98, 163].

3.2 Synthetic methods of preparation

The preparation of radiopharmaceuticals should ideally allow the incorporation of the radionuclide at the final step of synthesis. It also requires a rapid and simple isolation and purification of the final product. Therefore, it is important to find a suitable stable precursor for the synthesis of rhenium and technetium compounds bearing the cyclopentadienyl tricarbonyl motif.

3.2.1 Double ligand transfer reaction and improvements

Wenzel and co-workers were the first to propose a synthetic method for functionalised $CpM(CO)_3$ in 1992 [164]. The double ligand transfer (DLT) involves the one-pot transformation of substituted ferrocenes into their $[Cp^{99m}Tc(CO)_3]$ analogues, using pertechnetate $[^{99m}TcO_4]^-$, $SnCl_2$ as reducing agent, and manganese carbonyl as source of CO (Fig. 3-2). The reaction was named as such, because two different ligands (Cp and CO) on two different metals (Fe and Mn) were transferred to a third metal atom (Tc). However, a manganese byproduct was present in large excess and was not readily separable from the technetium compound.

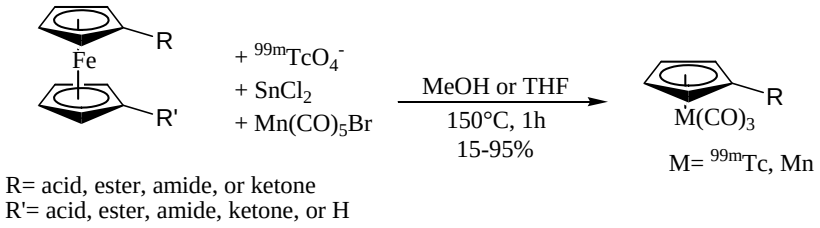

Figure 3-2: Wenzel's double ligand transfer reaction

The reaction conditions and yield have been improved later by Katzenellenbogen *et al.* [165–167]. The reducing agent has been changed to $CrCl_3$, and chromium hexacarbonyl was chosen to be the source of CO (Fig. 3-3). The procedure required methanol probably to facilitate the reduction of perrhenate and pertechnetate. Eventually, the experimental conditions were still too harsh for routine clinical preparations.

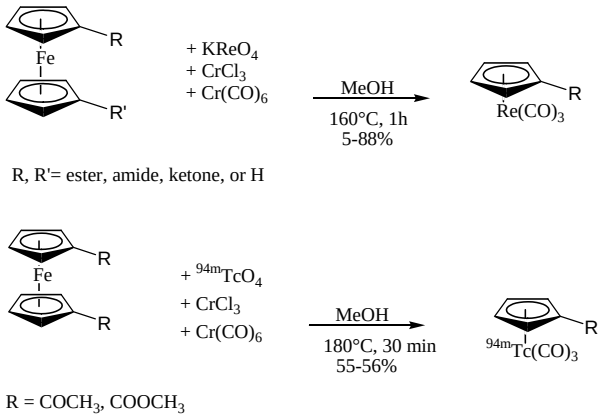

Figure 3-3: Katzenellenbogen's preparation of rhenium and technetium derivatives

Top *et al.* have proposed another method (Fig. 3-4) to convert ferrocenyl derivatives into their rhenium analogues, by using the $[Re(CO)_6]^+$ cation as a ligand transfer reagent [168,169]. The procedure is easier and more practical than that with perrhenate, because it does not need an external CO source, nor high pressure. The reagent $[^{188}Re(CO)_6]^+$ could be generated by the decay of $^{188}W(CO)_6$, in the same way as $[^{99m}Tc(CO)_6]^+$ had been obtained from $^{99}Mo(CO)_6$. Furthermore, this ligand transfer method is compatible with aqueous media, and promising results (up to 60% yield) in a water/DMSO 1:1 mixture have been obtained.

In the above methods, organic solvents were always compulsory to perform the synthesis. But Alberto *et al.* have reported successful preparations of technetium derivatives from esters in

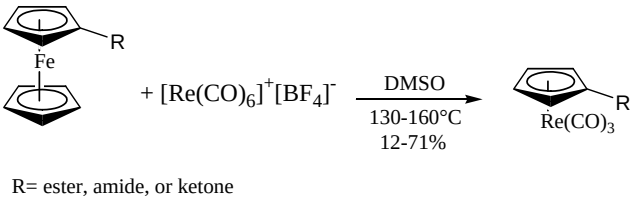

Figure 3-4: Ligand transfer reaction with the hexacarbonyl rhenium cation

aqueous media [111,169,170], by first linking Cp^- with the biomolecule, then adding the metal. Figure 3-5 shows the synthesis of a technetium phenyl acetyl derivative, a model for steroids and tamoxifen-type molecules [111]. The free Cp derivative was obtained by addition of NaCp to ethyl 2-phenylmethanoate. The water-soluble and stable reagent *fac*-$[^{99m}Tc(H_2O)_3(CO)_3]^+$ can be generated in physiological media from $^{99m}TcO_4^-$ by combining a Borax buffer, a complexing agent (tartrate) with $[H_3BCO_2]^{2-}$, which is the reducing agent and in situ CO source [110,171]. The latter reagents are available in a kit preparation (Isolink®, Mallinckrodt Med B.V.).

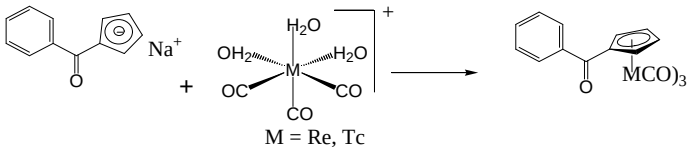

Figure 3-5: Synthesis of [Ph-CO-CpM$(CO)_3$]

3.2.2 Role of the ketone function in the DLT reaction

For all the proposed synthetic methods to be successful, it is crucial to have an electron-withdrawing group at the α position of the cyclopentadiene. In the proposed mechanism for the double ligand transfer reaction (Fig. 3-6), Katzenellenbogen and co-workers postulated that the ketone function must promote the difficult step of η^5 - η^3 Cp ring slippage [165]. The ketone unit probably stabilizes the transition state of the initial ring slip of ferrocene.

Yet, Alberto *et al.* have attributed another role to the ketone function. They have noticed that an acetyl group lowered the pKa value of cyclopentadiene from 15 to 8.7 [111]. This is because the deprotonated cyclopentadiene is stabilized by the keto-enol tautomerism. Once formed, the resulting negatively charged cyclopentadienyl ligand should bind more efficiently

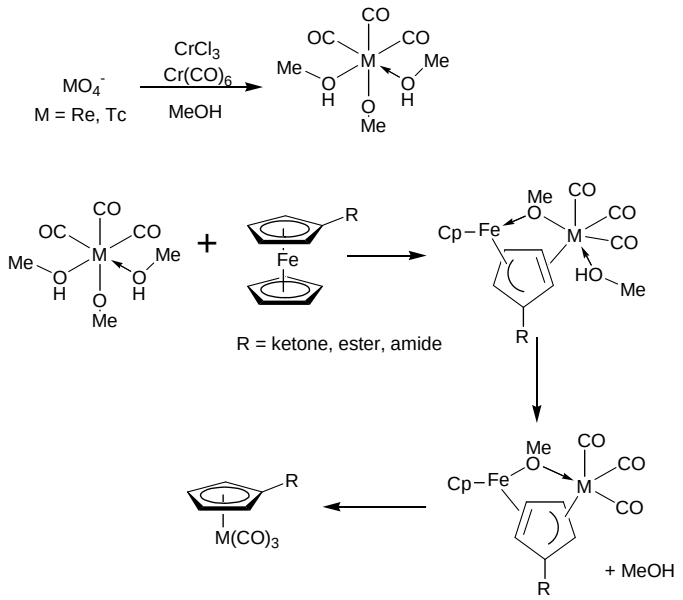

Figure 3-6: Mechanism for the DLT reaction proposed by Katzenellenbogen *et al.*

to Re/Tc. The ketone group not only facilitates the deprotonation of Cp, it could also offer an initial coordination site for the metal complex [170].

3.2.3 Design of Re/Tc ligands of estrogen receptors

As it has been explained earlier, we were interested in using the ferrocenyl derivatives as precursors for rhenium and technetium ligands of the ER. Many rhenium and technetium estradiol derivatives have been proposed, but most of them fail to have a strong enough affinity for the estrogen receptor [107, 109, 172–176]. Despite the high *in vitro* binding affinity of very few derivatives [107, 109, 174], none of the tested molecules gave satisfying tissue distribution *in vivo* [176, 177] (Fig. 3-7). In addition, only a few structures of these estradiol derivatives are suitable for the ligand transfer reaction. When the high affinity estradiol derivative **22** [174] was modified in order to allow the DLT, the binding affinity of the resulting molecule **23** [169] was much lower than the initial RBA value (16% for **22** and 1.6% for **23**).

Very few non-steroidal rhenium and technetium derivatives have been reported [167, 178]. Again, these molecules mostly have poor affinity for the estrogen receptor. Consequently, we sought to explore this field, by proposing suitable ferrocenyl tamoxifen-type molecules for the DLT. Compound **DFO**, presented in **Chapter 2** (Fig. 3-8), not only has the appropriate structure, but also shows a good affinity for the estrogen receptor [112]. A direct synthesis

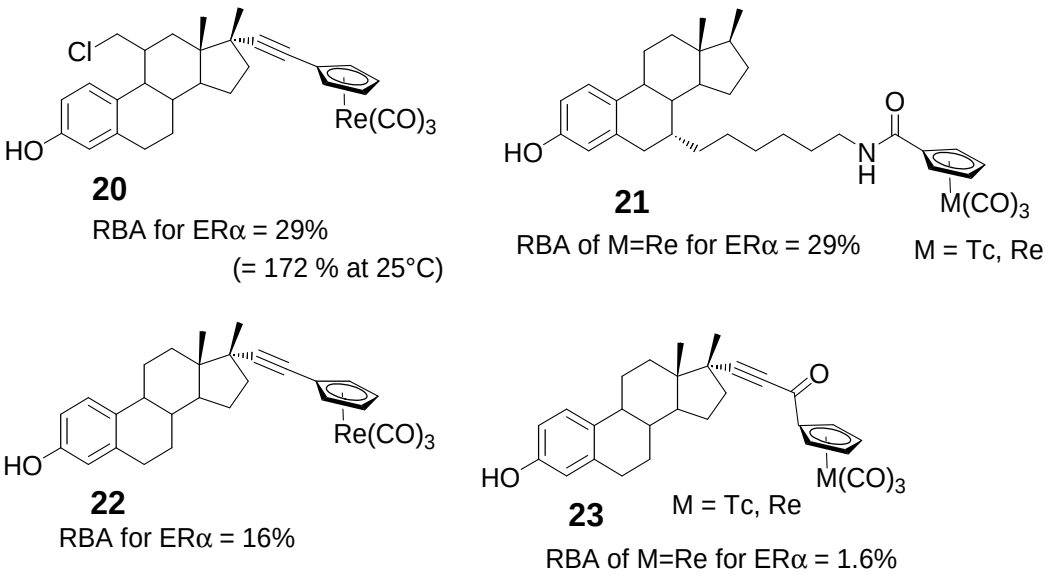

Figure 3-7: Rhenium and technetium estradiol derivatives (RBA values at 0°C)

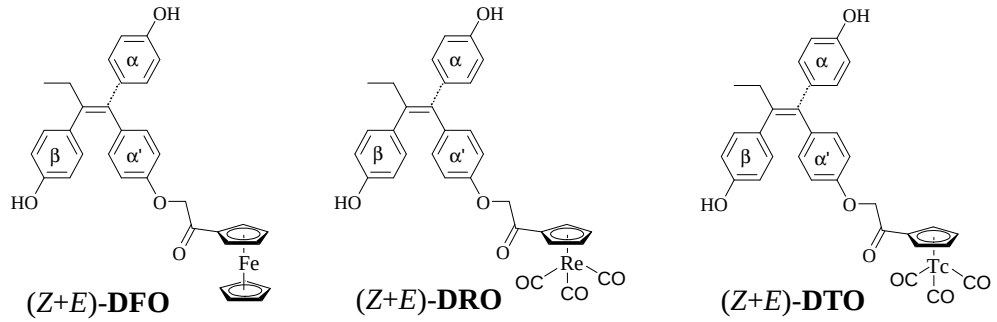

Figure 3-8: **DFO** and its rhenium & technetium derivatives proposed for study

of the non-radioactive rhenium analogue (**DRO** in Fig. 3-8) was performed first, in order to evaluate the biological interest of the compound. Then, the ferrocenyl precursor underwent the ligand transfer reaction, before the actual labelling (**DTO** in Fig.3-8).

3.3 Results and discussion

3.3.1 Direct synthesis of the rhenium compound

The synthesis of **DRO** followed the same steps as for **DFO**, except that a Friedel-Crafts reaction was not used to produce [(α-bromoacetyl)cyclopentadienyl]tricarbonyl rhenium like it was used for α-chloroacetylferrocene. Instead, bromoacetyl bromide was derivatized to the corresponding

Weinreb amide and reacted with lithiated cyclopentadienyltricarbonyl rhenium, to give the expected [(α-bromoacetyl)cyclopentadienyl]tricarbonyl rhenium (**24** in Fig 3-9). This synthetic method is more suitable for cyclopentadienylrhenium compounds, because bromoacetyl bromide did not react with $CpRe(CO)_3$ under Friedel-Crafts reaction conditions.

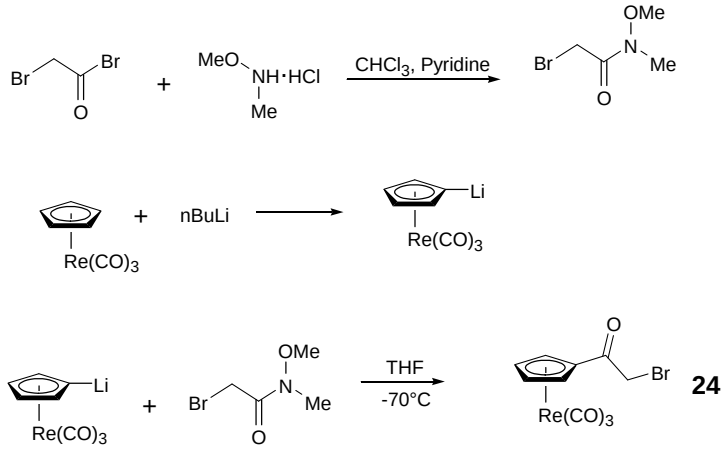

Figure 3-9: Synthesis of [(α-bromoacetyl)cyclopentadienyl] tricarbonyl rhenium

Similarly to **DFO**, the hydroxyl groups of 4-hydroxypropiophenone and 4,4'-dihydroxybenzophenone were protected prior to reaction with [(α-bromoacetyl)cyclopentadienyl]tricarbonyl rhenium (**24**). The pivaloate group was this time inappropriate, because its deprotection reaction conditions were too harsh, and all the compounds were degraded. Thus, the *tert*-butyldimethylsilyl protecting group was used instead, and the base KH was replaced by the milder Cs_2CO_3 (Fig. 3-10). Consequently, the yield was poor (16%), but **DRO** was finally produced, after deprotection of **29** by HCl in EtOH. It was possible to separate both the Z and E isomers of **27** by flash column chromatography. The following steps of the synthesis were performed on each isomer separately, with only a small isomerization occurring during the reaction time. **DRO** was eventually purified by HPLC.

3.3.2 Biological analysis of DRO

The next step was to evaluate the biological interest of the rhenium derivative **DRO**. Table 3.1 shows that the rhenium derivative is rather lipophilic, with a $\log P_{o/w}$ value (4.98 for the Z isomer) higher that of hydroxytamoxifen (3.2). According to this measurement, it may cross the cellular membranes more easily than hydroxytamoxifen.

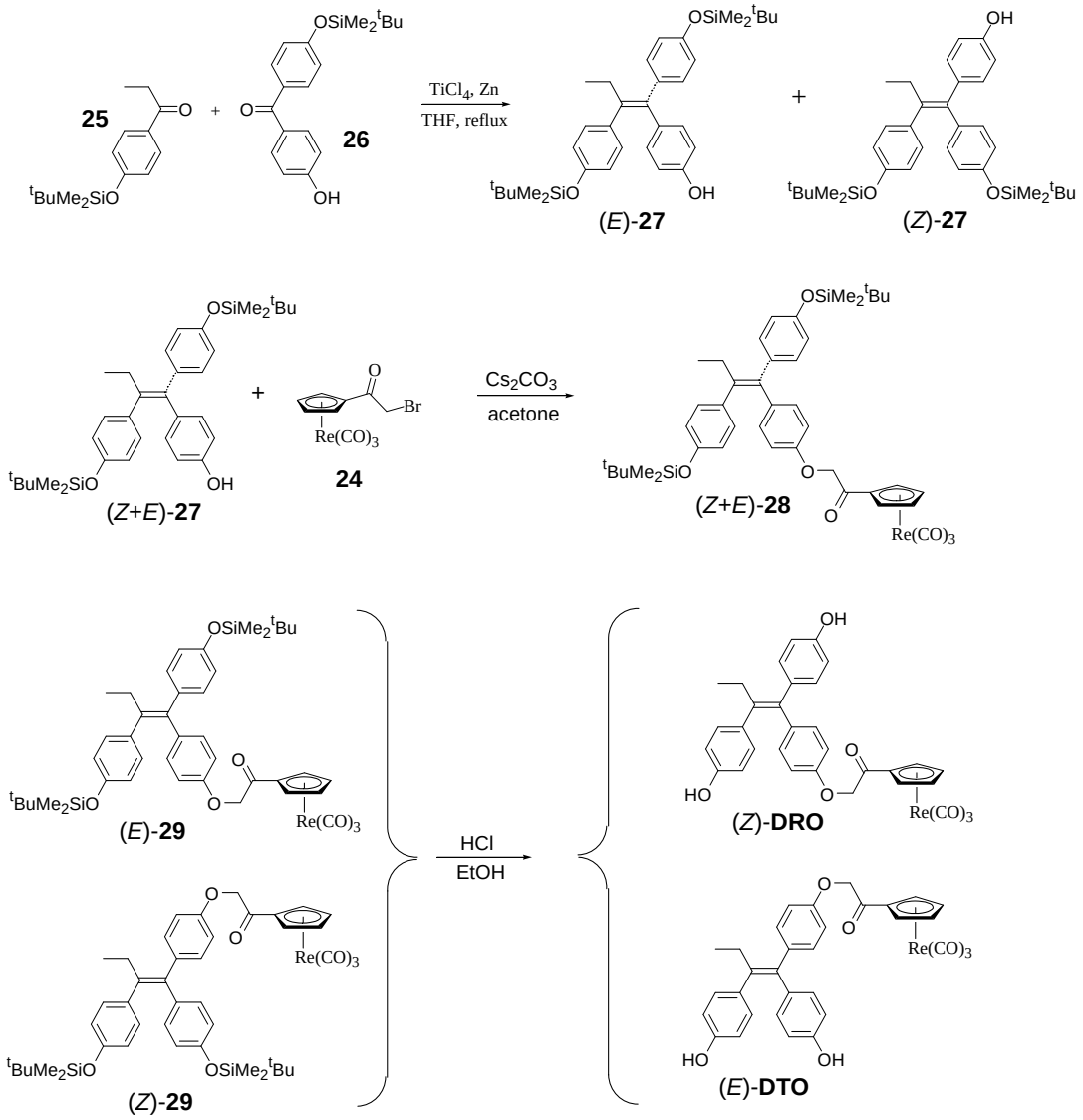

Figure 3-10: Direct synthesis of (Z)- and (E)-**DRO**

Table 3.1: Lipophilicity ($\log P_{o/w}$) and relative binding affinity values of **DRO** for ERα and ERβ, in DMSO at 4°C. Mean of 2*-3** experiments ± S.D.

	RBA		log Po/w
	ERα*	ERβ**	
(*Z*)-**DRO**	14.30 ± 0.70	11.80 ± 0.80	4.98
(*E*)-**DRO**	1.26 ± 0.25	1.80 ± 0.54	5.41

Likewise **DFO**, when the configuration of **DRO** changes from Z to E, there is a ten-fold decrease in the affinity with both receptor isoforms. Additionally, the similar binding affinities of (Z)-**DRO** (14.8% for ERα and 11.8% for ERβ) and (Z)-**DFO** (13.86% for ERα and 11.53% for ERβ) suggest that the hydrophobic pocket of the ERα LBD could still accommodate a cyclopentadienyltricarbonyl rhenium moiety, which is bulkier than the ferrocenyl group. Molecular modeling studies, in the same conditions as those described in **Chapter 2**, indicated that the [(Z)-**DRO**]-(ERα LBD) complex should have a stabilized conformation like that of [(Z)-**DFO**]-(ERα LBD). ΔE found for (Z)-**DRO** is similar (-90 kcal·mol^{-1}) to ΔE for (Z)-**DFO** (-89 kcal·mol^{-1}), if a direct interaction between Asp 351 and Fc is considered. This is consistent with the similar experimental RBA values of (Z)-**DRO** and (Z)-**DFO**.

The influence of (Z)-**DRO** and (E)-**DRO** on the proliferation of hormone-dependent MCF-7 cells and of hormone-independent PC-3 prostate cancer cells were studied, as described previously in **Chapter 2** (Fig. 3-11). The experiments on the hormone-independent MDA-MB-231 breast cancer cells are underway.

Both diastereoisomers Z and E of **DRO** exhibited similar biological behavior. Although the compound **DRO** induces only a slight proliferative activity at 1 μM on the MCF-7 breast cancer cells, it has no effect at 10 μM on these cells containing a high concentration of ERα. Moreover, the rhenium derivative has no influence on the growth of the PC-3 cancer cells, which have ERβ but no ERα. Since the technetium compound should have the same behaviour as its rhenium analogue, it might fulfill the requirement of a radioimaging agent to be as innocent as possible in the biological media.

3.3.3 The ligand transfer reaction

The biological experiments have demonstrated that the rhenium derivative **DRO** is an interesting potential agent for radiotherapy and imaging. Therefore, the following prerequisite is a simple method of synthesis. The procedure presented previously is too tedious, and the rhenium metal was not introduced at the last step of synthesis. Hence, it is more suitable to obtain the rhenium derivative from its stable ferrocenyl precursor, via the ligand transfer reaction.

The ferrocenyl precursor **DFO** was allowed to react for 20 min at 160°C with $[Re(CO)_6]^+[BF_4]^-$ in DMSO, and **DRO** was obtained in 35% yield (Fig. 3-12). The success of this ligand transfer reaction on **DFO**, with a reasonable yield, gives us hope that the labeling reaction with *Tc could be possible.

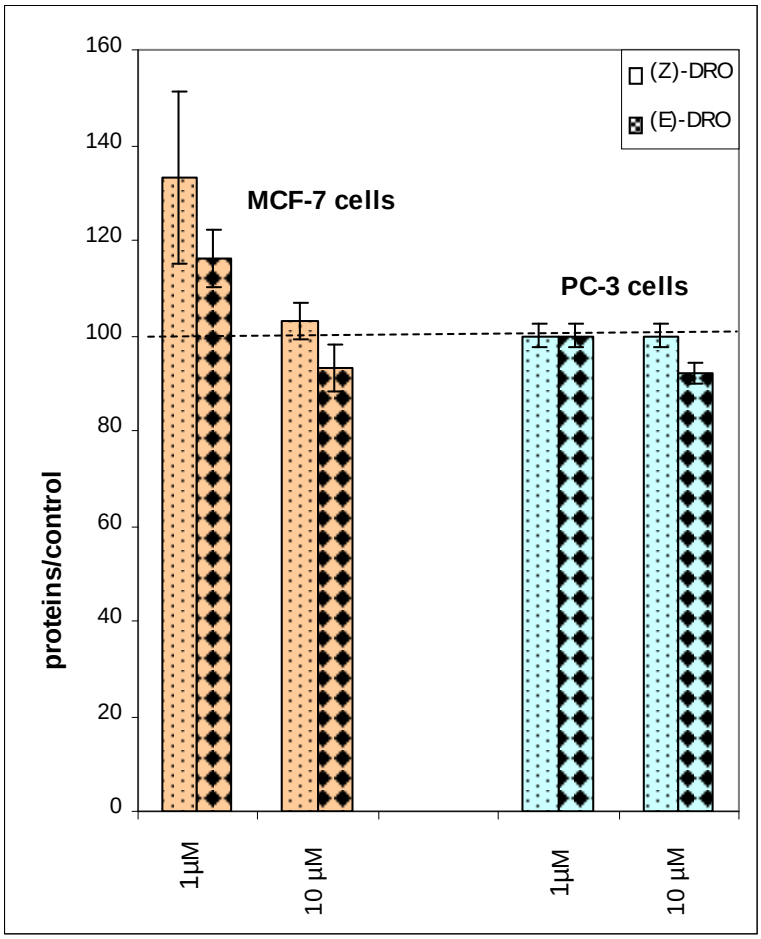

Figure 3-11: Effects of (*Z*)- and (*E*)-**DRO** on the growth of MCF-7 (orange) and PC-3 (blue) cancer cells. Mean of 2 experiments ± S.D.

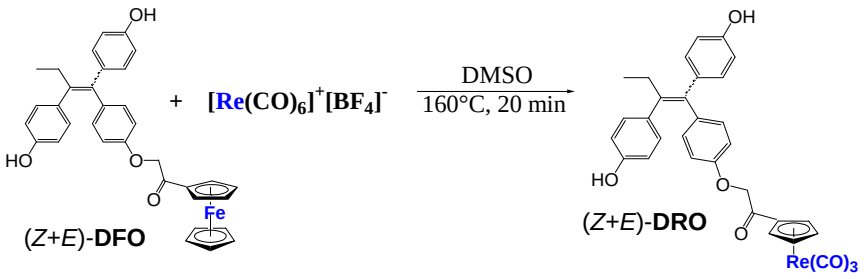

Figure 3-12: Synthesis of **DRO** from the ferrocenyl precursor **DFO**

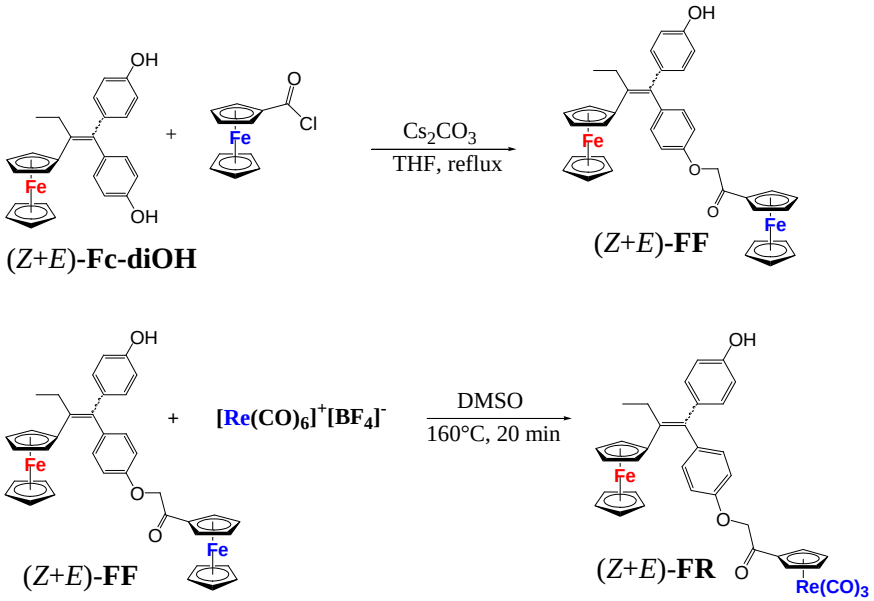

Figure 3-13: Syntheses of **FF** and **FR**

This ligand exchange reaction was further studied with the ferrocenyl analogue **FF** (Fig. 3-13). The molecule has the same chemical structure as **DFO**, but the β phenol has been replaced by another ferrocenyl group. According to prediction, only the ferrocenyl group which bears the electron withdrawing α-ketone unit underwent the ligand transfer, and the other ferrocenyl moiety was inert (**FR** in Fig. 3-13). This is consistent with the chemioselectivity of the ligand transfer reaction. Unfortunately, the ferrocenyl compound **FF** did not show any affinity for ERα, probably because of the steric hindrance of two bulky ferrocenyl groups, which may be too large to fit in the LBD. In addition, it did not have a significant influence on the proliferation of MCF-7 cancer cells at 1 μM.

3.3.4 Labeling with *Tc

Similarly to the mechanism proposed by Katzenellenbogen *et al.*, the first step of the ligand transfer reaction seems to be the substitution of three carbonyl ligands by three solvent molecules in the $[Re(CO)_6]^+$ cation [169, 179]. The intermediate *fac*-$[Re(DMSO)_3(CO)_3]^+$ could be formed, and then reacts with the cyclopentadienyl ligand the same way as the water-soluble reagent *fac*-$[^{99m}Tc(H_2O)_3(CO)_3]^+$ developed by Alberto *et al.* does. Thus, the work with ferrocene derivatives and the $[Re(CO)_6]^+$ cation has been extended to the preparation of $\{[R\text{-}CO\text{-}(\eta^5\text{-}C_5H_4)]^{99m}Tc(CO)_3\}$ from the same ferrocene precursors and using *fac*-$[^{99m}Tc(H_2O)_3(CO)_3]^+$

as the reagent. This method has been successfully applied to 4-methoxyphenylacetyl ferrocene and the ferrocenyl analogue of **23** (Fig. 3-7) [169].

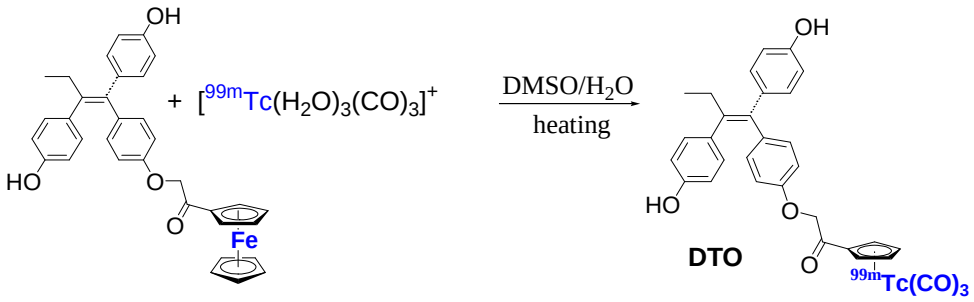

Figure 3-14: Synthesis of $\mathbf{D}^{99m}\mathbf{TO}$ from the corresponding ferrocene precursor

In consequence, the reaction of $[Re(CO)_6]^+$ with the ferrocenyl derivative **DFO** (Fig. 3-12) was adapted to Tc analogues. 50 μL of an aqueous solution containing $[^{99m}Tc(H_2O)_3(CO)_3]^+$ (nM-mM range) was allowed to react with 500 μL of a DMSO solution containing the ferrocenyl precursor **DFO** (mM range). The mixture was heated and the reaction (Fig. 3-14) was monitored by HPLC, equipped with a γ radiodetector. Since the ^{99m}Tc species are in very low concentration, characterization was only possible by HPLC and by comparison to the rhenium compound **DRO** used as a reference. The expected technetium analogue was formed in 70% radiochemical yield after heating for 40 min at 120°C. When the reaction was performed on the pure *Z* isomer (Fig. 3-15), a small isomerization probably occured.

Optimisation of the reaction was examined next, in order to gain higher yields or take advantage of milder conditions.

- The first parameter was temperature. Unluckily, higher temperatures than 120°C did not improve the yield, increased the yield of the by-product, and even degraded $[^{99m}Tc(H_2O)_3(CO)_3]^+$. At lower temperatures such as 90°C or 110°C, the reaction did not proceed.

- Secondly, the reaction time was studied. After about 1h30 min of reaction, the $[^{99m}Tc(H_2O)_3(CO)_3]^+$ was totally consumed, without improving the yield. In the end, the maximum yield was obtained for 40 min of reaction.

- Lastly, the pH of the reaction was also an important criterion. Either in alkaline or acidic medium, the reaction did not proceed. Only neutral pH led to the product.

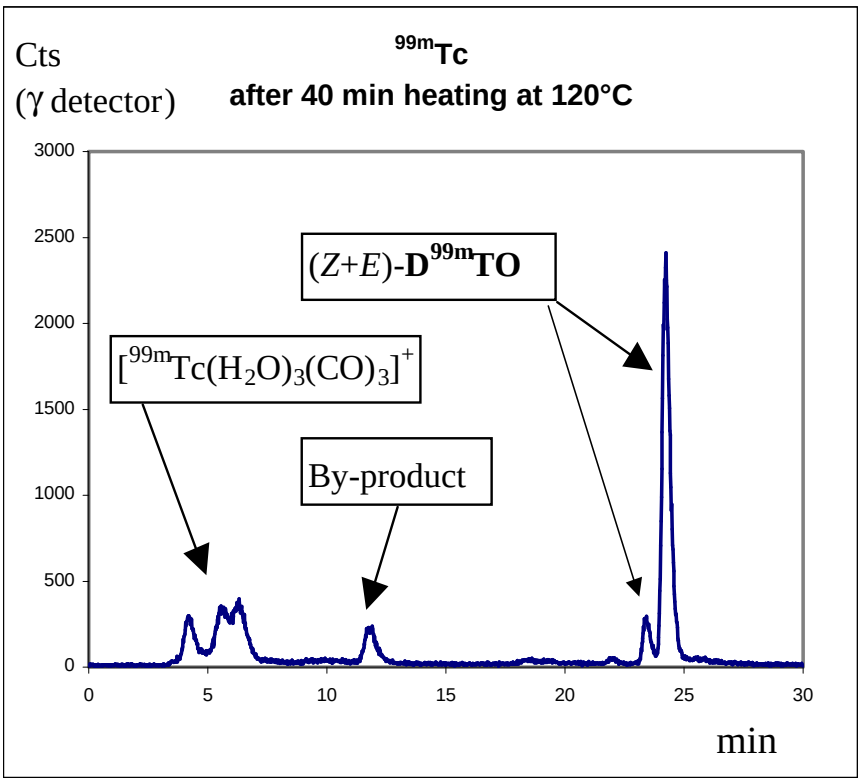

Figure 3-15: γ detection trace of the reaction mixture ((*Z*)-**DFO** with ^{99m}Tc) after 40 min of heating at 120°C

An attempt was conducted to determine whether the by-product could be the elusive *di*-carbonyl technetium ([$RTc(CO)_2$]), because the *di*-carbonyl rhenium complex has also a similar retention time. A ligand (*bis*-(2-pyridylmethyl)glycine) was added to the reaction mixture (Fig. 3-16). In the case of rhenium complexes, it has been noticed that this ligand prefers 4-fold coordination to 3-fold coordination, when binding to *di*-carbonyl rhenium [180]. Therefore, we hoped that if the by-product were a *di*-carbonyl technetium species, the (*bis*-(2-pyridylmethyl)glycine) ligand should bind to the by-product, and then we must see a change in the γ trace. However, nothing significant appeared on the γ trace.

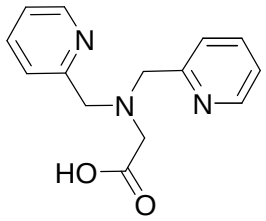

***bis*-(2-pyridylmethyl)glycine**

Figure 3-16: Structure of *bis*-(2-pyridylmethyl)glycine

It is also worthy to note that the reaction mixture underwent a color change: from orange-red to salmon after 30 min, then turned to violet at the end. This violet color may imply that ferrocenium ion could be formed during the reaction. Another observation was that the $[^{99m}Tc(H_2O)_3(CO)_3]^+$ peak disappeared while the signal for $^{99m}TcO_4^-$ increased slightly could mean that we have an oxidizing agent in the reaction mixture, which both oxidized $[^{99m}Tc(H_2O)_3(CO)_3]^+$ into $^{99m}TcO_4^-$ as a byproduct, and the ferrocene derivative into its ferrocenium ion analogue. Since the latter is less stable than the ferrocene precursor, the ferrocenium ion may be the reactive species for the Fe-Tc exchange.

This change in colour was not observed at lower temperature, where the reaction did not proceed. Since DMSO could act as an oxidant at high temperature, the solvent was then changed to DMF. The yield for the reaction was poor (10%). Thus, it is possible that DMSO acts as an oxidant at high temperatures, transforming the ferrocenyl precursor into its ferrocenium analogue. This molecule could then undergo the Fe-Tc exchange to generate the technetium analogue. However, the temperature should not be too high, in which case $[^{99m}Tc(H_2O)_3(CO)_3]^+$ degrades.

Once $\mathbf{D}^{99m}\mathbf{TO}$ was successfully synthesized, production of the technetium derivative on larger scale was undertaken, in order to better characterize the product. Larger quantities of $\mathbf{D}^{99}\mathbf{TO}$ can be synthesized and handled, starting from $[^{99}TcCl_3(CO)_3]^{2-}$, because of the weak radiation and the long half-life of ^{99}Tc [181] as compared to ^{99m}Tc. After 3h30 of heating the ferrocenyl precursor **DFO** with $[^{99}TcCl_3(CO)_3]^{2-}$ at 120°C in DMSO, $\mathbf{D}^{99}\mathbf{TO}$ (70% yield) was precipitated in water, and extracted with diethylether (Fig. 3-17). The reaction was again monitored by HPLC equipped with a β detector (Fig. 3-18). Both the similar retention times of $\mathbf{D}^{99}\mathbf{TO}$ (24.7 min) and $\mathbf{D}^{99m}\mathbf{TO}$ (24.2 min) in the radiodetectors, and the ^{99}Tc and ^{1}H NMR spectra satisfied us that the technetium analogue was indeed synthesized.

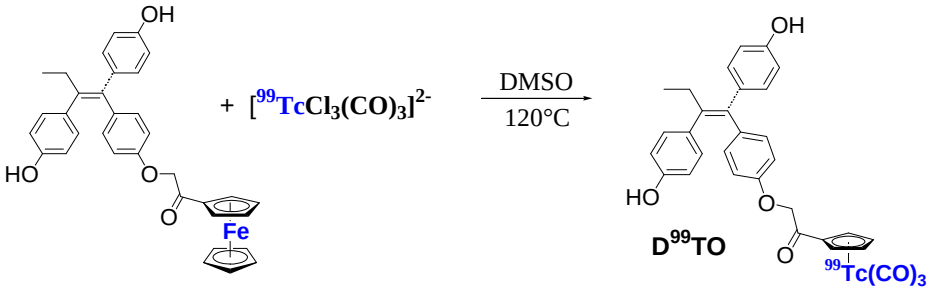

Figure 3-17: Synthesis of $\mathbf{D}^{99}\mathbf{TO}$

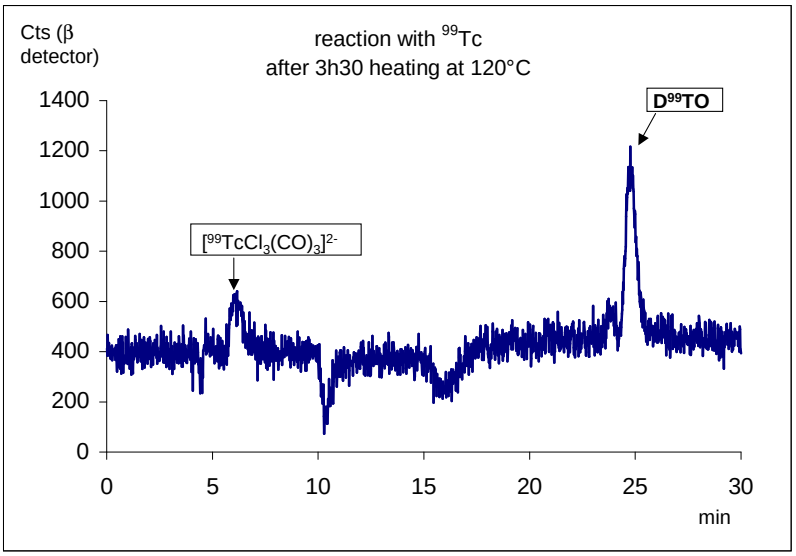

Figure 3-18: β detection trace of the reaction mixture ((*Z*)-**DFO** with ^{99}Tc) after 3h30 of heating at 120°C

The stability of the technetium derivative was investigated. $\mathbf{D}^{99m}\mathbf{TO}$ was isolated by HPLC, and its evolution was followed through time with a UV-vis detector and a γ detector. Since no new technetium species appeared over 24h, this suggested the stability of $\mathbf{D}^{99m}\mathbf{TO}$.

However, an isomerization probably occurred during the labeling reaction. They were carried out on the mixture of $(Z+E)$ isomers of **DFO**, but also on the (Z)-isomer alone. It seems, by both HPLC (Fig. 3-15) and NMR, that about 15% of the Z isomer was transformed into E during the reaction.

3.4 Conclusion

This work has shown for the first time that it is possible to produce a high affinity rhenium compound from a stable ferrocenyl derivative. The ferrocenyl precursor **DFO** could be converted into its rhenium analogue **DRO**, thanks to the ligand transfer reaction[†]. Incidentally, the chemioselectivity of this reaction has been demonstrated using **FF**, since only the keto-ferrocenyl moiety reacted.

The Z isomer of the rhenium derivative **DRO** exhibited a high recognition for both ERα and ERβ. It had no significant effect on the proliferation of the hormone-dependent MCF-7 breast cancer cells nor on the ER- PC-3 prostate cancer cells. For these reasons, the rhenium derivative could be presented as a potential agent for radiotherapy. For imaging, it has been shown that **DFO** could be successfully labeled with ^{99m}Tc[†], using the water-soluble reagent $[^{99m}\mathrm{Tc}(\mathrm{H_2O})_3(\mathrm{CO})_3]^+$. The encouraging result of this efficient radiochemical synthesis of a tamoxifen-like derivative is that it can be achieved with good yield, under rather mild conditions. These labelled compounds are likely to have also good affinities with ER and to be biologically inert, as in the case for their rhenium analogue. Therefore, the radioactive rhenium and technetium derivatives may be potential site-specific radiopharmaceuticals.

[†]It is worthy to note that the ligand transfer reaction on **DFO** was performed several times successfully with both Re and Tc. However, the reproductibility was not perfect, and the factors responsible for that are under investigation.

3.5 Experimental section

All air-sensitive reactions were carried out under argon atmosphere, using standard Schlenk and vacuum-line techniques. Anhydrous THF and ether were obtained by distillation from sodium/benzophenone. TLC chromatography was performed on silica gel 60 GF254. Flash chromatography was performed on silica gel Merck 60 (0.040-0.060 mm). Infrared spectra were obtained on a IR-FT BOMEM Michelson-100 spectrometer equipped with a DTGS detector. ^{1}H and ^{13}C NMR spectra were recorded on 300 MHz Bruker spectrometer, and the results δ given in ppm, if not specified otherwise. Mass spectrometry was performed with a Nermag R 10-10C spectrometer. High resolution mass spectrometry was done with a MStation 700 (JEOL) spectrometer. Melting points were measured with a Kofler device.

$[^{99m}TcO_4]^-$ was eluted from a Mallinckrodt Med. Inc. generator. HPLC to monitor the labelling were measured on two different Merck Hitachi LaChrom D-7000 instruments. One of them was interfaced with a EG & G Berthold LB 508 radioflow detector, while the other was interfaced with a Merck Hitachi M-8000 LCMS. HPLC system: RP-18 column, eluent gradient (A = 0.1% CF_3COOH in H_2O, B = MeOH): 0-3 min: 100% A; 3-9 min: 75% A; 9.1 min: 66% A; 9.1-20 min: 66% $\rightarrow$ 0% A; 20-25 min: 0% A; 25.1-30 min: 100% A.

[(2-bromo-1-oxo-ethyl)-cyclopentadienyl]tricarbonylrhenium (24)

$CpRe(CO)_3$ (335 mg, 1 mmol) was dissolved in 3 mL of THF under argon. The solution was cooled to -70°C, before *n*BuLi (0.48 mL, 1.2 mmol) was added. It was left stirring at -70°C for 1h30 min. A solution of $BrCH_2CON(OMe)Me$ (273 mg, 1.5 mL) in 2 mL of THF was then added. The mixture was stirred again for 1h at -70°C. 2 mL of 1/10 HCl solution were added and the cold bath was removed. After 5 min, 20 mL of 1/10 HCl solution were added and the product was extracted with 3 x 30 mL of diethyl ether. The organic layer was washed with 20 mL of water, dried over $MgSO_4$, and the solvent evaporated under reduced pressure. The crude product was purified by TLC using diethyl ether:pentane 1:1 as the eluent. Unreacted $CpRe(CO)_3$ was first eluted (123 mg). The second fraction was identified as [(2-bromoethyl)-cyclopentadienyl]tricarbonylrhenium **24** (colorless oil, 143 mg, 31% yield or 50% yield if recovered $CpRe(CO)_3$ is taken into account).

^{1}H *NMR* (300 MHz, $CDCl_3$): δ 4.00 (s, 2H, CH_2); 5.45 (t, 2H, C_5H_4), 5.09 (t, 2H, C_5H_4).
^{13}C *NMR* (75 MHz, $CDCl_3$): δ 29.4 (CH_2), 85.5 and 88.8 (C_5H_4); 91.8 (Cip, C_5H_4), 186.9

(CO), 191.2 (C≡O). *mp* = 96°C. *MS* (CI, NH_3): m/z = 474 $[M+NH_4]^+$, 457 $[M+H]^+$. *IR* (CH_2Cl_2, cm^{-1}): 2033 and 1942 ν(C≡O), 1683 ν(CO).

1,2-bis-[4-(tert-butyl-dimethylsilyloxy)phenyl]-1-(4-hydroxyphenyl)but-1-ene (27)

Titanium tetrachloride (3.6 mL, 33 mmol) was added dropwise to a suspension of zinc powder (4 g, 61 mmol) in 80 mL of dry THF at 0°C. The mixture was heated at reflux for 2h. A second solution was prepared by dissolving 4-(*tert*-butyl-dimethylsilyloxy)-propiophenone (2.64 g, 10 mmol) **25** and 4,4'-(*tert*-butyl-dimethylsilyloxy)hydroxy benzophenone (3.28 g, 10 mmol) **26** in 50 mL of dry THF. This latter solution was added dropwise to the first solution and then the reflux was continued for 2h. After cooling to room temperature, the mixture was stirred with water and dichloromethane. The mixture was acidified with diluted hydrochloric acid until dark color disappeared and was decanted. The aqueous layer was extracted with dichloromethane and the combination of all the organic layers was dried on $MgSO_4$. After concentration under reduced pressure, the crude product was separated on silica gel column with dichloromethane (eluent) to yield pure **27** as an oily mixture of *Z* and *E* isomers. 75% yield.

^1H *NMR* (300 MHz, $CDCl_3$): δ 0.12 and 0.17 (s, 6H, $(CH_3)_2Si$), 0.17 and 0.23 (s, 6H, $(CH_3)_2Si$), 0.94 and 0.97 (s, 9H, ^{t}Bu), 0.97 and 1.01 (s, 9H, ^{t}Bu), 0.99 (t, J = 7.3 Hz, 3H, CH_3), 2.45 (q, J = 7.3 Hz, 2H, CH_2), 4.84 and 5.13 (s, 1H, OH), 6.45 and 6.48 (d, J = 8.6 Hz, 2H, H_{arom}), 6.60-6.75 (m, 4H, H_{arom}), 6.79 and 6.81 (d, J = 8.5 Hz, 2H, H_{arom}), 6.94 and 6.95 (d, J = 8.6 Hz, 2H, H_{arom}), 7.08 and 7.09 (d, J = 8.5 Hz, 2H, H_{arom}). ^{13}C *NMR* (75 MHz, $CDCl_3$): δ -4.4 ($Si(CH_3)_2$); 13.7 (CH_3); 18.2 (Cq of ^{t}Bu); 25.7 (CH_3 of ^{t}Bu); 28.8 and 28.9 (CH_2); 114.2 and 114.9 (CH_{arom}); 118.8 and 119.5 (CH_{arom}); 119.5 and 119.6 (CH_{arom}); 130.6 and 130.7 (CH_{arom}); 130.7 and 130.8 (CH_{arom}); 131.9 and 132.1 (CH_{arom}); 135.5, 135.6, 136.2, 136.5, 136.6, 137.0, 137.4, 140.7 (C=C and C_{arom}); 153.3, 153.4, 153.7, 154.2 (Cq_{arom}-O). *mp* = 65°C. *MS* (EI) m/z : 560 $[M]^{\cdot+}$, 545 $[M\text{-}CH_3]^+$, 57 $[^tBu]^+$. *HRMS* (EI, $C_{34}H_{48}O_3Si_2$: $[M]^{\cdot+}$) calcd: 560.3142, found: 560.3132. *IR* (KBr, cm^{-1}): 3433 ν(OH), 1605 ν(C=C), 1507 ν(C=C_{arom}), 1254 $\delta_s(CH_3)$ of Si-CH_3.

(*Z*)- and (*E*)-1-[2-(cyclopentadienyltricarbonylrhenium)-2-oxo-ethoxy-phenyl]-1,2-*di*(*p*-*tert*-butyldimethylsiloxyphenyl)but-1-ene (28)

Cs_2CO_3 (177 mg, 0.5 mmol) was added into a solution of $[BrCH_2CO\text{-}(\eta^5\text{-}C_5H_4)]Re(CO)_3$ (228 mg, 0.5 mmol) in 3 mL of acetone. A solution of 1-(p-hydroxyphenyl)-1,2-di(*p*-

tbutyldimethylsiloxy-phenyl)-but-1-ene (280 mg, 0.56 mmol) **27** in acetone (2 mL) was added dropwise (15 min). The mixture was stirred for 1h30 min. 10 mL of diethyl ether was added and the mixture was filtered over silica gel and evaporated under reduced pressure. The crude product obtained was purified by TLC using diethyl ether:pentane 1:2 as the eluent.

(*E*)-28: 25 mg, colorless oil, 5% yield, minor isomer.

^1H *NMR* (300 MHz, $CDCl_3$): δ 0.16 (s, 6H, $(CH_3)_2Si$), 0.22 (s, 6H, $(CH_3)_2Si$); 0.92 (t, J = 7.4 Hz, 3H, CH_3); 0.96 (s, 9H, CH_3 of ^{t}Bu), 0.99 (s, 9H, CH_3 of ^{t}Bu); 2.44 (q, J = 7.4 Hz, 2H, CH_2); 4.64 (s, 2H, CH_2CO); 5.39 (t, 2H, C_5H_4); 6.15 (t, 2H, C_5H_4); 6.55, 6.64, 6.79, 6.80, 6.93, 7.05 (6 d, 6×2H, CH_{arom}). ^{13}C *NMR* (75 MHz, $CDCl_3$): δ -4.4 ($Si(CH_3)_2$); 13.6 (CH_3); 18.2 (Cq of ^{t}BuSi); 25.6 (CH_3 of ^{t}Bu); 28.7 (CH_2); 71.9 (CH_2CO); 85.2, 88.9 and 92 (C_5H_4); 113.3, 119.5, 119.6, 130.5, 130.6, 132.2 (CH_{arom}); 135.4, 136.7, 137.2, 137.5, 141.2, 153.8, 154.2 and 155.2 (C=C and C_{arom}); 191.43 ($(CO)CH_2$ and (CO)Re). *IR* (CH_2Cl_2) : 2033 and 1940 ν(C≡O), 1704 and 1683 (C=O), 1604 (C=C). *MS* (CI): m/z = 937 $[M+H]^+$.

(*Z*)-23: 59 mg, colorless oil, 11% yield (*Z* structure identified by 2D NMR), major isomer.

^1H *NMR* (300 MHz, $CDCl_3$): δ 0.10 (s, 6H, CH_3), 0.15 (s, 6H, CH_3), 0.91 (s, 9H, CH_3 of ^{t}Bu), 0.93 (t, 3H, CH_3), 0.97 (s, 9H, CH_3 of ^{t}Bu), 2.43 (q, 2H, CH_2); 4.80 (s, 2H, CH_2CO), 5.43 (t, 2H, C_5H_4), 6.25 (t, 2H, C_5H_4), 6.46, 6.62, 6.68, 6.90, 6.92, 7.17 (6 d, 6×2H, C_6H_4). ^{13}C *NMR* (75 MHz, $CDCl_3$): δ -4.4 ($Si(CH_3)_2$); 13.6 (CH_3); 18.2 (Cq of ^{t}Bu); 25.6 (CH_3 of ^{t}Bu); 28.7 (CH_2); 71.9 (CH_2CO); 85.2, 88.9, 92 (C_5H_4); 114.1, 118.9, 119.4, 130.6, 130.9, 131.9 (CH_{arom}); 135.3, 136.4, 137.0, 137.9, 141.0, 153.4, 153.8, 156.1 (C=C and C_{arom}); 191.3 (C=O and C≡O). *IR* (CH_2Cl_2, cm^{-1}) : 2033 and 1939 ν(C≡O), 1704 and 1683 ν(C=O), 1604 ν(C=C). *MS* (CI, NH_3): m/z = 937 $[M+H]^+$.

(*Z*)-1-[2-(cyclopentadienyltricarbonylrhenium)-2-oxo-ethoxy-phenyl]-1,2-*di*-(*p*-hydroxyphenyl)but-1-ene ((*Z*)-DRO)

Direct synthesis: (*Z*)-1-[2-(cyclopentadienyltricarbonylrhenium)-2-oxo-ethoxy-phenyl]-1,2-di(*p*-*tert*-butyldimethylsiloxyphenyl)-but-1-ene **28** was dissolved in 5 mL of ethanol (41 mg, 0.044 mmol). After the addition of HCl (0.1 mL), the solution was stirred at 80°C for 20 min. The heating bath was removed, 20 mL of diethyl ether was added. The mixture was washed with 3 x 7 mL of water, dried over $MgSO_4$, filtered and evaporated under re-

duced pressure. The solid obtained was dissolved in diethyl ether, and pentane was added to precipitate the compound. 15 mg of (*Z*)-1-(2-(cyclopentadienyltricarbonylrhenium)-2-oxo-ethoxy-phenyl)-1,2-di(*p*-hydroxyphenyl)-but-1-ene DRO was isolated as colorless solid (48% yield).

^{1}H NMR (300 MHz, CD_3COCD_3): δ 0.88 (t, J = 7.5 Hz, 3H, CH_3); 2.45 (q, J = 7.5 Hz, 2H, CH_2); 4.96 (s, 2H, CH_2CO); 5.75 (t, 2H, C_5H_4), 6.41 (t, 2H, C_5H_4); 6.63, 6.64, 6.81, 6.82, 6.95, 7.03 (6 d, 6×2H, CH_{arom}), 8.17 (s, 1H, OH), 8.32 (s, 1H, OH). *^{13}C NMR* (100 MHz, CD_3COCD_3): δ 14.1 (CH_3); 22.8 (CH_2); 71.1 (CH_2CO); 87.1, 89.8, 94.0 (C_5H_4); 114.1, 115.5, 115.6, 131.2, 131.4, 132.5 (CH_{arom}); 134.1, 135.8, 137.9, 138.1, 141.4, 156.4, 156.7, 156.9 (C=C and C_{arom}); 191.1 and 193.3 (C=O and C≡O). *IR* (CH_2Cl_2, cm^{-1}): 2033 and 1941 ν(C≡O), 1704 and 1681 ν(C=O), 1608 ν(C=C). *MS* (ESI): m/z = 731 $[MNa]^+$, 726 $[MNH_4]^+$. *HRMS* (FAB, $C_{32}H_{25}O_7Re$: $[M]^{\cdot+}$) calcd: 708.1160, found: 708.1138.

(*E*)-1-[2-(cyclopentadienyltricarbonylrhenium)-2-oxo-ethoxy-phenyl]-1,2-*di*-(*p*-hydroxyphenyl)but-1-ene ((*E*)-DRO)

Direct synthesis: (*E*)-1-[2-(cyclopentadienyltricarbonylrhenium)-2-oxo-ethoxy-phenyl]-1,2-di(*p*-*tert*-butyldimethylsiloxyphenyl)-but-1-ene **28** was dissolved in 5 mL of ethanol (40 mg, 0.042 mmol). After the addition of HCl (0.1 mL), the solution was stirred at 80°C for 20 min. The heating bath was removed, 20 mL of diethyl ether was added. The mixture was washed with 3 x 7 mL of water, dried over $MgSO_4$, filtered and evaporated under reduced pressure. The crude product was purified by HPLC using acetonitrile:water 80:20 as the eluent. 16 mg of (*E*)-1-[2-(cyclopentadienyltricarbonylrhenium)-2-oxo-ethoxy-phenyl]-1,2-di(*p*-hydroxyphenyl)-but-1-ene were isolated as colorless solid (54% yield).

^{1}H NMR (300 MHz, CD_3COCD_3): δ 0.89 (t, J = 7.5 Hz, 3H, CH_3); 2.41 (q, J = 7.5 Hz, 2H, CH_2); 5.11 (s, 2H, CH_2CO); 5.79 (t, 2H, C_5H_4), 6.45 (t, 2H, C_5H_4); 6.49, 6.65, 6.70, 6.95, 6.96, 7.14 (6 d, 6×2H, C_6H_4), 8.08 (s, 1H, OH), 8.15 (s, 1H, OH). *^{13}C NMR* (100 MHz, CD_3COCD_3): δ 13.1 (CH_3); 70.6 (CH_2CO); 86.5, 89.1 and 93.3 (C_5H_4); 114.2, 114.3, 114.8, 130.5, 130.8, 131.9 (CH_{arom}); 133.5, 134.9, 137.4, 137.6, 140.5, 155.3, 155.7, 156.9 (C=C and C_{arom}); 190.5 and 192.6 (C=O and C≡O). *IR* (CH_2Cl_2, cm^{-1}) : 2033

and 1941 ν(C≡O), 1704 and 1682 ν(C=O), 1608 ν(C=C). *MS* (ESI): m/z = 731 $[MNa]^+$, 1439 $[2MNa]^+$. *HRMS* (FAB, $C_{32}H_{25}O_7Re$: $[M]^{\cdot+}$) calcd: 708.1160, found: 708.1152.

(*Z*+*E*)-1-[2-(cyclopentadienyltricarbonylrhenium)-2-oxo-ethoxy-phenyl]-1,2-di-(*p*-hydroxyphenyl)but-1-ene ((*Z*+*E*)-DRO)

Ligand transfer reaction: $[Re(CO)_6]^+[BF_4]^-$ (88.8 mg, 0.2 mmol) was dissolved in 1.5 mL of DMSO, and heated at 160°C for 30 min. The oil bath was removed, and 1-(2-ferrocenyl-2-oxoethoxyphenyl)-1-(*p*-hydroxyphenyl)-2-(*p*-hydroxyphenyl)but-1-ene (**DFO**) (111.6 mg, 0.2 mmol) was added to the reaction mixture 5 min later. The reaction mixture was heated again for 20 min. The blackened solution was cooled down to room temperature, hydrolysed by an acidic aqueous solution, and extracted with diethylether. The organic layers were collected, dried over $MgSO_4$, and concentrated by evaporation under reduced pressure. The crude product obtained was purified by TLC using diethyl ether:pentane 4:1 as the eluent. The final product (35 % yield) was a mixture of *Z* and *E* isomers.

HPLC retention time = 24.0 min (UV detection, A/B gradient as eluent)

1-[(2-ferrocenyl-2-oxo-ethoxy)phenyl]-1-(*p*-hydroxyphenyl)-2-ferrocenylbut-1-ene (FF)

In a three neck round flask, under inert atmosphere, NaH (132 mg, 3.3 mmol) at 60% in oil was dispersed in 100 mL of dry THF. **Fc-diOH** (1.27 g, 3 mmol) was introduced in the flask, and the mixture was left stirring for 10 min. α-chloroacetylferrocene (787 mg, 3 mmol) was then added slowly. The mixture was heated under reflux for 24h. A slightly acidic aqueous solution was poured into the reaction mixture. The reaction mixture was extracted by dichloromethane. The collected organic layers were finally dried over $MgSO_4$ and evaporated under reduced pressure. The crude product was separated by flash chromatography using diethyl ether:dichloromethane 1:9 as the eluent. The purified product was a mixture of *Z* and *E* isomers (1:1 ratio). Yield 36%.

^{1}*H NMR* (300 MHz, $CDCl_3$): δ 0.99 (t, 3H, CH_3), 2.56 (q, J = 7.4 Hz, 2H, CH_2), 3.89 (m, 2H, (η^5-C_5H_4)-C=C), 4.05 (m, 2H, (η^5-C_5H_4)-C=C), 4.10 (s, 5H, Cp of CpFe(η^5-C_5H_4)-C=C), 4.21 and 4.22 (s, 5H, Cp of CpFe(η^5-C_5H_4)-CO), 4.57 (m, 2H, (η^5-C_5H_4)-CO), 4.91 (m, 4H, (η^5-C_5H_4)-CO + O-CH_2-CO), 5.22 (s, 1H, OH), 5.31 (s, 1H, OH), 6.68-7.13 (m, 8H, CH_{arom}). ^{13}*C NMR* (75 MHz, $CDCl_3$): δ 15.7 (CH_3); 28.1 (CH_2); 68.2, 69.3, 69.4, 69.5, 70.3, 72.9 (Cp or (η^5-C_5H_4)); 71.5 and 71.7 (O-CH_2-CO); 114.6, 114.8, 115.2, 115.3, 130.7, 130.7, 131.3 (CH_{arom}); 137.1, 137.2, 138.4, 138.6 (C=C and Cq_{arom});

154.3 and 156.7 (C_{arom}-O.); 199.8 (C=O). *MS* (EI): m/z = 650 $[M]^{\cdot+}$. *HRMS* (FAB, Na, $C_{38}H_{34}O_3Fe_2$: $[MNa]^+$) calcd: 673.1106, found: 673.1093. *IR* (KBr, cm^{-1}) : 1663 ν(C=O), 1605 ν(C=C), 1507 ν(C=C_{arom}).

1-[2-(cyclopentadienyltricarbonylrhenium)-2-oxo-ethoxy-phenyl]-1-(*p*-hydroxyphenyl)-2-ferrocenylbut-1-ene (FR)

$[Re(CO)_6]^+[BF_4]^-$ (132 mg, 0.3 mmol) was dissolved in 2 mL of DMSO, and heated at 160°C for 30 min. The oil bath was removed, and 1-[(2-ferrocenyl-2-oxo-ethoxy)phenyl]-1-(*p*-hydroxyphenyl)-2-ferrocenylbut-1-ene (**FF**) (205 mg, 0.32 mmol) was added to the reaction mixture 5 min later. The reaction mixture was heated again for 20 min. The blackened solution was cooled down to room temperature, hydrolysed by an acidic aqueous solution, and extracted with diethylether. The organic layers were collected, dried over $MgSO_4$, and concentrated by evaporation under reduced pressure. The crude product obtained was purified by preparative TLC using diethyl ether:pentane 3:1 as the eluent. Yield 21 %.

^{1}H NMR (300 MHz, $CDCl_3$): δ 1.01 (t, J = 7.4 Hz, 3H, CH_3), 2.57 (m, 2H, CH_2), 3.88 (m, 2H, η^5-C_5H_4 of Fc), 4.06 (m, 2H, η^5-C_5H_4 of Fc), 4.10 (s, 5H, Cp), 5.42 (m, 2H, (η^5-C_5H_4)Re), 6.20 (m, 2H, (η^5-C_5H_4)Re), 6.68-7.14 (m, 8H, CH_{arom}). *^{13}C NMR* (75 MHz, $CDCl_3$): δ 15.6 (CH_3); 28.0 (CH_2); 53.9, 68.2, 69.3, 69.4, 85.4 and 89.1 (CH of Cp or η^5-C_5H_4); 72.0 (O-CH_2-CO); 87.0, 87.2 and 92.4 (Cq of η^5-C_5H_4); 114.3, 114.5, 115.2, 115.3, 130.7, 130.8, 131.3, 131.5 (CH_{arom}); 136.8, 137.3 and 137.3 (C=C and Cq_{arom}); 154.3 and 156.0 (Cq_{arom}-O); 191.6 (C=O). *MS* (EI): m/z = 800 $[M]^{\cdot+}$. *HRMS* (FAB, Na, $C_{36}H_{29}O_6FeRe$: $[MNa]^+$) calcd: 823.0771, found: 823.0757. *IR* (CH_2Cl_2, cm^{-1}) : 2032 and 1937 ν(C≡O), 1702 ν(C=O), 1506 ν(C=C_{arom}).

1-[2-(cyclopentadienyltricarbonyltechnetium-99m)-2-oxo-ethoxy-phenyl]-1,2-di-(*p*-hydroxyphenyl)but-1-ene ($D^{99m}TO$)

1 mL of an aqueous solution containing [99mTc(H2O)3(CO)3]+ was prepared as described in the literature [110, 111]:

A vial was charged with 4 mg of boranocarbonate ($K_2H_3BCO_2$), 7 mg of $Na_2B_4O_7$, and 7 mg of sodium tartrate, sealed, and flushed with nitrogen. 1 mL of generator eluate containing $[^{99m}TcO_4]^-$ was added and the vial heated to 90°C for 30 min to generate

$[^{99m}Tc(H_2O)_3(CO)_3]^+$ in >95% yield (HPLC). The pH of the solution was set to pH 7.4 with phosphate buffer.

50 μL of this solution was then added to a 0.5 mL solution of the ferrocenyl compound **DFO** (10^{-3} mol·L^{-1}) in DMSO. Heating from 90°C to 120°C for 40 min in a sealed vial afforded D^{99m}TO in 70% yield. HPLC retention time = 24.2 min (γ detection).

1-[2-(cyclopentadienyltricarbonyltechnetium-99)-2-oxo-ethoxy-phenyl]-1,2-*di*-(*p*-hydroxyphenyl)but-1-ene (D^{99}TO)

Compound (*Z*)-**DFO** (17 mg, 30 μmol) in 1 mL of DMSO was added to purified white powder $[NEt_4]_2[^{99}TcCl_3(CO)_3]$ (26 μmol) in a Schlenk tube equipped with a magnetic stirring bar. The dark red mixture was heated for 3h30 at 120°C under N_2. Water was added and left to precipitate overnight. A brown-black precipitate was filtered and **D^{99}TO** (70%) was extracted by ether (yellow-orange solution). The product was identified by HPLC with β-detection and NMR (^{1}H and ^{99}Tc). The NMR spectra of this compound were recorded on a Varian Mercury 200 MHz instrument.

HPLC retention time = 24.4 min (UV detection, A/B gradient as eluent) and 24.7 min (β-detection).

^{1}H NMR (200 MHz, CD_3COCD_3): δ 0.85 (t, J = 7.6 Hz, 3H, CH_3); 2.41 (m, 2H, CH_2); 4.99 (s, 2H, CH_2CO); 5.61 (t, J = 2.2 Hz, 2H, C_5H_4), 6.31 (t, J = 2.4 Hz, 2H, C_5H_4), 6.61 (m, 12H, CH_{arom}), 8.23 (s, 1H, OH), 8.38 (s, 1H, OH). *^{99}Tc NMR* (67.37 MHz, CD_3COCD_3): -2506 (major); -2657 (minor)

Chapter 4

Improved bioavailability of ferrocenyl tamoxifen derivatives by nanoparticle coating

Before a bioactive compound discovered in research laboratories reaches the market and is prescribed as treatment, a decade-long, tedious and costly road awaits pharmaceutical companies. Thousands of novel compounds are synthesized, passed on to biologists who then test them for the required activity. The most interesting candidates are then selected to undergo toxicology testing. Once their compliance to the strict requirements defined by the government (e.g. the Food and Drug Administraton in the USA) is proven, the drug has to be formulated. This involves the decision of how the drug is to be given to the patients. Finally, after successful clinical testing, the goverment committees will examine the potential drug and give approval for commercial distribution.

4.1 Introduction

Among the various organometallic compounds we synthesised in this thesis work, compound **DFO** was singled out for its antiproliferative activity and good binding affinity with the estrogen receptors. Another compound of interest is **Fc-diOH**. This molecule is an analogue of OH-Tam, where the tamoxifen β-aromatic benzyl ring has been replaced by the aromatic ferrocene moiety, and the amino side-chain has been replaced by a second hydroxyl group (Fig. 4-1). It is the most efficacious cytotoxic compound to date in the laboratory ($IC_{50} \simeq 0.7$ μM on MCF-7 cells, 0.44 μM on MDA-MB-231 cells) [133]. Interestingly, both compounds are active against ER+ and ER- cancer cells, suggesting that they do not target only the ERs in cancer cells.

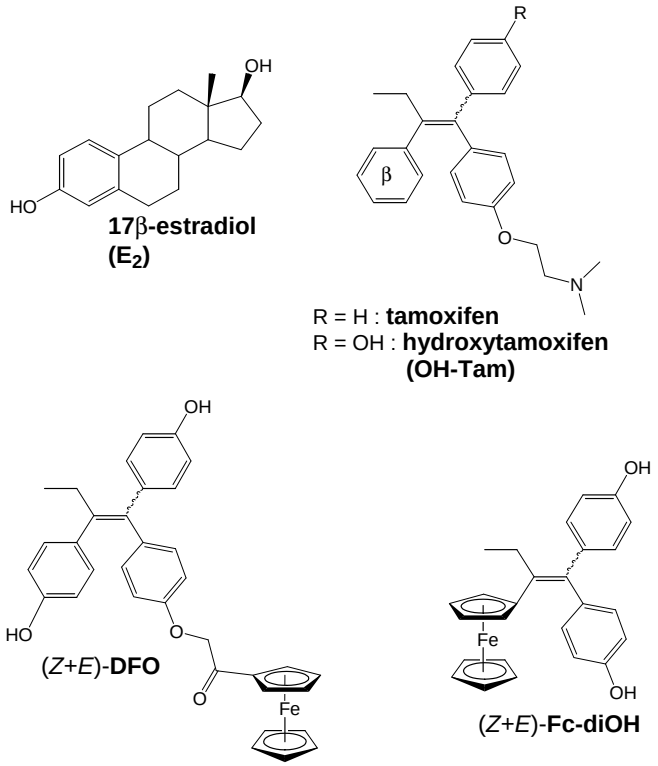

Figure 4-1: Structures of **Fc-diOH** and **DFO** as compared to hydroxytamoxifen and 17β-estradiol

Although **Fc-diOH** and **DFO** appear to be promising potential drugs, they still encounter the problem of bioavailibility, so common to active biomolecules discovered in laboratories, especially for polyphenols [182]. They are also rather lipophilic, making its solubility in physiological media and distribution in the body difficult. Moreover, administration of anticancer drugs increasingly requires intravenous perfusion. However, once injected in the bloodstream,

the substance is distributed throughout the body, not specifically to the target [183]. In addition, as a foreign entity, the drug is often detected by the physiological defence system of the organism: the mononuclear phagocyte system or MPS. For instance, in the opsonization process, one or more receptors of the MPS cells interact with the foreign substance and promote its uptake by these cells. Once captured or/and degraded by the metabolism, the substance is removed from blood circulation by macrophages of the MPS [183]. Therefore, only a small amount of the active metabolite reaches the tumours. Since high doses have to be administered, toxicological problems arise as side-effects. To summarize, the ferrocenyl derivatives encounter serious problems before reaching the target: insolubility in physiological media, poor bioavailability as a polyphenol, non-specific distribution and degradation by the MPS.

Hence, in order to increase the circulation time in the bloodstream and to enhance the probability of the molecule effectively reaching the target tissue, we chose to trap the hydrophobic active molecule in the lipophilic layer of submicronic long-circulating colloidal carrier systems. One of the first and intensively investigated colloidal particles is the liposome [184, 185]. Liposomes possess a lipidic bilayer that encapsulates an internal aqueous phase (Fig. 4-2). The drug could be either in the aqueous layer or carried within the lipid membrane. Despite the long circulation time of liposomes in the bloodstream, these vesicles have limited physical and chemical stability [184]. Additionally, they do not very efficiently incorporate lipophilic substances [186]. For this type of compound, nanoparticles (NP) are prefered.

Nanoparticles are defined as solid colloidal particles of a polymeric nature, ranging in size from 10 to 1000 nm [187]. They are subdivided into two classes: nanospheres and nanocapsules (Fig. 4-3). On one hand, a nanosphere is a dense matrix of polymer into which the active molecules are trapped. On the other hand, a nanocapsule is a vesicular system, whose oily core retains the active molecules, and is surrounded by a protective polymeric membrane. These drug carriers have hydrophilic PolyEthyleneGlycol (PEG) chains (Fig. 4-4) at their surface. The presence of these highly hydrophilic groups sterically inhibits hydrophobic and electrostatic interactions of the carrier with blood components [188], and thus avoids recognition of the drug carriers by opsonins, and eventually the destruction by the MPS.

The other important issue in drug delivery is the ability of drug carriers to accumulate in the target. To address this problem, the particular "leaky property" of tumour blood vessels is exploited. Solid tumours are heterogeneously vascularized. Some regions are richly and densely vascularized, with constant formation of new capillarities from pre-existing vessels (angiogen-

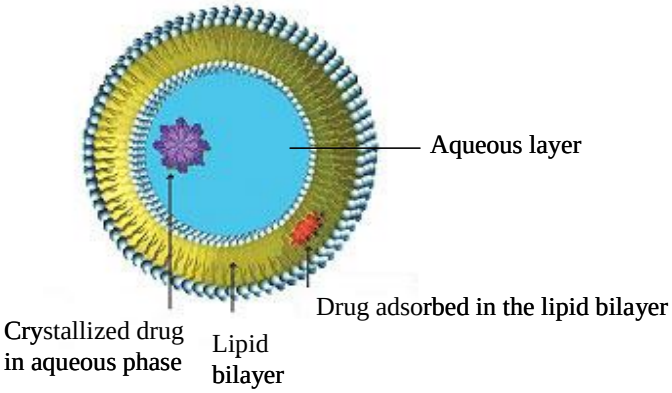

Figure 4-2: Structure of a liposome [189]

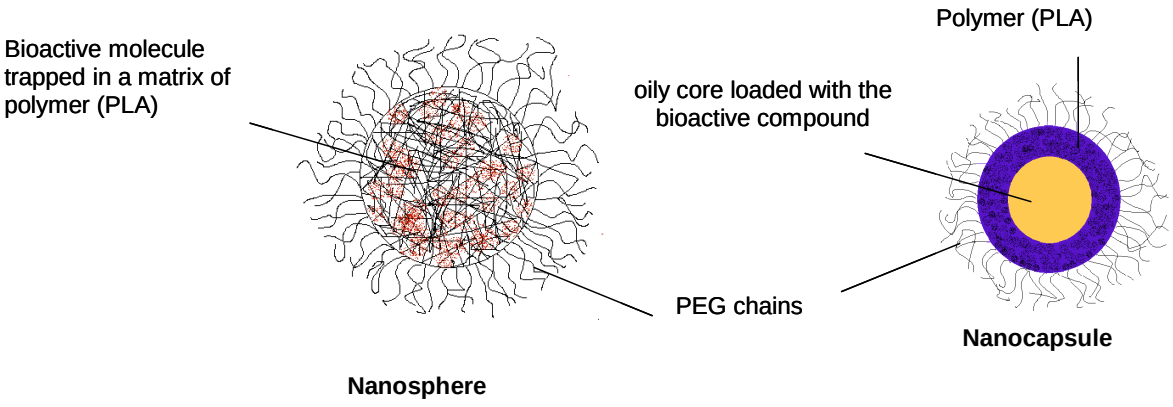

Figure 4-3: Structures of the PEG/PLA nanosphere and nanocapsule

esis). Because of the irregular growth, tumour blood vessels present various abnormalities, resulting in an enhanced permeability of tumour vasculature. A major consequence is the presence of gaps in their discontinuous endothelium [190]. Their pore size cut-off is quite diverse depending on the tissue, but it roughly lies in the range of 300-900 nm [190–192]. Hence, it is possible to produce suitable nanoparticles which can cross the vascular endothelium (extravasation process) and deliver the therapeutic agents in the tumour [190,193]. In other words, the drug nanocarriers could transport and concentrate the antiproliferative agents in the tumours by passive targeting [194]. This method to improve bioavailibility has already been used for many bioactive molecules, including tamoxifen [195–197] and the lipophilic pure antiestrogen RU 58 668 [51,198,199].

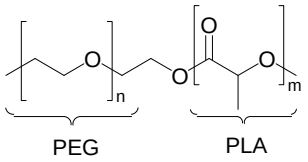

Figure 4-4: Structure of the PEG/PLA copolymer

Therefore, for a more targeted and effective drug delivery, **Fc-diOH** and **DFO** were loaded inside nanospheres (NS) and nanocapsules (NC). The polymer chosen is biodegradable poly(D, L-lactic acid), or PLA (Fig. 4-4). Hydrophilic PEG chains are covalently bound to PLA, and extrude at the surface of the NPs. The ability of the nanospheres and nanocapsules to modulate the antiproliferative activity of **Fc-diOH** and **DFO** was then assessed by *in vitro* biological evaluation.

4.2 Materials and Methods

4.2.1 Chemicals

Soy phosphatidylcholine Lipoïd S75® (about 70% phosphatidylcholine) was purchased from Lipoïd GmbH (Germany). Miglyol 810N was kindly provided by Hüls (Germany). Poly(D,L-lactide) PLA_{50} of MW 42 kDa was purchased from Phusis (France). PLA/PEG (D,L-PLA50 MW 45 kDa and PEG MW 5 kDa) was synthesized and characterized as previously described [200].

Compounds **Fc-diOH** and **DFO** were prepared as described in Chapter 2, and in literature [93, 112].

The solvents were analytical grade, and all other chemicals were commercially available at reagent grade. Water was purified by reverse osmosis (MilliQ, Millipore®).

4.2.2 Preparation of PEG-coated nanoparticles

The preparation of nanospheres (NS) according to Fessi *et al.* [201] was based on interfacial deposition of preformed polymer, following solvent displacement (nanoprecipitation).

Briefly, 20 mg of polymer or copolymer were dissolved in 1 mL of acetone containing 1 mM of **Fc-diOH** or **DFO**, and rapidly dispersed into 2 mL of demineralised and sterilised water, followed by acetone evaporation under nitrogen flow.

In the case of the nanocapsules (NC), only 5 mg of preformed polymer was dissolved in 1 mL of acetone. 2.1 mg of **Fc-diOH** or 5.9 mg of **DFO** was dissolved in a mixture of lipophilic surfactant (Lipoïd S75®, 66 mg/mL of acetone) and oil (Miglyol 810, 25 μL/mL of acetone). 25 μL of this preparation was added to the organic phase, before dispersion in water.

Control particles without **Fc-diOH** and **DFO** were prepared under the same conditions.

4.2.3 Physicochemical characterization of nanoparticles

The size of the nanoparticles was measured by QuasiElastic Laser Light Scattering using a Nanosizer N4 Plus (Coulter Electronics, Florida, USA). The potential measurements (ζ potentials) were determined with a Zetasizer 4 (Malvern Instruments, UK) after dilution of the NS or NC suspensions in 1 mM KCl in a 1:2 volume ratio (NP suspension/ 1mM KCl).

4.2.4 Measurement of encapsulation efficacy

The incorporation efficiency of the ferrocenyl derivatives was expressed both as encapsulation rate (w/w ratio) and percentage of encapsulation (%). The amount of **Fc-diOH** and **DFO** associated with the drug carriers was indirectly determined by UV-vis spectroscopy (Jenway 6405 UV/vis Spectrometer). These values were calculated as the difference between the total amount of **Fc-diOH** or **DFO** used to prepare the loaded nanoparticles and the amount of free molecules in the aqueous phase, after separation by centrifugation (60 000 g, 1h, 4°C) for nanospheres, or by ultrafiltration/centrifugation (450 000 g, 1 h, 4°C) using Millicon eppendorfs (10 000 NMWL, Millipore®, France) for nanocapsules. The concentrations of **Fc-diOH** and

DFO in the aqueous phase after centrifugation were determined by the absorbance at $\lambda = 304$ nm for **Fc-diOH** and at $\lambda = 276$ nm for **DFO**.

4.2.5 Cell culture and transcription measurements

We used a method based on the capacity of free and encapsulated antiestrogens to inhibit estradiol-induced transcription in MELN cells, as previously described [51]. MELN cells are MCF-7 cells stably transfected with a construct in which the luciferase (LUC) reporter gene is placed downstream of an estrogen response element (ERE) linked to the minimal β-globin promoter (ERE-β-globin-LUC). MELN and MCF-7 cells were cultured in DMEM (DMEM Biological Industries, Inc., Kibbutz Beit Haemek, Israel) supplemented with L-glutamine (2 mM), penicillin (50 UI/mL), streptomycin (50 UI/mL) and 10% FCS (fetal calf serum) and maintained at 37°C, with 5% CO_2 in a humidified atmosphere. Before steroid treatment, MELN cells were grown for 3 days in phenol red free DMEM containing 10% charcoal-stripped FCS. Under these experimental conditions, 0.1 nM of 17β-estradiol (E_2) was found to induce the maximum LUC transcription. In order to evaluate the release of **Fc-diOH** and **DFO** from the formulations, NCs and NSs containing **Fc-diOH** or **DFO** were added to the culture medium containing 0.1 nM E_2. After a total incubation time of 18h at 37°C, cells were collected, rinsed and lysed in 250 μL of LUC buffer (25 mM Tris/HPO_4 at pH 7.8, 10 mM $MgCl_2$, 1% Triton X100, 15% glycerol, 1 mM EDTA, 1 mM DTT). Protein concentration was determined by the Biorad assay (Bio-Rad GmbH, Munich, Germany). Quantification of LUC activity was performed in triplicate in a luminometer (TD 20/20, Tuner Designs, Sunnyvale, CA), after injection of the LUC buffer (100 μL) supplemented with 100 mM ATP and 87 μg of luciferin/mL to 100 μL of cellular extract.

4.2.6 Cell cycle analyses and apoptosis estimation

MCF-7 cells ($2{\cdot}10^5$) were exposed or not to the free or the encapsulated drugs (1 or 10 μM) during 48h and 72h. The cells were washed twice in cold phosphate-buffered saline (PBS), pelleted and suspended in ice-cold ethanol (80% in MilliQ water). In some experiments, 10 μM α-tocopherol was added for 1h to the cell medium prior to further treatment. Fixed cells were then centrifuged and resuspended in PBS at 25°C containing 100 μg/mL RNase A (Roche Molecular Biochemicals, Meylan, France) and 20 μg/mL propidium iodide (PI, Sigma-Aldrich) for 30 min at 37°C. Cells were further analysed with a FACS Calibur (Becton-Dickinson, Le

Pont de Claix, France) equipped with an argon laser tuned at 488 nm and data were obtained with the CellQuest 1.2.2 and the ModFit LT 1.01 softwares (Becton-Dickinson).

4.3 Results

4.3.1 Characterization of NPs

The PEG/PLA nanoparticles were formed by nanoprecipitation [187]. This conventional technique consists of dissolving the copolymer and the drug in an organic solvent miscible with water, such as acetone. The organic solvent/water mixture and organic solvent evaporation lead to polymer precipitation in the form of nanospheres. In the case of nanocapsules, the oily phase is dissolved together with the copolymer and the drug in the organic layer. Following solvent evaporation, the polymer precipitates around the oily droplets to yield the nanocapsules.

Table 4.1: Characterization of the nanoparticles (mean value ± S.D., n = 6)

	Mean diameter (nm)	**Zeta potential** (mV)	**Encapsulation efficiency** (µg/mg polymer)	**Encapsulation yield** (%)
Nanospheres				
empty	50 ±18	-1.1 ± 0.5	-	-
Fc-diOH	52 ± 16	-7.3 ± 0.6	198 ± 4	95 ± 2
DFO	56 ± 18	-2.9 ± 0.4	255 ± 20	93 ± 7
Nanocapsules				
empty	178 ± 77	-73.5 ± 1.4	-	-
Fc-diOH	180 ± 56	-44. 0 ± 0.7	8 ± 1	83 ± 4
DFO	130 ± 35	- 57.8 ± 4.0	25 ± 1	93 ± 5

The size and the zeta (ζ) potential of both empty NSs and NCs, and those loaded with the organometallic compounds **Fc-diOH** and **DFO** are summarized in Table 4.1. The ζ potential indicates the surface charge of the NP. While the size of the NCs was in the range of 150-200 nm, that of the NSs was three times smaller. The incorporation of the drug did not modify this parameter for either formulation. This was not the case for the ζ potential: the decrease of the ζ potential of **Fc-diOH**- and **DFO**-charged NSs, as well as the increase of NC ζ potential indicate that some amount (though small) of the compounds were adsorbed at the

NP surface. Indeed, the ζ potential of the aqueous suspension of **Fc-diOH** and **DFO** at 1 mM was definitely negative, and measured as -35.5 $\pm$ 5.2 and -36.6 $\pm$ 0.5 mV, respectively. These values are lower than the ζ potential of the unloaded NSs. Hence, if the organometallic compounds were adsorbed at the surface of the NSs, the ζ potential of the loaded NSs should decrease. On the other hand, the ζ potentials of the free **Fc-diOH** and **DFO** are higher than those of the empty NCs. Therefore, we expected the ζ potential of the loaded NCs to increase, if the organometallic compounds were adsorbed at the surface of the NCs.

The encapsulation yield of both molecules in the NSs was higher than that in the NCs. The maximum concentrations of encapsulated **Fc-diOH** and **DFO** were similar in the NSs (1 mM) and were estimated at 70 μM and 160 μM in the NCs respectively. The encapsulation efficiency and encapsulation yield of both types of NPs showed that the organometallic compounds have a high affinity for the copolymer. Nevertheless, NCs had a tendency to incorporate a lower concentration of both compounds, a feature characteristic of such nanoparticles, because of the reduced drug solubility in oil [51].

4.3.2 Modulation of the antiestrogenic activity by loaded NPs

We wondered next about the biological activity of the NPs. In a previous work, we showed that unloaded PEG/PLA NPs have no inhibitory activity on the luciferase gene expression in MELN cells [51]. As shown in Fig. 4-5, free **Fc-diOH** had a weak inhibition on estradiol-induced transcription in MELN cells at 16h, with an IC_{50} value about 100-fold that of OH-Tam. However, the trapped **Fc-diOH** has an even weaker ability to inhibit the expression of luciferase than the free compound at 16h. This feature suggests that only a limited amount of drug was released from the NPs. Surprisingly, the type of NP does not seem to affect the transcription inhibition activity.

Data from Fig. 4-6 indicate that **DFO** has a better anti-estrogenic activity than **Fc-diOH**. Precisely, its luciferase inhibition activity is ten times stronger than that of **Fc-diOH**. Again, both **DFO**-loaded NCs and NSs have a weaker transcription inhibition activity than free **DFO**. Interestingly, **DFO** released from the NC has an inhibitory activity somewhat similar to that of **Fc-diOH** trapped in the NPs (data from Fig. 4-5 compared to data from Fig. 4-6). However, in the case of **DFO**, the type of NP in which the molecule is encapsulated seems to influence its activity. Comparatively, the **DFO**-loaded NS inhibits the luciferase activity 100 times more

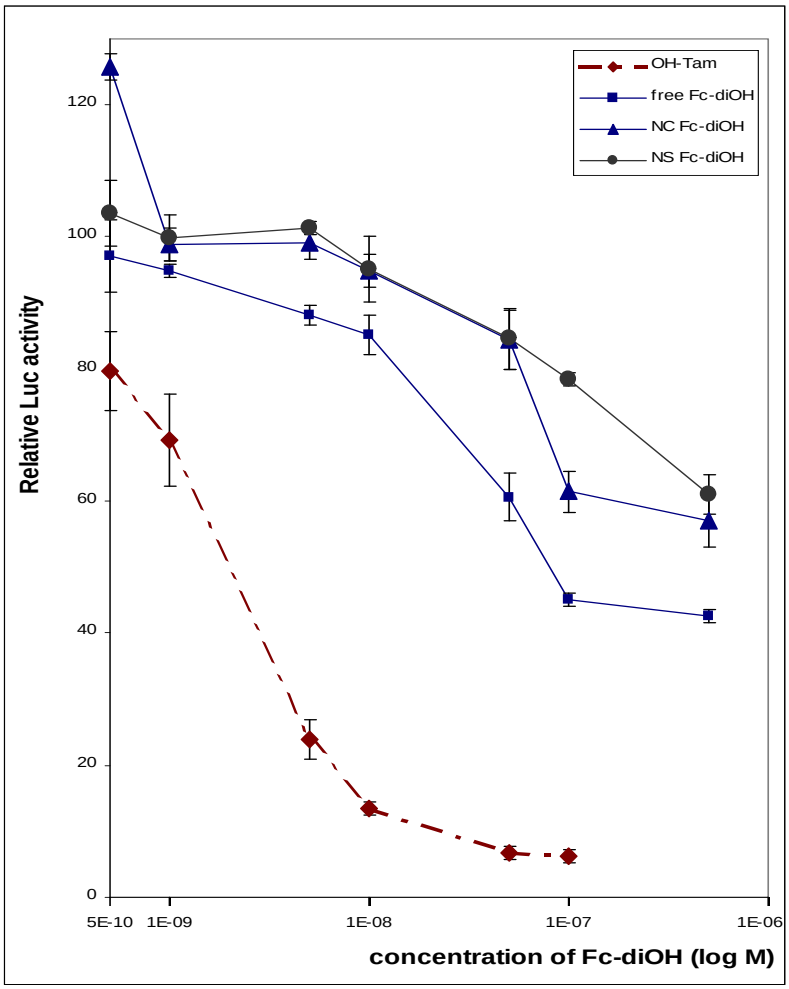

Figure 4-5: Inhibitory capacity of free **Fc-diOH** and **Fc-diOH**-loaded PEG/PLA NS and NC on E_2-mediated transcription.
MELN cells (10^6) grown in phenol red free medium for 3 days were treated in triplicates during one night (16h) with increasing concentrations of **Fc-diOH**, free and entrapped in either NS or NC as described in Materials and Methods. In the control experiment, E_2- induced transcription (at 1 nM) was estimated as 100%. It corresponds to a 8-9 fold increase as compared to the basal level of transcription (obtained without E_2, but only vehicle). After harvest and lysis, luciferase activity was measured. Data are expressed as mean % ± S.D. (n=3) of inhibition of the E_2-induced luciferase (LUC) activity.

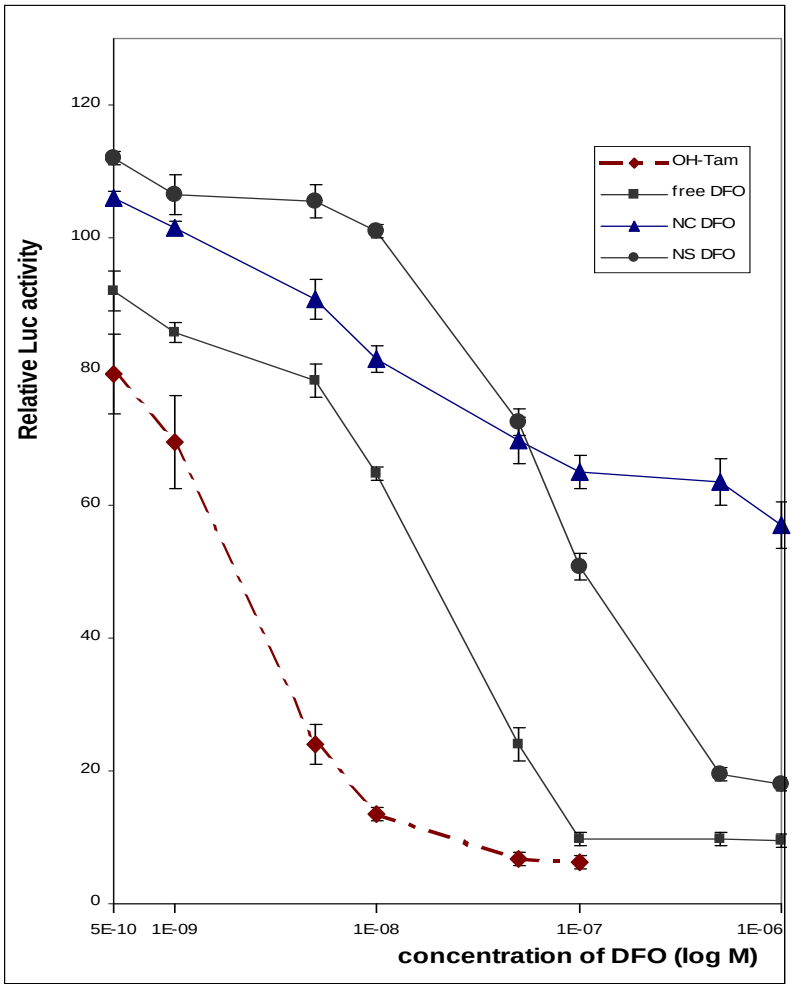

Figure 4-6: Inhibitory capacity of free **DFO** and **DFO**-loaded PEG/PLA NS and NC on E_2-mediated transcription.
MELN cells were treated as described in Fig. 4-5 with free and NS, NC-trapped compound **DFO**. Results are expressed as in Fig. 4-5.

than **DFO** trapped in a NC at high concentrations (0.1 - 1 μM). This suggests that NCs release **DFO** more slowly than NSs at these concentrations.

4.3.3 Activity of loaded NPs on cell cycle and apoptosis

We then wanted to know if these nanosystems behave differently towards MCF-7 cell cycle. Flow cytometry experiments were carried out at 48h and 72h with both free and encapsulated **Fc-diOH** and **DFO** at 1 μM and/or at 10 μM. Data (FACS analysis) are summarized in Tables 4.2 and 4.3. Both empty NSs (Table 4.2) and empty NCs (Table 4.3) had no effect on the cell distribution as already observed [202]. Interestingly, when compared to control, the number of cells in the S phase of the cycle increased more clearly with **Fc-diOH** than with **DFO**, whether the compounds were trapped or not in NS. Altogether, this suggests that at 10 μM, **Fc-diOH** has a greater capacity to arrest the cell cycle in the S phase than **DFO**. At a similar concentration, once trapped in the NS, **DFO** had a strong capacity to arrest cell cycle in the G0/G1 phase at 48h, unlike the free drug. This effect was no longer observed at 72h, suggesting maybe some instability of **DFO**, which is protected only as long as it stays encapsulated.

Table 4.2: FACS analysis on MCF-7 cells exposed to free and encapsulated ferrocenyl derivatives in nanospheres (NS) of PEG/PLA. Data given in number of cells.

	G0 /G1		**S**		**G2 /M**		**Sub G1**	
	48h	72h	48h	72h	48h	72h	48h	72h
Control	69	79	14	12	14	8	3	2
Fc-diOH (10 µM)	63	54	24	37	6	6	11	10
DFO (10 µM)	66	62	13	18	19	16	5	10
NS **Fc-diOH**	64	52	25	38	8	7	8	17
NS **DFO**	80	66	10	20	9	9	5	15
Empty NS	70	73	13	11	14	9	2.5	3

Interestingly, an increase of cells in apoptosis (sub G1) was noticed after cell exposure to both free **Fc-diOH** and **DFO**. This fate was stronger in the case of cell incubation with the trapped compounds. **Fc-diOH** and **DFO** have comparable ability to induce apoptosis in MCF-7 cells and this potency is enhanced and delayed by entrapment in PEG/PLA nanospheres.

Table 4.3: FACS analysis on MCF-7 cells exposed to free and encapsulated ferrocene derivatives in nanocapsules (NC) of PEG/PLA. Data given in number of cells.

	G0 /G1		S		G2 /M		Sub G1	
	48h	72h	48h	72h	48h	72h	48h	72h
Control	67	72	16	15	17	13	1.1	1.25
Fc-diOH (1µM)	36	44	38	36	25	19	4	3
DFO (1µM)	66	73.5	16	14	17	12	2	2
NC **Fc-diOH**	49	59	28.5	24	22	16	1.6	2.3
NC **DFO**	63	65	17	21	20	12	1.1	3
Empty NC	66	69	18	19	16	15	1.6	2

We also compared the activity of **Fc-diOH**/**DFO**-loaded NCs on the cell cycle. Since the encapsulation loading was weaker in the NCs than in the NSs, MCF-7 cells were exposed to weaker drug concentrations in the case of the NC experiments, in order to avoid too high an amount of polymer in the cell culture. Results presented in Table 4.3 clearly indicate that **Fc-diOH** at 1 μM, whether free or encapsulated in the NCs, arrests cell cycle in the S phase, and to a more limited extent in the G2/M phase. This feature is less clearly observed at 10 μM, a concentration which rather induces apoptosis (see Table 4.4). Additionally, a smaller number of cells in apoptosis were noticed after 48h when the compounds were encapsulated, hence suggesting again the delay induced by the nanovectors. At this low concentration, free **DFO** at 1 μM had no significant effect on MCF-7 cells, contrary to the encapsulated drug which slightly increased the number of cells in the S phase.

4.3.4 Influence of α-tocopherol on cell cycle and apoptosis.

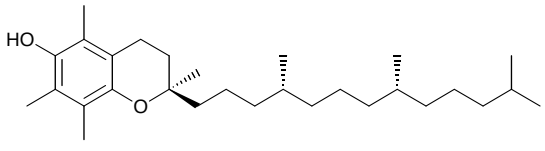

α-tocopherol

Figure 4-7: Structure of α-tocopherol (Vitamine E)

It has been suggested that OH-Tam at high concentrations may induce the production of Reactive Oxygen Species (ROS) in breast cancer cells [203]. Similarly, ferrocene derivatives have also been suspected of producing ROS [127, 129, 130]. We next examined if the effects of the ferrocene derivatives observed in MCF-7 cells could imply ROS production. Similar experiments to those described in Table 4.3 were performed in the presence or absence of the anti-oxidant α-tocopherol (Fig. 4-7), as it is known to prevent ROS production [204]. Data from Table 4.4 suggest that α-tocopherol alone has practically no effect on the MCF-7 cell cycle in the experimental conditions, although it slightly induced apoptosis. However, we predicted that the presence of α-tocopherol would decrease apoptosis of cells exposed to **Fc-diOH** and **DFO**. Indeed, in the presence of α-tocopherol, the number of cells in subG1 dropped from 7 to 4.7, and from 7.7 to 5.6 respectively, after 72h of treatment. These data also indicate that **DFO** could have a dual effect on MCF-7 cells, an anti-proliferative effect through its inhibitory capacity towards ERα activation and downstream consequences, and the capacity to produce free radicals.

Table 4.4: Effect on free radical inhibition by α-tocopherol (α-toco) on MCF-7 cells exposed to free compounds **Fc-diOH** and **DFO**. Data given in number of cells.

	G0 /G1		**S**		**G2 /M**		**Sub G1**	
	48h	72h	48h	72h	48h	72h	48h	72h
Control	65	67	20	18	15	12	2.25	1.9
Fc-diOH (10 µM)	55	59	36	31	7	9	8	7
DFO (10 µM)	72	71	14	15	9	11	6.7	7.7
α-toco	54	67	24	18	21	14	3.9	3.9
Fc-diOH + α-toco	52	64	39	27	8.5	8.6	3.5	4.7
DFO + α-toco	71	72	14.5	14	12	13	5.9	5.6

4.4 Discussion

In the present work, we have designed two types of nanovectors, aiming at the *in vivo* delivery of insoluble anticancer molecules. We took advantage of previously well established formulations based on the copolymer PEG/PLA, which proved to be capable of incorporating high concentrations of a SERM like OH-Tam [195, 202] and a pure antiestrogen like RU 58 668 [51, 198, 199]. Ameller *et al.* demonstrated that PEG/PLA (PEG-poly(D,L-lactic acid)

nanoparticles are non-toxic [199], in contrast to the PEG/PACA (PEG-poly(alkylcyanoacrylate) copolymer. They also have a loading efficiency three fold higher than the tamoxifen-loaded (PEG/PACA) nanoparticles. The RU 58 668-loaded nanospheres were able to inhibit E_2-induced tumours growth with a quantity 50 to 100 times less than what was needed for free RU 58 668, when administred by i.v. in mice bearing MCF-7 breast cancer xenografts.

Both organometallic compounds **Fc-diOH** and **DFO** were incorporated in these formulations at a high yield, although the NS incorporated higher concentrations than the NC. The size of the resulting NPs were within the range of the gaps in the discontinuous cancerous endothelium, and thus they are possible vectors for the organometallic bioligands. Both compounds showed efficiency in inhibiting estradiol-induced transcription in ER+ breast cancer cells, arresting cell cycle, and inducing apoptosis in the same cells. A great benefit of such devices is their endocytosis ability, leading to the delivery of their trapped drug inside the cell [194]. They have, among others, the advantage of protecting the drugs against hydrolysis and oxidation. The synthesised nanovectors tend to promote the activity of **Fc-diOH** and **DFO**, maybe because encapsulation reduces their degradation. This observation is consistent with the results from the estradiol-induced transcription experiments on MELN cells and from the flow cytometry experiments.

It is worthwhile to differentiate the results from antiestrogenic experiments on MELN cells and those from the FACS Analysis. The distinction lies in the concentrations used for each method. In the anti-estrogenic experiments, the concentrations reached very small values such as 0.5 nM, whereas in the FACS experiments the concentrations were 1 μM and 10 μM. Therefore, in the MELN cells where the NPs were very diluted, a greater percentage of **Fc-diOH** or **DFO** was liberated. This is a function of the partition coefficient between oily/polymeric medium and water for the NCs and the NSs. Moreover, diffusion of the active species through the polymeric matrix of the NSs was favoured for small concentrations. Thus, there was a greater percentage of organometallic compounds liberated from the NPs in the estradiol-induced transcription experiments than in the flow cytometry experiments. So the relative reduced activity of the trapped compounds compared to the free ones was different according to the type of experiment.

The mechanism of action of both organometallic compounds has been investigated, in order to better understand their antiproliferative effects. **Fc-diOH** and **DFO** probably each follow different mechanisms, due to their structural differences. Indeed, it has been proposed that the

ferrocene moiety in **Fc-diOH** acts as an intramolecular oxidation assistant [133, 135]. However, in the structure of **DFO**, the ferrocene moiety cannot act as an intramolecular oxidation "antenna", having no electron carrier π system to link the ferrocene moiety to a phenol group. So the antiproliferative effect observed must follow another mechanism. It might involve the oxidation of the ferrocene to a ferrocenium salt and production of hydroxyl radicals via the Fenton process [205].

Our experiments suggest that α-tocopherol does reverse the antiproliferative effect of both organometallic compounds, since the number of cells in subG1 dropped when the anti-oxidant agent was added. This result is consistent with our hypothesis that Fe plays an important role in inhibiting the proliferation of breast cancer cells. As a well-known anti-oxidant, α-tocopherol could prevent the oxidation of Fe(II) into Fe(III), and also help to reduce the downstream production of ROS, thus lowering the number of cells in subG1.

4.5 Conclusion

Interest in nanovectors of highly cytotoxic compounds has fostered many drug formulations, such as the lipid-coated aggregates of the metal coordination complex *cis*-platin [186]. This article describes for the first time an efficient encapsulation of organometallic compounds, which should possess stronger metal-ligand bonds than classical metal coordination complexes. The ferrocene derivatives **Fc-diOH** and **DFO** have shown interesting cytotoxic effects on MCF-7 cells, which very likely involve ROS production. But since their water-insolubility impedes their potential biological activity, both were successfully loaded at high yield in nanospheres and nanocapsules. Thanks to their appropriate physico-chemical characteristics, the nanoparticles were able to deliver the water-insoluble compounds to cancer cells, and shield the active molecules from degradation by delaying their release.

Futhermore, according to the metal introduced, organometallic compounds could offer different possibilities. As suggested in **Chapter 3**, the Fe atom of **DFO** may be exchanged with radioactive Re or Tc, without changing the good binding affinity with ERα and β. Then it would be possible to follow the bioavailibility of the labeled bioligands in the body, once released from their protective nanovectors. To date, biodistribution of labelled nanocarriers have been studied, but not that of labelled bioligands coated in nanoparticles.

Chapter 5

Conclusion

Despite huge progress since the mid-twentieth century, current breast cancer treatments would still benefit by becoming milder, safer and more successful. This presentation illustrated the rich possibilities that the emerging field of bioorganometallic chemistry can offer to oncology research, by bringing together a metallic entity and bioactive organic molecules.

Chapter 1 presented an introduction to the treatments and diagnosis techniques available for breast cancer. It focused on hormone therapy and the development of novel bioactive molecules, from pure antiestrogens to SERMs. The way the natural hormone estradiol favours cell proliferation was briefly discussed, and then a mechanism of action of the antiestrogen drug tamoxifen was presented. Despite its popularity for the treatment of hormone-dependent breast tumours, the drug resistance problems have stimulated the synthesis of various compounds with new therapeutic spectra. Of particular interest are the benefits offered by metal-based compounds. An overview was given on their use in medicine. Although the discovery of the platinum inorganic complex *cis*-platin is a landmark in this field, organometallic compounds present the advantage of more robust metal-ligand bonds, having a more covalent character. Therefore, insights in the biological applications of organometallic compounds, especially of ferrocenyl, rhenium and technetium derivatives, were outlined. This last part introduced the main topics of the research described in this thesis.

The coupling of organometallic moieties tethered to SERMs has led to the synthesis of different types of compounds showing variable affinities for the two main ER isoforms ERα and ERβ. In such a program, a ferrocenyl substituent was tethered to the 4-hydroxytamoxifen scaffold, the active metabolite of tamoxifen. In **Chapter 2**, we have designed and studied the first ferrocenyl tamoxifen-like compounds (the **DF** and **FO** series), whose chemical structures bear a ferrocenyl chain instead of the key amino side-chain of 4-hydroxytamoxifen (Fig. 5-1). The biological results demonstrated that shorter ferrocenyl chain lengths induced a stronger biological activity; and when two phenol groups in *trans* configuration were present, a better RBA and an antiproliferative effect were observed. Additionally, molecular modelling suggested that a ketone functionality on the side-chain of the ligand would favour the binding to ERα thanks to a stabilizing interaction with Asp 351. This is consistent with the high RBA values registered for compound **DFO**. Moreover, this molecule displayed an antiproliferative activity both on ER+ and ER- cancer cells. This inhibition potency probably stemmed more from the ER-independent cytotoxicity of the compound, rather than its antiestrogenic character. Nevertheless, this issue needs a more thorough investigation. In particular, the question remains open on why the antiproliferative activity of the ferrocenyl derivatives on the MDA-MB-231 cells was significantly weaker than on the PC-3 cells.

A further exploitation of the ligand-receptor studies prompted us to propose the **AC** series, where a carboxylic acid side-chain was coupled to the structure of the cytotoxic **Fc-diOH**.

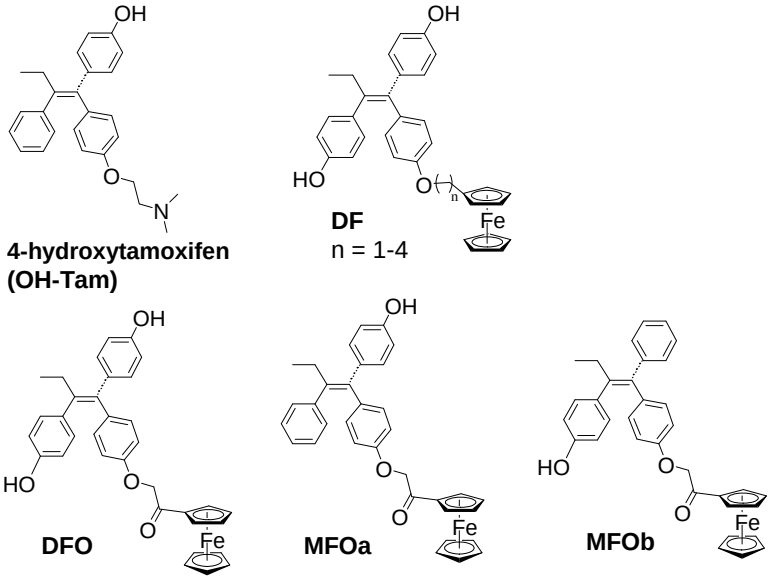

Figure 5-1: Ferrocenyl compounds studied in **Chapter 2**

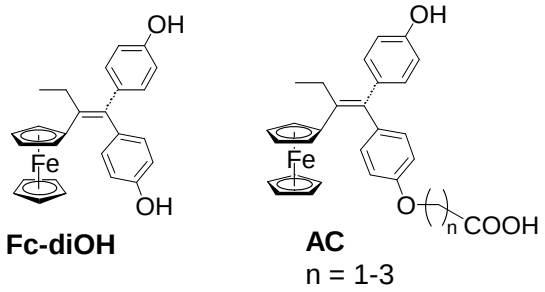

Figure 5-2: **AC** compounds and **Fc-diOH**

Since our previous experiments as well as those done by Willson *et al.* and Ruenitz *et al.* all suggested the importance of the ketone functionality in conveying an antiproliferative effect, we hoped to increase this inhibition activity by combining it to the **Fc-diOH** scaffold. However, the biological results were less satisfactory than expected. Complementary biological experiments (such as checking Ruenitz's results) and additional studies in molecular modelling and in electrochemistry are needed to understand these poor behaviours.

Although ferrocenyl derivatives have shown antiproliferative effects, it is worthy to note that the simple presence of a ferrocenyl group is not always sufficient to yield cytotoxic compounds. For example, a proliferative activity was found for the **DF**s, **MFOa** and **MFOb** on ER+ cancer cells. Both the position and the structural pattern in which ferrocene is inserted are important.

While the motif "(ferrocene)-(conjugated spacer)-(*para*-phenol)" has seemed to be crucial for the cytotoxic effects of ferrocenyl derivatives until now [132], the early results on the **AC** series may challenge this idea.

Interestingly, the ferrocenyl derivative **DFO** possesses a particular structure which enables it to be both a potential drug and a stable precursor for the synthesis of radiopharmaceuticals. In **Chapter 3**, the successful conversion of the compound into a rhenium and a technetium derivative by a ligand exchange reaction was described (Fig. 5-3). Optimization of the reaction parameters was studied. The ligand transfer reaction was chemioselective, and required the presence of a ketone unit adjacent to the ferrocene moiety. The radioactive organometallic rhenium and technetium compounds should have high affinity with ER, as was the case for the non-radioactive rhenium derivative **DRO**. Thus, they could be either potential site-specific drugs (^{188}Re derivatives), or targeted radiopharmaceuticals (^{99m}Tc derivatives). However, since the conversion of **DFO** into the technetium derivative **DTO** was not complete, a more thorough optimization of the experimental conditions is needed before *in vivo* testing. The synthesis of the radioactive ^{188}Re derivative and its study still await us. In addition, a close look at the evolution of the ligand transfer reaction had opened some paths towards a possible mechanism for the reaction. Further experiments could be useful to elucidate this reaction. For instance, it may be interesting to probe the implication of the ferrocenium salt in the mechanism.

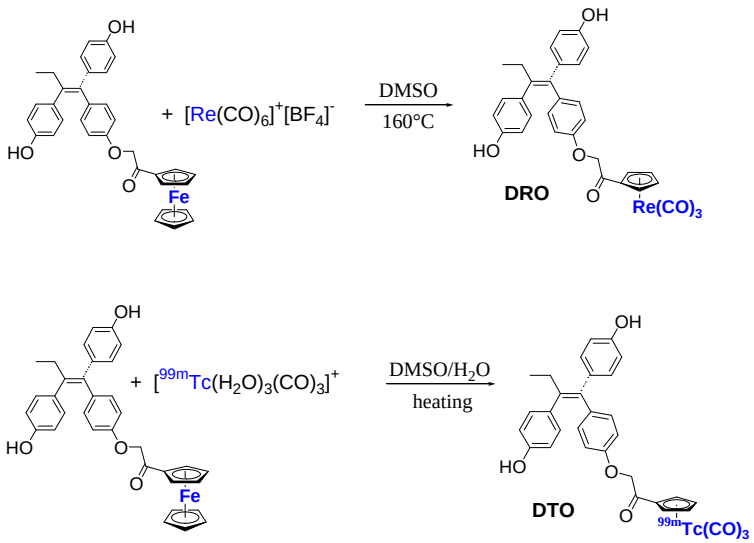

Figure 5-3: Synthesis of **DRO** and **DTO** by the ligand transfer reaction

Eventually, the bioavailibility of bioactive compounds was addressed in **Chapter 4**. Although **Fc-diOH** and **DFO** have an interesting antiproliferative activity in breast cancer cells, they are insoluble in biological fluids, and are prone to degradation once introduced in the body. To overcome this problem, they were incorporated in two types of stealth nanoparticles: PEG/PLA nanospheres (NS) and nanocapsules (NC). Their physico-chemical parameters were measured (size, ζ potential, encapsulation and loading efficiency), and their biological activity was assessed. Notwithstanding potential drug adsorption at the NP surface, **Fc-diOH** and **DFO** were incorporated efficiently in NC and NS, which slowly released both compounds. They induced apoptosis, and this effect was more prominent with loaded NS. A decrease in their antiproliferative activity by the addition of the anti-oxidant α-tocopherol indicated that ROS may be involved. Therefore, nanosystems, containing for the first time a high load of anticancer organometallic triphenylethylenes, have been developed. Their small size and delayed drug release are compatible with an increased persistence in the blood. Moreover, their enhanced apoptotic potential by the encapsulation reveals a promising antitumour activity. We could extend the bioavailibility study to other protection forms, such as tailoring the compounds with sugar units or lipidic chains.

Since the rhenium compound **DRO** is the non-steroidal ligand with the highest affinity for both ER isoforms to date, crystallization of this ligand with ERα is currently underway, in collaboration with Prof. G. Greene (University of Chicago, USA). The same experiments are also underway with **DFO** and **Fc-diOH**. It would be of great interest to assess if there is indeed an interaction between the ketone group and Asp 351 in ERα LBD, as predicted by molecular modelling studies. Moreover, in protein crystal structure analysis, crystallographers often have to add heavy metals to the ligand-receptor complex in order to solve the phase problem. With an organometallic ligand itself bearing a heavy metal, it might be not necessary to add these salts during crystallization. Thus, a more precise ligand-receptor structure, without exogenous molecules to disturb the conformation, could hopefully be produced.

The biological results on the organometallic compounds described in this work provided a further refinement of our understanding of ligand structure-binding affinity correlations for the ERs. They also outlined prototypes for potent cytotoxic molecules on breast cancer cells. Although some questions remain unclear and require further studies, the results from the thesis contribute to the general perspective that bioorganometallic chemistry could be useful in medicine. This concept could indeed offer a plausible alternative to chemotherapy (with its

drastic side-effects), and tamoxifen (with its problems of resistance). The combination of the antiestrogenic quality of the biovector hydroxytamoxifen with a cytotoxic ferrocenyl moiety did confer a different antiproliferative activity to the SERM, and gave rise to broader therapeutic possibilities, especially in the tamoxifen-resistant cases.

References

[1] American Cancer Society, *Breast Cancer Facts and Figures: 2005-2006*. American Cancer Society, Inc., 2005.

[2] J. Breasted, *The Edwin Smith Surgical Papyrus*. University of Chicago Press, 1930.

[3] J. Ferley, F. Bray, P. Pisani, and D. Parkin, *GLOBOCAN 2002: Cancer Incidence, Mortality and Prevalence Worldwide*. Lyon: IARCPress, 2004.

[4] A. Jemal, R. Siegel, E. Ward, T. Murray, J. Xu, and M. J. Thun, "Cancer statistics, 2007," *CA Cancer J Clin*, vol. 57, pp. 43–66, January 1, 2007.

[5] La Ligue contre le Cancer, *Le Cancer du Sein, grand public*. Paris: La Ligue Nationale contre le Cancer, 2006.

[6] C. Maggio, "State of the art of current modalities for the diagnosis of breast lesions," *European Journal of Nuclear Medicine and Molecular Imaging*, vol. 31, pp. S56–S69, 2004.

[7] R. Smith-Bindman, P. Chu, D. L. Miglioretti, C. Quale, R. D. Rosenberg, G. Cutter, B. Geller, P. Bacchetti, E. A. Sickles, and K. Kerlikowske, "Physician predictors of mammographic accuracy," *J. Natl. Cancer Inst.*, vol. 97, pp. 358–367, March 2, 2005.

[8] D. S. M. Buist, P. L. Porter, C. Lehman, S. H. Taplin, and E. White, "Factors contributing to mammography failure in women aged 40-49 years," *J. Natl. Cancer Inst.*, vol. 96, pp. 1432–1440, October 6, 2004.

[9] L. Berlin, "The missed breast cancer redux: Time for educating the public about the limitations of mammography?," *Am. J. Roentgenol.*, vol. 176, pp. 1131–1134, May 1, 2001.

[10] A. Mavroforou, D. Mavrophoros, and E. Michalodimitrakis, "Screening mammography, public perceptions, and medical liability," *European Journal of Radiology*, vol. 57, no. 3, pp. 428–435, 2006.

[11] K. Scheidhauer, C. Walter, and M. D. Seemann, "FDG PET and other imaging modalities in the primary diagnosis of suspicious breast lesions," *European Journal of Nuclear Medicine and Molecular Imaging*, vol. 31, no. 0, pp. S70–S79, 2004.

[12] F. Benard and E. Turcotte, "Imaging in breast cancer: Single-photon computed tomography and positron-emission tomography," *Breast Cancer Res.*, vol. 7, no. 4, pp. 153 – 162, 2005.

[13] C. Lehman and M. Schnall, "Imaging in breast cancer: Magnetic resonance imaging," *Breast Cancer Res.*, vol. 7, no. 5, pp. 215 – 219, 2005.

[14] W. Liang, W. F. Lawrence, C. B. Burnett, Y.-T. Hwang, M. Freedman, B. J. Trock, J. S. Mandelblatt, and M. E. Lippman, "Acceptability of diagnostic tests for breast cancer," *Breast Cancer Research and Treatment*, vol. 79, no. 2, pp. 199–206, 2003.

[15] J. C. Reubi, "Peptide receptors as molecular targets for cancer diagnosis and therapy," *Endocr. Rev.*, vol. 24, pp. 389–427, August 1, 2003.

[16] G. Beatson, "On the treatment of inoperable cases of carcinoma of the mamma: suggestions for a new method of treatment, with illustrative cases," *Lancet*, vol. 148, no. 3802, pp. 101–107, 1896.

[17] E. Jensen, *Steroid hormones, receptors and antagonists*, pp. 1–17. (L. Castagnetta, I. Nenci, H.L. Bradlow, Eds.) Annals New York Academy of Sciences, 1996.

[18] E. R. DeSombre, P. P. Carbone, E. Jensen, W. L. McGuire, S. A. Wells, J. L. Wittliff, and M. B. Lipsett, "Special report. Steroid receptors in breast cancer.," *N Eng. J. Med.*, vol. 301, pp. 1011–1012, 1979.

[19] S. Green, P. Walter, V. Kumar, A. Krust, J.-M. Bornert, P. Argos, and P. Chambon, "Human oestrogen receptor cDNA: sequence, expression and homology to v-erb-A," *Nature*, vol. 320, no. 6058, pp. 134–139, 1986.

[20] G. L. Greene, P. Gilna, M. Waterfield, A. Baker, Y. Hort, and J. Shine, "Sequence and expression of human estrogen receptor complementary DNA," *Science*, vol. 231, pp. 1150–1154, March 7, 1986.

[21] G. Kuiper, E. Enmark, M. Pelto-Huikko, S. Nilsson, and J.-A. Gustafsson, "Cloning a novel estrogen receptor expressed in rat prostate and ovary," *Proc. Natl. Acad. Sci. USA*, vol. 93, pp. 5925–5930, 1996.

[22] S. Mosselman, J. Polman, and R. Dijkema, "ERß: Identification and characterization of a novel human estrogen receptor," *FEBS Lett.*, vol. 392, pp. 49–53, 1996.

[23] G. G. Kuiper, B. Carlsson, K. Grandien, E. Enmark, and J. Haggblad, "Comparison of the ligand binding specificity and transcript tissue distribution of estrogen receptors alpha and ß," *Endocrinology*, vol. 138, pp. 863–870, 1997.

[24] B. Hanstein, S. Djahansouzi, P. Dall, M. W. Beckmann, and H. G. Bender, "Insights into the molecular biology of the estrogen receptor define novel therapeutic targets for breast cancer," *Eur. J. Endocrinol.*, vol. 150, pp. 243–255, 2004.

[25] E. Enmark, M. Pelto-Huikko, K. Grandien, S. Lagercrantz, J. Lagercrantz, G. Fried, M. Nordenskjold, and J.-A. Gustafsson, "Human estrogen receptor ß-gene structure, chromosomal localization and expression pattern.," *J. Clin. Endocrinol. Metab.*, vol. 82, pp. 4258–4265, 1997.

[26] K. Dahlman-Wright, V. Cavailles, S. A. Fuqua, V. C. Jordan, J. A. Katzenellenbogen, K. S. Korach, A. Maggi, M. Muramatsu, M. G. Parker, and J.-A. Gustafsson, "International union of pharmacology. LXIV. Estrogen receptors," *Pharmaceutical Review*, vol. 58, pp. 773–781, December 1, 2006.

[27] V. C. Jordan, "Antiestrogens and selective estrogen receptor modulators as multifunctional medicines. 1. Receptor interactions," *J. Med. Chem.*, vol. 46, no. 6, pp. 883–908, 2003.

[28] C. A. Hudis, "Trastuzumab–mechanism of action and use in clinical practice," *N. Engl. J. Med.*, vol. 357, pp. 39–51, Jul 5 2007.

[29] G. Ismael, D. D. Rosa, E. de Azambuja, S. Braga, and M. Piccart-Gebhart, "Trastuzumab (herceptin) for early-stage breast cancer," *Hematol. Oncol. Clin. North. Am.*, vol. 21, pp. 239–56, Apr 2007.

[30] EBTCG, "Effects of chemotherapy and hormonal therapy for early breast cancer on recurrence and 15-year survival: an overview of the randomised trials," *Lancet (Early Breast Cancer Trialists'Collaborative Group)*, vol. 365, pp. 1687–1717, 2005.

[31] G. N. Hortobagyi and A. U. Buzdar, "Current status of adjuvant systemic therapy for primary breast cancer: progress and controversy," *CA Cancer J Clin*, vol. 45, pp. 199–226, July 1, 1995.

[32] V. C. Jordan, "Antiestrogens and selective estrogen receptor modulators as multifunctional medicines. 2. Clinical considerations and new agents," *J. Med. Chem.*, vol. 46, no. 7, pp. 1081–1108, 2003.

[33] V. C. Jordan, *Tamoxifen for the treatment and prevention of breast cancer.* PRR, Inc., 1999.

[34] J. F. R. Robertson, "Selective oestrogen receptor modulators/new antioestrogens: a clinical perspective," *Cancer Treatment Reviews*, vol. 30, no. 8, pp. 695–706, 2004.

[35] M. N. Singh, H. F. Stringfellow, E. Paraskevaidis, P. L. Martin-Hirsch, and F. L. Martin, "Tamoxifen: Important considerations of a multi-functional compound with organ-specific properties," *Cancer Treatment Reviews*, vol. 33, no. 2, pp. 91–100, 2007.

[36] J. M. Dixon, "Exemestane and aromatase inhibitors in the management of advanced breast cancer," *Expert. Opin. Pharmacother.*, vol. 5, pp. 307–316, Feb 2004.

[37] E. P. Winer, C. Hudis, H. J. Burstein, A. C. Wolff, K. I. Pritchard, J. N. Ingle, R. T. Chlebowski, R. Gelber, S. B. Edge, J. Gralow, M. A. Cobleigh, E. P. Mamounas, L. J. Goldstein, T. J. Whelan, T. J. Powles, J. Bryant, C. Perkins, J. Perotti, S. Braun, A. S. Langer, G. P. Browman, and M. R. Somerfield, "American society of clinical oncology technology assessment on the use of aromatase inhibitors as adjuvant therapy for postmenopausal women with hormone receptor-positive breast cancer: status report 2004," *J Clin Oncol*, vol. 23, pp. 619–629, Jan 20 2005.

[38] M. J. Meegan and D. G. Lloyd, "Advances in the science of estrogen receptor modulation," *Curr. Med. Chem.*, vol. 10, pp. 181–210, 2003.

[39] R. A. Magarian, L. B. Overacre, S. Singh, and K. L. Meyer, "The medicinal chemistry of nonsteroidal antiestrogens : a review," *Curr. Med. Chem.*, vol. 1, p. 61, 1994.

[40] A. M. Brzozowski, A. C. Pike, Z. Dauter, R. E. Hubbard, T. Bonn, O. Engstrom, L. Ohman, G. L. Greene, J.-A. Gustafsson, and M. Carlquist, "Molecular basis of agonism and antagonism in the oestrogen receptor," *Nature*, vol. 389, pp. 753–758, 1997.

[41] C. K. Osborne, H. Zhao, and S. A. W. Fuqua, "Selective estrogen receptor modulators: structure, function and clinical use.," *J. Clin. Oncol.*, vol. 18, pp. 3172–3186, 2000.

[42] K. Paech, P. Webb, G. G. Kuiper, S. Nilsson, J.-A. Gustafsson, P. J. Kushner, and T. S. Scanlan, "Differential ligand activation of oestrogen receptors ERalpha and ERbeta at AP1 sites," *Science*, vol. 277, pp. 1508–1510, 1997.

[43] P. Webb, P. Nguyen, C. Valentine, G. N. Lopez, G. R. Kwok, E. McInerney, B. S. Katzenellenbogen, E. Enmark, J.-A. Gustafsson, S. Nilsson, and P. J. Kushner, "The estrogen receptor enhances AP-1 activity by two distinct mechanisms with different requirements for receptor transactivation functions," *Mol. Endocrinol.*, vol. 13, pp. 1672–1685, October 1, 1999.

[44] L. J. Lerner, J. F. Holthaus, and C. R. Thompson, "A non-steroidal estrogen antagonist 1-(p-2-diethylaminoethoxyphenyl)-1-phenyl-2-p-methoxyphenyl-ethanol," *Endocrinology*, vol. 63, pp. 295–318, 1958.

[45] J. I. MacGregor and V. C. Jordan, "Basic guide to the mechanisms of antiestrogen action," *Pharmacol. Rev.*, vol. 50, pp. 151–196, 1998.

[46] F. S. Zeelen and E. W. Bergink, *Structure-activity relationships of the steroid estrogens*, pp. 39–48. (J. Raus, H. Martens, G Leclercq, Eds.) Academic Press, 1980.

[47] J. P. Raynaud, T. Ojasoo, M. M. Bouton, E. Bignon, M. Pons, and A. Castres de Paulet, *Structure-activity relationships of steroids estrogens.* (McLachlan Ed.) Elsevier, 1985.

[48] A. E. Wakeling, M. Dukes, and J. Bowler, "A potent specific pure antiestrogen with clinical potential," *Cancer Res.*, vol. 51, pp. 3867–73, Aug 1 1991.

[49] A. E. Wakeling and J. Bowler, "ICI 182,780, a new antioestrogen with clinical potential," *J. Steroid Biochem. Mol. Biol.*, vol. 43, pp. 173–7, Sep 1992.

[50] P. Van de Velde, F. Nique, F. Bouchoux, J. Bremaud, M. C. Hameau, D. Lucas, C. Moratille, S. Viet, D. Philibert, and G. Teutsch, "RU 58,668, a new pure antiestrogen inducing a regression of human mammary carcinoma implanted in nude mice," *J. Steroid Biochem. Mol. Biol.*, vol. 48, pp. 187–96, Feb 1994.

[51] T. Ameller, V. Marsaud, P. Legrand, R. Gref, and J.-M. Renoir, "In vitro and in vivo biologic evaluation of long-circulating biodegradable drug carriers loaded with the pure antiestrogen RU 58668," *Int. J. Cancer*, vol. 106, no. 3, pp. 446–454, 2003.

[52] S. Maillard, T. Ameller, J. Gauduchon, A. Gougelet, F. Gouilleux, P. Legrand, V. Marsaud, E. Fattal, B. Sola, and J.-M. Renoir, "Innovative drug delivery nanosystems improve the anti-tumor activity in vitro and in vivo of anti-estrogens in human breast cancer and multiple myeloma," *The Journal of Steroid Biochemistry and Molecular Biology*, vol. 94, no. 1-3, pp. 111–121, 2005.

[53] A. K. Shiau, D. Barstad, P. M. Loria, L. Cheng, P. J. Kushner, D. A. Agard, and G. L. Greene, "The structural basis of estrogen receptor/coactivator recognition and the antagonism of this interaction by tamoxifen," *Cell*, vol. 95, pp. 927–937, 1998.

[54] V. C. Jordan, J. Mac Gregor Schafer, A. S. Levenson, H. Liu, K. M. Pease, L. A. Simons, and J. W. Zapf, "Molecular classification of estrogens," *Cancer Research*, vol. 61, pp. 6619–6623, 2001.

[55] H. Liu, E.-S. Lee, A. De Los Reyes, J. W. Zapf, and C. V. Jordan, "Silencing and reactivation of the selective estrogen receptor modulator-estrogen receptor alpha complex," *Cancer Research*, vol. 61, no. 9, pp. 3632–3639, 2001.

[56] T. M. Willson, B. R. Henke, T. M. Momtahen, P. S. Charifson, K. W. Batchelor, D. B. Lubahn, L. B. Moore, B. B. Oliver, H. R. Sauls, J. A. Triantafillou, S. G. Wolfe, and P. G. Baer, "3-[4-(1,2-diphenylbut-1-enyl)phenyl]acrylic acid: A non-steroidal estrogen with functional selectivity for bone over uterus in rats," *J. Med. Chem*, vol. 37, no. 11, pp. 1550–1552, 1994.

[57] T. M. Willson, J. D. Norris, B. L. Wagner, I. Asplin, P. Baer, H. R. Brown, S. A. Jones, B. Henke, H. Sauls, S. Wolfe, D. C. Morris, and D. P. McDonnell, "Dissection of the

molecular mechanism of action of GW5638, a novel estrogen receptor ligand, provides insights into the role of estrogen receptor in bone," *Endocrinology*, vol. 138, pp. 3901–3911, September 1, 1997.

[58] D. J. Bentrem, R. C. Dardes, H. Liu, J. MacGregor-Schafer, J. W. Zapf, and V. C. Jordan, "Molecular mechanism of action at estrogen receptor alpha of a new clinically relevant antiestrogen (GW7604) related to tamoxifen," *Endocrinology*, vol. 142, pp. 838–846, February 1, 2001.

[59] Y.-L. Wu, X. Yang, Z. Ren, D. P. McDonnell, J. D. Norris, T. M. Willson, and G. L. Greene, "Structural basis for an unexpected mode of SERM-mediated ER antagonism," *Molecular Cell*, vol. 18, no. 4, pp. 413–424, 2005.

[60] J. A. Clemens, D. R. Bennett, L. J. Black, and C. D. Jones, "Effects of a new antiestrogen, keoxifene (LY156758), on growth of carcinogen-induced mammary tumors and on LH and prolactin levels," *Life Sci.*, vol. 32, pp. 2869–2875, Jun 20 1983.

[61] E. Von Angerer and J. Prekajac, "2-(hydroxyphenyl)indoles: a new class of mammary tumor-inhibiting compounds," *J. Med. Chem*, vol. 26, no. 1, pp. 113–116, 1983.

[62] E. Von Angerer, N. Knebel, M. Kager, and B. Ganss, "1-(aminoalkyl)-2-phenylindoles as novel pure estrogen antagonists," *J. Med. Chem*, vol. 33, no. 9, pp. 2635–2640, 1990.

[63] C. P. Miller, M. Collini, B. D. Tran, H. A. Harris, Y. P. Kharode, J. T. Marzolf, R. A. Moran, R. A. Henderson, R. H. W. Bender, R. J. Unwalla, L. M. Greenberger, J. P. Yardley, M. A. Abou-Gharbia, C. R. Lyttle, and B. S. Komm, "Design, synthesis, and preclinical characterization of novel, highly selective indole estrogens," *J. Med. Chem.*, vol. 44, pp. 1654–1657, 2001.

[64] C. K. Osborne, "Tamoxifen in the treatment of breast cancer," *N. Eng. J. Med.*, vol. 339, pp. 1609–1618, November 26, 1998.

[65] J. S. Lewis and V. C. Jordan, "Selective estrogen receptor modulators (SERMs): Mechanisms of anticarcinogenesis and drug resistance," *Mutation Research/Fundamental and Molecular Mechanisms of Mutagenesis*, vol. 591, no. 1-2, pp. 247–263, 2005.

[66] G. Jaouen, *Bioorganometallics: Biomolecules, Labeling, Medicine.* Wiley-VCH, 2005.

[67] B. Rosenberg, L. Vancamp, and T. Krigas, "Inhibition of cell division in Escherichia Coli by electrolysis products from a platinum electrode," *Nature*, vol. 205, pp. 698–699., 1965.

[68] B. Rosenberg, L. Vancamp, J. E. Trosko, and V. H. Mansour, "Platinum compounds: a new class of potent antitumour agents," *Nature*, vol. 222, pp. 385–386, 1969.

[69] B. Rosenberg and L. VanCamp, "The successful regression of large solid Sarcoma 180 tumors by platinum compounds," *Cancer Res.*, vol. 30, pp. 1799–1802, 1970.

[70] E. Wong and C. M. Giandomenico, "Current status of platinum-based antitumor drugs," *Chem. Rev.*, vol. 99, pp. 2451–2466, 1999.

[71] B. Lippert, *Cisplatin: Chemistry and Biochemistry of a Leading Anticancer Drug.* John Wiley and Sons, 1999.

[72] M. A. Jakupec, M. Galanski, and B. K. Keppler, "Tumour-inhibiting platinum complexes-state of the art and future perspectives," *Rev. Physiol. Biochem. Pharmacol.*, vol. 146, pp. 1–53, 2003.

[73] C. R. Culy, D. Clemett, and L. R. Wiseman, "Oxaliplatin. a review of its pharmacological properties and clinical efficacy in metastatic colorectal cancer and its potential in other malignancies," *Drugs*, vol. 60, pp. 895–924, Oct 2000.

[74] O. Gandolfi, J. Blum, and F. Mandelbaum-Shavit, "Antitumor steroidal-cis-platinum(II)-o-catecholato conjugates: preliminary evaluation on breast cancer MCF-7-cells," *Inorg. Chim. Acta*, vol. 91, pp. 257–261, 1984.

[75] E. von Angerer, *Platinum complexes with specific activity against hormone dependent tumors*, pp. 73–83. (B. K. Keppler Ed.) VCH, 1993.

[76] C. Chesne, G. Leclercq, P. Pointeau, and H. Patin, "Synthesis and biological studies of aminoestradiol-platinum (II) conjugates," *Eur. J. Med. Chem.*, vol. 21, pp. 321–327, 1986.

[77] R. Gust, H. Schönenberger, U. Klement, and K. J. Range, "Aqua 51-(2,6-dichloro-4-hydroxyphenyl)-2-(2-halo-4-hydroxyphenyl) ethylenediamine]sulfoplatinum(II) complexes with variable substituents in the 2-phenyl ring. II: correlation of molecular structure and estogenic activity of breast and prostate cancer inhibiting [erythro-1-(2,6-dichloro-4-hydroxy-phenyl)-2-(2-halo-4-hydroxyphenyl) ethylenediamine]platinum(II) complexes," *Arch. Pharm. (Weinheim)*, vol. 326, pp. 967–976, 1993.

[78] J. Altman, T. Castrillo, W. Beck, G. Bernhardt, and H. Schönenberger, "Metal complexes with biologically important ligands. 62. Platinum(II) complexes of 3-(2-aminoethoxy)estrone and -estradiol," *Inorg. Chem.*, vol. 30, pp. 4085–4088, 1991.

[79] A. Jackson, J. Davis, R. J. Pither, A. Rodger, and M. J. Hannon, "Estrogen-derived steroidal metal complexes: agents for cellular delivery of metal centers to estrogen receptor-positive cells," *Inorg. Chem.*, vol. 40, no. 16, pp. 3964–3973, 2001.

[80] J. Karl, R. Gust, T. Spruß, M. R. Schneider, H. Schönenberger, J. Engel, K. H. Wrobel, F. Lux, and S. Trebert Haeberlin *J. Med. Chem.*, vol. 31, pp. 72–83, 1988.

[81] S. Top, E. B. Kaloun, A. Vessières, G. Leclercq, I. Laïos, M. Ourevitch, C. Deuschel, M. J. McGlinchey, and G. Jaouen, "Tamoxifen derivatives for delivery of the antitumoral DACH-Pt group : Selective synthesis by McMurry coupling, and biochemical behaviour," *ChemBioChem*, vol. 4, pp. 754–761, 2003.

[82] G. Grenier, G. Bérubé, and C. Gicquaud, "Effects of new triphenylethylene platinum(II) complexes on the interaction with phosphatidylcholine liposomes," *Chem. Pharm. Bull.*, vol. 46, pp. 1480–1483, 1998.

[83] R. H. Crabtree, *The Organometallic Chemistry of the Transition Elements.* J. Wiley and Sons, 4th edition ed., 2005.

[84] M. Herberhold, *Ferrocenes.* (A. Togni, T. Hayashi, Eds.) VCH, 1995.

[85] E. I. Edwards, R. Epton, and G. Marr, "1,1'-ferrocenyldiacetic acid anhydride and its use in the preparation of heteroannularly substituted ferrocenyl-penicillins and -cephalosporins.," *J. Organomet. Chem.*, vol. 122, no. 3, pp. C49–C53, 1976/12/21.

[86] E. I. Edwards, R. Epton, and G. Marr, "Organometallic derivatives of penicillins and cephalosporins a new class of semi-synthetic antibiotics," *J. Organomet. Chem.*, vol. 85, no. 2, pp. C23–C25, 1975/2/4.

[87] A. N. Nesmeyanov, L. G. Bogomolova, V. Viltchevskaya, N. Palitsyne, I. Andrianova, and O. Belozerova, "Patent ferrocerone," 1971.

[88] C. Biot, G. Glorian, L. A. Maciejewski, and J. S. Brocard, "Synthesis and antimalarial activity in vitro and in vivo of a new ferrocene-chloroquine analogue," *J. Med. Chem.*, vol. 40, no. 23, pp. 3715–3718., 1997.

[89] O. Domarle, G. Blampain, H. Agnaniet, T. Nzadiyabi, J. Lebibi, J. Brocard, L. Maciejewski, C. Biot, A. J. Georges, and P. Millet, "In vitro antimalarial activity of a new organometallic analog, ferrocene-chloroquine," *Antimicrob Agents Chemother*, vol. 42, no. 3, pp. 540–4., 1998.

[90] S. Top, J. Tang, A. Vessières, D. Carrez, C. Provot, and G. Jaouen, "Ferrocenyl hydroxytamoxifen: a prototype for a new range of oestradiol receptor site-directed cytotoxics," *Chem. Commun.*, pp. 955–956, 1996.

[91] S. Top, B. Dauer, J. Vaissermann, and G. Jaouen, "Facile route to ferrocifen, 1-[4-(2-dimethylaminoethoxy)]-1(phenyl-2-ferrocenyl-but-1-ene), first organometallic analogue of tamoxifen, by the McMurry reaction," *J. Organomet. Chem.*, vol. 541, pp. 355–361, 1997.

[92] G. Jaouen, S. Top, A. Vessières, G. Leclercq, J. Quivy, L. Jin, and A. Croisy, "The first organometallic antioestrogens and their antiproliferative effects," *C. R. Acad. Sci. Paris,*, vol. Série IIc, pp. 89–93, 2000.

[93] S. Top, A. Vessières, G. Leclercq, J. Quivy, J. Tang, J. Vaissermann, M. Huché, and G. Jaouen, "Synthesis, biochemical properties and molecular modelling studies of organometallic specific estrogen receptor modulators (SERMs), the ferrocifens and hydroxyferrocifens: evidence for an antiproliferative effect of hydroxyferrocifens on both hormone-dependent and hormone-independent breast cancer cell lines," *Chem. Eur. J.*, vol. 9, pp. 5223–5236, 2003.

[94] S. Top, A. Vessières, C. Cabestaing, I. Laios, G. Leclercq, C. Provot, and G. Jaouen, "Studies on organometallic selective receptor modulators (SERMs). dual activity in the hydroxy ferrocifen series," *J. Organomet. Chem.*, vol. 637, pp. 500–506, 2001.

[95] G. Jaouen, S. Top, and A. Vessières, *Organometallics targeted to specific biological sites: The development of new therapies*, pp. 65–95. (G. Jaouen Ed.) Wiley-VCH, 2005.

[96] S. Liu, "The role of coordination chemistry in the development of target-specific radiopharmaceuticals," *Chem. Soc. Rev.*, vol. 33, no. 7, pp. 445–461, 2004.

[97] R. Alberto, *Radiopharmaceuticals*, pp. 97–124. (G. Jaouen Ed.) Wiley-VCH, 2005.

[98] R. Schibli and A. P. Schubiger, "Current use and future potential of organometallic radiopharmaceuticals," *European Journal of Nuclear Medicine and Molecular Imaging*, vol. 29, no. 11, pp. 1529–1542, 2002.

[99] R. K. Hom and J. A. Katzenellenbogen, "Technetium-99m-labeled receptor-specific small-molecule radiopharmaceuticals: recent developments and encouraging results.," *Nucl. Med. Biol.*, vol. 24, pp. 485–498, 1997.

[100] S. S. Jurisson and J. D. Lydon, "Potential technetium small molecule radiopharmaceuticals," *Chem. Rev.*, vol. 99, no. 9, pp. 2205–2218, 1999.

[101] M. J. Abrams, A. Davison, A. G. Jones, C. E. Costello, and H. Pang, "Synthesis and characterization of hexakis(alkyl isocyanide) and hexakis(aryl isocyanide) complexes of technetium(I)," *Inorg. Chem.*, vol. 22, pp. 2798–2800, 1983.

[102] I. Khalkhali, I. Mena, E. Jouanne, L. Diggles, R. Venegas, J. Block, K. Alle, and S. Klein, "Prone scintimammography in patients with suspicion of carcinoma of the breast," *J. Am. Coll. Surg.*, vol. 178, no. 5, pp. 491–497, 1994.

[103] I. Khalkhali, I. Mena, and L. Diggles, "Review of imaging techniques for the diagnosis of breast cancer: a new role of prone scintimammography using technetium-99m sestamibi," *Eur J Nucl Med.*, vol. 21, no. 4, pp. 357–362, 1994.

[104] M. G. Pomper, H. VanBrocklin, A. M. Thieme, R. D. Thomas, D. O. Kiesewetter, K. E. Carlson, C. J. Mathias, M. J. Welch, and J. A. Katzenellenbogen, "11ß-methoxy, 11ß-ethyl- and 17alpha-ethynyl-substituted 16alpha-fluoroestradiols: receptor based imaging agents with enhanced uptake efficiency and selectivity," *J. Med. Chem.*, vol. 33, pp. 3143–3155, 1990.

[105] J. W. Seo, J. S. Comninos, D. Y. Chi, D. W. Kim, K. E. Carlson, and J. A. Katzenellenbogen, "Fluorine-substituted cyclofenil derivatives as estrogen receptor ligands: Synthesis and structure-affinity relationship study of potential positron emission tomography agents for imaging estrogen receptors in breast cancer," *J. Med. Chem*, vol. 49, no. 8, pp. 2496–2511, 2006.

[106] F. Lumachi, G. Ferretti, M. Povolato, M. Marzola, P. Zucchetta, O. Geatti, A. Brandes, and F. Bui, "Accuracy of technetium-99m sestamibi scintimammography and X-ray mam-

mography in premenopausal women with suspected breast cancer," *European Journal of Nuclear Medicine and Molecular Imaging*, vol. 28, no. 12, pp. 1776–1780, 2001.

[107] M. B. Skaddan, F. R. Wüst, and J. A. Katzenellenbogen, "Synthesis and binding affinities of novel Re-containing 7alpha-substituted estradiol complexes: models for breast cancer imaging agents," *J. Org. Chem.*, vol. 64, pp. 8108–8121, 1999.

[108] W. F, K. E. Carlson, J. A. Katzenellenbogen, H. Spies, and B. Johannsen, "Synthesis and binding affinities of a new 17a-substituted estradiol-rhenium "n+1" mixed-ligand and thioether-carbonyl complexes.," *Steroids*, vol. 63, no. 665-671, 1998.

[109] S. Top, H. El Hafa, A. Vessières, J. Quivy, J. Vaissermann, D. Huges, M. J. McGlinchey, J. Mornon, E. Thoreau, and G. Jaouen, "Rhenium carbonyl complexes of beta-estradiol derivatives with high affinity for the estradiol receptor: an approach to selective organometallic radiopharmaceuticals.," *J. Am. Chem. Soc.*, vol. 117, pp. 8372–8380, 1995.

[110] R. Alberto, K. Ortner, N. Wheatley, R. Schibli, and A. P. Schubiger, "Synthesis and properties of boranocarbonate: A convenient in situ CO source for the aqueous preparation of [99mTc(OH2)3(CO)3]+," *J. Am. Chem. Soc.*, vol. 123, no. 13, pp. 3135–3136, 2001.

[111] J. Wald, R. Alberto, K. Ortner, and L. Candreia, "Aqueous one-pot synthesis of derivatized cyclopentadienyl-tricarbonyl complexes of 99mTc with an in situ CO source: Application to a serotonergic receptor ligand," *Angew. Chem., Int. Ed.*, vol. 40, no. 16, pp. 3062–3066, 2001.

[112] A. Nguyen, S. Top, A. Vessieres, P. Pigeon, M. Huche, E. A. Hillard, and G. Jaouen, "Organometallic analogues of tamoxifen: Effect of the amino side-chain replacement by a carbonyl ferrocenyl moiety in hydroxytamoxifen," *Journal of Organometallic Chemistry (ISBOMC bioorganometallics special issue)*, vol. 692, no. 6, pp. 1219–1225, 2007.

[113] P. C. Ruenitz, C. S. Bourne, K. J. Sullivan, and S. A. Moore, "Estrogenic triarylethylene acetic acids: Effect of structural variation on estrogen receptor affinity and estrogenic potency and efficacy in MCF-7 cells," *Journal of Medicinal Chemistry*, vol. 39, no. 24, pp. 4853–4859, 1996.

[114] P. C. Ruenitz and X. Bai, "Acidic metabolites of tamoxifen. Aspects of formation and fate in the female rat," *Drug Metabolism and Disposition*, vol. 23, no. 9, pp. 993–8, 1995.

[115] A. Nguyen, V. Marsaud, B. Céline, S. Top, A. Vessières, P. Pigeon, R. Gref, P. Legrand, G. Jaouen, and J.-M. Renoir, "Nanoparticles loaded with ferrocenyl tamoxifen derivatives for breast cancer treatment," *Int. J. Pharm.*, vol. in press, no. doi: 10.1016/j.ijpharm.2007.06.033, 2007.

[116] J. F. Miquel and J. Gilbert, "A chemical classification of nonsteroidal antagonists of sex-steroid hormone action," *J. Steroid Biochem.*, vol. 31, no. 4B, pp. 525–544, 1988.

[117] D. W. Robertson, J. A. Katzenellenbogen, J. R. Hayes, and B. S. Katzenellenbogen, "Antiestrogen basicity-activity relationships: a comparison of the estrogen receptor binding and antiuterotrophic potencies of several analogs of (Z)-1,2-diphenyl-1-[4-[2-(dimethylamino)ethoxy]phenyl]-1-butene (Tamoxifen, Nolvadex) having altered basicity," *J. Med. Chem*, vol. 25, no. 2, pp. 167–171, 1982.

[118] A. B. Foster, R. McCague, A. Seago, G. Leclercq, S. Stoessel, and F. Roy, "Modification of the basic side chain in tamoxifen: effects on microsomal metabolism and in vitro biological activity," *Anticancer Drug Des.*, vol. 1, pp. 245 – 257, 1986.

[119] M. Jarman, O. T. Leung, G. Leclercq, N. Devleeschouwer, S. Stoessel, R. C. Coombes, and R. A. Skilton, "Analogues of tamoxifen: the role of the basic side-chain. applications of a whole-cell oestrogen-receptor binding assay to N-oxides and quaternary salts.," *Anticancer Drug Des.*, vol. 1, pp. 259 – 268, 1986.

[120] V. Agouridas, I. Laios, A. Cleeren, E. Kizilian, E. Magnier, J.-C. Blazejewski, and G. Leclercq, "Loss of antagonistic activity of tamoxifen by replacement of one N-methyl of its side chain by fluorinated residues," *Bioorg Med Chem*, vol. 14, no. 22, pp. 7531–7538, 2006.

[121] K. S. Kraft, P. C. Ruenitz, and M. G. Bartlett, "Carboxylic acid analogues of tamoxifen: (Z)-2-[p-(1,2-diphenyl-1-butenyl)phenoxy]-N,N-dimethylethylamine. estrogen receptor affinity and estrogen antagonist effects in MCF-7 cells," *Journal of Medicinal Chemistry*, vol. 42, no. 16, pp. 3126–3133, 1999.

[122] V. N. Rubin, P. C. Ruenitz, F. D. Boudinot, and J. L. Boyd, "Identification of new triarylethylene oxyalkanoic acid analogues as bone selective estrogen mimetics," *Bioorganic and Medicinal Chemistry*, vol. 9, no. 6, pp. 1579–1587, 2001.

[123] V. C. Jordan, R. R. Bain, R. R. Brown, B. Gosden, and M. A. Santos, "Determination and pharmacology of a new hydroxylated metabolite of tamoxifen observed in patient sera during therapy for advanced breast cancer," *Cancer Res.*, vol. 43, pp. 1446–1450, March 1, 1983.

[124] M. W. DeGregorio, G. T. Wurz, T. L. Taras, R. U. Erkkola, K. H. Halonen, and R. K. Huupponen, "Pharmacokinetics of (deaminohydroxy)toremifene in humans: a new, selective estrogen-receptor modulator," *European Journal of Clinical Pharmacology*, vol. 56, no. 6, pp. 469–475, 2000.

[125] Q. Qu, H. Zheng, J. Dahllund, A. Laine, N. Cockcroft, Z. Peng, M. Koskinen, K. Hemminki, L. Kangas, K. Vaananen, and P. Harkonen, "Selective estrogenic effects of a novel triphenylethylene compound, FC1271a, on bone, cholesterol level, and reproductive tissues in intact and ovariectomized rats," *Endocrinology*, vol. 141, no. 2, pp. 809–820, 2000.

[126] P. Köpf-Maier, H. Köpf, and E. W. Neuse, "Ferrocenium salts- the first antineoplastic iron compounds," *Angew. Chem. Int. Ed. Engl.*, vol. 23, pp. 456–457, 1984.

[127] A. M. Joy, D. M. L. Goodgame, and I. J. Stratford, "High efficiency of ferricenium salts as radiosensitizers of V79 cells in vitro and the KHT tumor in vivo,"

[128] H. Tamura and M. Miwa, "DNA cleaving activity and cytotoxic activity of ferricenium cations," *Chem. Lett.*, pp. 1177–1178, 1997.

[129] D. Osella, M. Ferrali, P. Zanello, F. Laschi, M. Fontani, C. Nervi, and G. Cavigiolio, "On the mechanism of the antitumor activity of ferrocenium derivatives," *Inorg. Chim. Acta*, vol. 306, pp. 42–48, 2000.

[130] G. Tabbi, C. Cassino, G. Cavigiolio, D. Colangelo, A. Ghiglia, I. Viano, and D. Osella, "Water stability and cytotoxic activity relationship of a series of ferricenium derivatives. ESR insights on the radical production during the degradation process," *J. Med. Chem.*, vol. 45, pp. 5786–5796, 2002.

[131] J. P. Kehrer, "The Haber-Weiss reaction and mechanisms of toxicity," *Toxicology*, vol. 149, no. 1, pp. 43–50., 2000.

[132] A. Nguyen, A. Vessieres, E. A. Hillard, S. Top, P. Pigeon, and G. Jaouen, "Ferrocifens and ferrocifenols as new potential weapons against breast cancer," *Chimia, in press.*

[133] A. Vessières, S. Top, P. Pigeon, E. A. Hillard, L. Boubeker, D. Spera, and G. Jaouen, "Modification of the estrogenic properties of diphenols by the incorporation of ferrocene. Generation of antiproliferative effects in vitro.," *J. Med. Chem.*, vol. 48, pp. 3937–3940, 2005.

[134] E. A. Hillard, P. Pigeon, A. Vessières, C. Amatore, and G. Jaouen, "The influence of phenolic hydroxy substitution on the electron transfer and anti-cancer properties of compounds based on the 2-ferrocenyl-1-phenyl-but-1-ene motif," *Dalton Trans.*, vol. in press, 2007.

[135] E. A. Hillard, A. Vessières, L. Thouin, G. Jaouen, and C. Amatore, "Ferrocene-mediated proton-coupled electron transfer in a series of ferrocifen-type breast cancer drug candidates.," *Angew. Chem. Int. Ed.*, vol. 45, pp. 285–290, 2006.

[136] P. W. Fan, F. Zhang, and J. L. Bolton, "4-hydroxylated metabolites of the antiestrogens tamoxifen and toremifene are metabolized to unusually stable quinone methides.," *Chem. Res. Toxicol.*, vol. 13, pp. 45–52, 2000.

[137] F. Zhang, P. W. Fan, X. Liu, L. Shen, R. B. van Breeman, and J. L. Bolton, "Synthesis and reactivity of a potential carcinogenic metabolite of tamoxifen: 3,4-dihydroxytamoxifen-o-quinone," *Chem. Res. Toxicol.*, vol. 13, pp. 53–62, Jan 2000.

[138] S. Shibutani, L. Dasaradhi, I. Terashima, E. Banoglu, and M. W. Duffel, "alpha-hydroxytamoxifen is a substrate of hydroxysteroid (alcohol) sulfotransferase, resulting in tamoxifen DNA adducts," *Cancer Res*, vol. 58, pp. 647–653, 1998.

[139] S. Gauthier, J. Mailhot, and F. Labrie, "New highly stereoselective synthesis of (Z)-4-hydroxytamoxifen and (Z)-4-hydroxytoremifene via McMurry reaction," *J. Org. Chem.*, vol. 61, pp. 3890–3893, 1996.

[140] K. Schloegl and H. Egger, "Synthesis and reaction of ferrocenylacetylene," *Monatshefte fuer Chemie*, vol. 94, no. 2, pp. 376–92, 1963.

[141] B. T. Kilbourn and P. G. Owston *J. Chem. Soc.*, vol. B26, p. 1, 1970.

[142] G. Precigoux, C. Courseille, S. Geoffre, and M. Hospital *Acta Crystallogr.*, vol. B35, p. 3070, 1979.

[143] W. L. Davis, R. F. Shago, E. H. G. Langner, and J. C. Swarts, "Synthesis and electrochemical properties of a series of ferrocene-containing alcohols," *Polyhedron*, vol. 24, no. 12, pp. 1611–1616, 2005.

[144] E. A. Hillard, A. Vessieres, S. Top, P. Pigeon, K. Kowalski, M. Huche, and G. Jaouen, "Organometallic diphenols: The importance of the organometallic moiety on the expression of a cytotoxic effect on breast cancer cells," *Journal of Organometallic Chemistry*, vol. 692, no. 6, pp. 1315–1326, 2007.

[145] D. J. Minick, J. H. Frenz, M. A. Patrick, and D. A. Brent, "A comprehensive method for determining hydrophobicity constants by reversed-phase high- performance liquid chromatography," *J. Med. Chem.*, vol. 31, pp. 1923–1933, 1988.

[146] "MacSpartan Pro. 18401 Von Karman Avenue, Irvine, CA 92612, USA," *Odyssey Wavefunction Society.*

[147] V. Marsaud, A. Gougelet, S. Maillard, and J.-M. Renoir, "Various phosphorylation pathways, depending on agonist and antagonist binding to endogenous estrogen receptor alpha (ERalpha), differentially affect ERalpha extractability, proteasome-mediated stability, and transcriptional activity in human breast cancer cells," *Mol. Endocrinol.*, vol. 17, no. 10, pp. 2013–2027, 2003.

[148] A. Rivas, M. Lacroix, F. Olea-Serrano, I. Laïos, G. Leclercq, and N. Olea, "Estrogenic effect of a series of bisphenol analogues on gene and protein expression in MCF-7 breast cancer cells.," *J. Steroid Biochem. Mol. Biol.*, vol. 82, no. 1, pp. 45–53, 2002.

[149] J. MacGregor Schafer, H. Liu, A. S. Levenson, J. Horiguchi, Z. Chen, and V. C. Jordan, "Estrogen receptor [alpha] mediated induction of the transforming growth factor [alpha] gene by estradiol and 4-hydroxytamoxifen in MDA-MB-231 breast cancer cells," *The Journal of Steroid Biochemistry and Molecular Biology*, vol. 78, pp. 41–50, 2001.

[150] A. S. Levenson, J. I. M. Schafer, D. J. Bentrem, K. M. Pease, and V. C. Jordan, "Control of the estrogen-like actions of the tamoxifen-estrogen receptor complex by the surface amino acid at position 351," *Journal of Steroid Biochemistry and Molecular Biology*, vol. 76, no. 1-5, pp. 61–70, 2001.

[151] W. S. Marshall, T. Goodson, G. J. Cullinan, D. Swanson-Bean, K. D. Haisch, L. E. Rinkema, and J. H. Fleisch, "Leukotriene receptor antagonists. 1. Synthesis and structure-activity relationships of alkoxyacetophenone derivatives," *J. Med. Chem*, vol. 30, no. 4, pp. 682–689, 1987.

[152] T. A. Woods, T. E. Boyd, E. R. Biehl, and P. C. Reeves, "Directive effects in the hydroboration of vinylferrocenes," *J. Org. Chem.*, vol. 40, no. 16, pp. 2416–2418, 1975.

[153] G. M. Sheldrick, "SHELXS-97: Program for crystal structure solution.," *University of Göttingen, Göttingen, Germany.*

[154] G. M. Sheldrick, "SHELXL-97: Program for crystal structure refinement.," *University of Göttingen, Göttingen, Germany*, 1997.

[155] S. J. Mather, "Design of radiolabelled ligands for the imaging and treatment of cancer," *Mol. BioSyst.*, vol. 3, pp. 30–35, 2007.

[156] S. Liu and D. S. Edwards, "99mTc-labeled small peptides as diagnostic radiopharmaceuticals," *Chem. Rev.*, vol. 99, no. 9, pp. 2235–2268, 1999.

[157] W. A. Volkert and T. J. Hoffman, "Therapeutic radiopharmaceuticals," *Chem. Rev.*, vol. 99, no. 9, pp. 2269–2292, 1999.

[158] R. Chandra, *Introductory physics of nuclear medicine.* Philadelphia: Lea and Febiger, 1992.

[159] M. Comet and M. Vidal, *Radiopharmaceutiques: Chimie des radiotraceurs et applications biologiques.* Grenoble: Presses Universitaires de Grenoble, 1998.

[160] K. Schwochau, "Technetium radiopharmaceuticals: Fundamentals, synthesis, structure, and development," *Angew. Chem. Int. Ed. Engl.*, vol. 33, pp. 2258–2267, 1994.

[161] D. J R and P. S J, "The biomedical chemistry of technetium and rhenium," *Chem. Soc. Rev.*, vol. 27, pp. 43–55, 1998.

[162] P. A. Schubiger, R. Alberto, and A. Smith, "Vehicles, chelators, and radionuclides: Choosing the "building blocks" of an effective therapeutic radioimmunoconjugate," *Bioconjugate Chem.*, vol. 7, pp. 165–167, 1996.

[163] R. Alberto, "The particular role of radiopharmacy within bioorganometallic chemistry," *Journal of Organometallic Chemistry*, vol. 692, no. 6, pp. 1179–1186, 2007.

[164] M. Wenzel, "Tc-99m-Markierung von Cymantren-analogen Verbindungen mit verschiedenen Substituenten- Ein neuer Zugang zu Tc-99m Radiodiagnostika," *J. Labelled Comp. Radiopharm.*, vol. 31, no. 9, pp. 641–650, 1992.

[165] T. W. Spradau and J. A. Katzenellenbogen, "Preparation of cyclopentadienyltricarbonylrhenium complexes using a double ligand-transfer reaction," *Organometallics*, vol. 17, p. 2009, 1998.

[166] L. G. Luyt, E. S. Mull, J. A. Katzenellenbogen, H. M. Bigott, and M. J. Welch, "Preparation of cyclopentadienyltricarbonyl technetium-94m complexes," *J. Labelled Cpd. Radiopharm.*, vol. 4, no. suppl. 1, pp. S489–S490, 2001.

[167] H. M. Bigott, E. Parent, L. G. Luyt, J. A. Katzenellenbogen, and M. J. Welch, "Design and synthesis of functionalized cyclopentadienyl tricarbonylmetal complexes for technetium-94m PET imaging of estrogen receptors," *Bioconjugate Chem.*, vol. 16, no. 2, pp. 255–264, 2005.

[168] S. Top, S. Masi, and G. Jaouen, "The [Re(CO)6]+ cation as a ligand-transfer reagent with ferrocene derivatives," *Eur. J. Inorg. Chem.*, pp. 1848–1853, 2002.

[169] S. Masi, S. Top, L. Boubeker, G. Jaouen, S. Mundwiler, B. Spingler, and R. Alberto, "Direct synthesis of tricarbonyl(cyclopentadienyl)rhenium and tricarbonyl(cyclopentadienyl)technetium units from ferrocenyl moieties. preparation of 17alpha-ethynylestradiol derivatives bearing a tricarbonyl(cyclopentadienyl)technetium group.," *Eur. J. Inorg. Chem.*, vol. 10, pp. 2013–2017, 2004.

[170] J. Bernard, K. Ortner, B. Spingler, H. J. Pietzsch, and R. Alberto, "Aqueous synthesis of derivatized cyclopentadienyl complexes of technetium and rhenium directed toward radiopharmaceutical application," *Inorg. Chem.*, vol. 42, no. 4, pp. 1014–1022, 2003.

[171] M. E. Dyszlewski, M. J. Bushman, R. Alberto, J. W. Brodack, H. Knight, J. MacDonald, L. K. Chinen, E. G. Webb, E. Vries, M. Pattipawaej, and J.-L. Vanderheyden, "Kit formulation and preliminary toxicity of [99m-Tc(CO)3]+ intermediate: a novel technetium radiopharmaceutical platform," *J. Labelled Compd. Radiopharm.*, vol. 44, no. suppl 1, pp. S483–S485, 2001.

[172] M. Wenzel and C. Klinge, "Estradiol-derivatives. synthesis, organ distribution and tumour affinity," *J. Labelled Compd. Radiopharm.*, vol. 34, pp. 981–987, 1994.

[173] S. Top, A. Vessières, and G. Jaouen, "Synthetic strategy for organometallic complexes of rhenium with exceptionnally high affinity for the estradiol receptor. Their potential use as imaging and therapeutic agents.," *J. Chem. Soc. Chem. Commun.*, pp. 453–454, 1994.

[174] D. Osella, C. Nervi, F. Gaelotti, G. Cavigiolio, A. Vessières, and G. Jaouen, "The ferrocenyl-ethynyl unit : a stable hormone tag," *Helv. Chim. Acta*, vol. 84, pp. 3289–3298, 2001.

[175] T. W. Spradau and J. A. Katzenellenbogen, "Ligands for the estrogen receptor, containing cyclopentadienyltricarbonylrhenium units," *Bioorg Med Chem Lett*, vol. 8, no. 22, pp. 3235–3240, 1998.

[176] S. Mundwiler, R. Waibel, B. Spingler, S. Kunze, and R. Alberto, "Picolylaminemethylphosphonic acid esters as tridentate ligands for the labeling of alcohols with the fac-[M(CO)3]+ core (M=99mTc, Re): synthesis and biodistribution of model compounds and of a 99mTc-labeled cobinamide," *Nuclear Medicine and Biology*, vol. 32, no. 5, pp. 473–484, 2005.

[177] L. G. Luyt, H. M. Bigott, M. J. Welch, and J. A. Katzenellenbogen, "7alpha- and 17alpha-substituted estrogens containing tridentate tricarbonyl rhenium/technetium complexes: synthesis of estrogen receptor imaging agents and evaluation using microPET with technetium-94m," *Bioorg. Med. Chem.*, vol. 11, pp. 4977–4989, 2003.

[178] E. S. Mull, V. J. Sattigeri, A. L. Rodriguez, and J. A. Katzenellenbogen, "Aryl cyclopentadienyl tricarbonyl rhenium complexes: Novel ligands for the estrogen receptor with potential use as estrogen radiopharmaceuticals," *Bioorganic and Medicinal Chemistry*, vol. 10, no. 5, pp. 1381–1398, 2002.

[179] S. Masi, S. Top, and G. Jaouen, "Reaction of [Re(CO)6]+ cation with cyclopentadienylthallium derivatives. formation of cyclopentadienylrheniumtricarbonyl derivatives via [Re(CO)3L3]+ (L=solvent)," *Inorg. Chim. Acta*, vol. 350, pp. 665–668, 2003.

[180] N. Marti, B. Spingler, F. Breher, and R. Schibli, "Comparative studies of substitution reactions of rhenium(I) dicarbonyl-nitrosyl and tricarbonyl complexes in aqueous media," *Inorg. Chem.*, vol. 44, no. 17, pp. 6082–6091, 2005.

[181] F. Tisato, M. Porchia, C. Bolzati, F. Refosco, and A. Vittadini, "The preparation of substitution-inert 99Tc metal-fragments: Promising candidates for the design of new 99mTc radiopharmaceuticals," *Coordination Chemistry Reviews*, vol. 250, no. 15-16, pp. 2034–2045, 2006.

[182] A. Scalbert and G. Williamson, "Dietary intake and bioavailability of polyphenols," *J. Nutr.*, vol. 130, pp. 2073S–2085, August 1, 2000.

[183] R. K. Jain, "Delivery of molecular and cellular medicine to solid tumors," *Advanced Drug Delivery Reviews*, vol. 26, no. 2-3, pp. 71–90, 1997.

[184] A. Sharma and U. S. Sharma, "Liposomes in drug delivery: Progress and limitations," *International Journal of Pharmaceutics*, vol. 154, no. 2, pp. 123–140, 1997.

[185] D. C. Drummond, O. Meyer, H. Keelung, D. B. Kirpotin, and D. Papahadjopoulos, "Optimizing liposomes for delivery of chemotherapeutic agents to solid tumours," *Pharmacological Reviews*, vol. 51, no. 4, pp. 691–743, 1999.

[186] K. N. J. Burger, R. W. H. M. Staffhorst, H. C. de Vijlder, M. J. Velinova, P. H. Bomans, P. M. Frederik, and B. de Kruijff, "Nanocapsules: lipid-coated aggregates of cisplatin with high cytotoxicity," *Nat Med*, vol. 8, no. 1, pp. 81–84, 2002.

[187] R. Gref, *Surface-engineered nanoparticles as drug carriers*, pp. 233–256. (M-I Baraton Ed.) American Scientific Publishers, 2003.

[188] G. Storm, S. O. Belliot, T. Daemen, and D. D. Lasic, "Surface modification of nanoparticles to oppose uptake by the mononuclear phagocyte system," *Advanced Drug Delivery Reviews*, vol. 17, no. 1, pp. 31–48, 1995.

[189] "http://www.life-enhancement.com."

[190] S. K. Hobbs, W. L. Monsky, F. Yuan, W. G. Roberts, L. Griffith, V. P. Torchilin, and R. K. Jain, "Regulation of transport pathways in tumor vessels: Role of tumor type and microenvironment," *Proc. Natl. Acad. Sci. USA*, vol. 95, pp. 4607–4612, April 14, 1998.

[191] F. Yuan, M. Dellian, D. Fukumura, M. Leunig, D. A. Berk, V. P. Torchilin, and R. K. Jain, "Vascular permeability in a human tumor xenograft: Molecular size dependence and cutoff size," *Cancer Res*, vol. 55, pp. 3752–3756, September 1, 1995.

[192] W. L. Monsky, D. Fukumura, T. Gohongi, M. Ancukiewcz, H. A. Weich, V. P. Torchilin, F. Yuan, and R. K. Jain, "Augmentation of transvascular transport of macromolecules and nanoparticles in tumors using vascular endothelial growth factor," *Cancer Res*, vol. 59, pp. 4129–4135, August 1, 1999.

[193] S. Maillard, E. Fattal, V. Marsaud, B. Sola, and J.-M. Renoir, *Colloidal systems for the delivery of anticancer agents in breast cancer and multiple myeloma*, pp. 371–403. (C. Kumar Ed.) Wiley-VCH, 2006.

[194] A. Gabizon and D. Papahadjopoulos, "Liposome formulations with prolonged circulation time in blood and enhanced uptake by tumors," *Proc. Natl. Acad. Sci. USA*, vol. 85, pp. 6949–6953, September 15, 1988.

[195] I. Brigger, P. Chaminade, V. Marsaud, M. Appel, M. Besnard, R. Gurny, M. Renoir, and P. Couvreur, "Tamoxifen encapsulation within polyethylene glycol-coated nanospheres. A new antiestrogen formulation," *International Journal of Pharmaceutics*, vol. 214, no. 1-2, pp. 37–42, 2001.

[196] J. S. Chawla and M. M. Amiji, "Biodegradable poly([epsilon]-caprolactone) nanoparticles for tumor-targeted delivery of tamoxifen," *International Journal of Pharmaceutics*, vol. 249, no. 1-2, pp. 127–138, 2002.

[197] F. X. Hu, K. G. Neoh, and E. T. Kang, "Synthesis and in vitro anti-cancer evaluation of tamoxifen-loaded magnetite/PLLA composite nanoparticles," *Biomaterials*, vol. 27, no. 33, pp. 5725–5733, 2006.

[198] T. Ameller, V. Marsaud, P. Legrand, R. Gref, B. Gillian, and J.-M. Renoir, "Polyester-poly(ethylene glycol) nanoparticles loaded with the pure antiestrogen RU 58668: Physicochemical and opsonization properties," *Pharmaceutical Research*, vol. 20, pp. 1063–1070, 2003.

[199] T. Ameller, V. Marsaud, P. Legrand, R. Gref, and J.-M. Renoir, "Pure antiestrogen RU 58668–loaded nanospheres: morphology, cell activity and toxicity studies," *European Journal of Pharmaceutical Sciences*, vol. 21, no. 2-3, pp. 361–370, 2004.

[200] R. Gref, A. Domb, P. Quellec, T. Blunk, R. H. Muller, J. M. Verbavatz, and R. Langer, "The controlled intravenous delivery of drugs using PEG-coated sterically stabilized nanospheres," *Advanced Drug Delivery Reviews*, vol. 16, no. 2-3, pp. 215–233, 1995.

[201] H. Fessi, F. Puisieux, J. P. Devissaguet, N. Ammoury, and S. Benita, "Nanocapsule formation by interfacial polymer deposition following solvent displacement," *International Journal of Pharmaceutics*, vol. 55, no. 1, pp. R1–R4, 1989.

[202] J.-M. Renoir, B. Stella, T. Ameller, E. Connault, P. Opolon, and V. Marsaud, "Improved anti-tumoral capacity of mixed and pure anti-estrogens in breast cancer cell xenografts after their administration by entrapment in colloidal nanosystems," *The Journal of Steroid Biochemistry and Molecular Biology*, vol. 102, no. 1-5, pp. 114–127, 2006.

[203] M. Obrero, D. V. Yu, and D. J. Shapiro, "Estrogen receptor-dependent and estrogen receptor-independent pathways for tamoxifen and 4-hydroxytamoxifen-induced programmed cell death," *J. Biol. Chem.*, vol. 277, pp. 45695–45703, November 15, 2002.

[204] M. Valko, C. J. Rhodes, J. Moncol, M. Izakovic, and M. Mazur, "Free radicals, metals and antioxidants in oxidative stress-induced cancer," *Chemico-Biological Interactions*, vol. 160, pp. 1–40, 2006.

[205] E. A. Hillard, A. Vessières, F. Le Bideau, D. Plazuk, D. Spera, M. Huché, and G. Jaouen, "A series of unconjugated ferrocenyl phenols: prospects as anticancer agents," *ChemMedChem*, vol. 1, pp. 551–559, 2006.

List of Figures

List of Tables

List of abbreviations and Glossary

Ac	acetyl group -CO-CH_3
arom	belong to an aromatic ring
Asp	aspartate
^{t}Bu	*tert*-butyl group -$C(CH_3)_3$
CI	chemical ionization (MS)
Cp	cyclopentadiene ligand $C_5H_5^-$
Cq	quaternary carbon
Cip	ipso carbon
d	doublet
DLT	double ligand transfer (reaction), p. 83
DMF	*N,N*-dimethylformamide
DMSO	dimethylsulfoxide
DNA	deoxyribonucleic acid
E_2	17β-estradiol, p. 8
ER	estrogen receptor, p.5
ER+	hormone-dependent, p. 5
ER-	hormone-independent, p. 1.1.3
ESI	electrospray ionization (MS)
Et	ethyl group -C_2H_5
EtOH	ethanol
FAB	fast atom bombardment (MS)
FACS	fluorescence-activated cell sorting, a flow cytometry system
Fc	ferrocenyl group -[(η^5-C_5H_4)Fe(C_5H_5)]
GSH	glutathione
HPLC	high pressure liquid chromatography
HRMS	high resolution mass spectroscopy

IC_{50}	concentration of a compound that induces 50% of growth inhibition of cells compared to untreated cells
IR	infrared spectroscopy
J	coupling constant in NMR
LBD	ligand binding domain
Leu	leucine
LUC	luciferase
m	multiplet
M	concentration unit: $mol \cdot L^{-1}$
MCF-7	hormone-dependent breast cancer cell line, p. 39
MDA-MB-231	hormone-independent breast cancer cell line, p. 39
Me	methyl group -CH_3
MELN	MCF-7 cell line transfected with the luciferase reporter gene
MeOH	methanol
MS	mass spectroscopy
m/z	mass to charge ratio (MS)
n.a.	(data) non available
NC	nanocapsule, p. 107
NMR	nuclear magnetic resonance
NP	nanoparticle, p. 107
NS	nanosphere, p. 107
PC-3	hormone-independent prostate cancer cell line, p. 39
PBS	phosphate buffered saline
PEG	polyethyleneglycol, p. 107
PET	positron emission tomography
Ph	phenyl group
PLA	poly(D, L-lactic acid), a biodegradable polymer
ppm	parts per million
Pv	pivaloate protecting group -CO-$C(CH_3)_3$
q	quartet

RBA	relative binding affinity, p.36
ROS	reactive oxygen species
s	singlet
S.D.	standard deviation
SERM	selective estrogen receptor modulator, p. 9
SPECT	single photon emission computed tomography
t	triplet
$\tau_{\frac{1}{2}}$	physical half-time of a radionuclide, p. 81
THF	tetrahydrofuran
Tyr	tyrosine
UV-vis	ultraviolet visible spectroscopy